DESIGN AND WIND TUNNEL TESTING OF A SIZE SAMPLING IN-SITU NET SYSTEM (SSISNET)

Robert Paul Mitchke

NAVAL POSTGRADUATE SCHOOL
Monterey, California

THESIS

DESIGN AND WIND TUNNEL TESTING OF

A SIZE SAMPLING IN-SITU NET SYSTEM
(SSISNET)

by

Robert Paul Mitchke

September 1976

Thesis Advisor: E. D. Traganza

Approved for public release; distribution unlimited.

SECURITY CLASSIFICATION OF THIS PAGE (When Data Entered)

REPORT DOCUMENTATION PAGE		READ INSTRUCTIONS BEFORE COMPLETING FORM
1. REPORT NUMBER	2. GOVT ACCESSION NO.	3. RECIPIENT'S CATALOG NUMBER
4. TITLE (and Subtitle) Design and Wind Tunnel Testing of a Size Sampling in-situ Net System (SSISNET)		5. TYPE OF REPORT & PERIOD COVERED Master's Thesis; September 1976 6. PERFORMING ORG. REPORT NUMBER
7. AUTHOR(s) Robert Paul Mitchke		8. CONTRACT OR GRANT NUMBER(s)
9. PERFORMING ORGANIZATION NAME AND ADDRESS Naval Postgraduate School Monterey, California 93940		10. PROGRAM ELEMENT, PROJECT, TASK AREA & WORK UNIT NUMBERS
11. CONTROLLING OFFICE NAME AND ADDRESS Naval Postgraduate School Monterey, California 93940		12. REPORT DATE September 1976 13. NUMBER OF PAGES 94
14. MONITORING AGENCY NAME & ADDRESS(if different from Controlling Office) Naval Postgraduate School Monterey, California 93940		15. SECURITY CLASS. (of this report) Unclassified 15a. DECLASSIFICATION/DOWNGRADING SCHEDULE

16. DISTRIBUTION STATEMENT (of this Report)

Approved for public release; distribution unlimited.

17. DISTRIBUTION STATEMENT (of the abstract entered in Block 20, if different from Report)

18. SUPPLEMENTARY NOTES

19. KEY WORDS (Continue on reverse side if necessary and identify by block number)

20. ABSTRACT (Continue on reverse side if necessary and identify by block number)

A number of plankton sampling devices have been designed and tested and their physical properties (filtration, efficiency, filtration pressure drop, net filtration ratio and mesh approach speed) have been calculated and compared. The data necessary to make these calculations were collected by mounting 1/4 scale sampler models in a wind tunnel, the wind speed having been adjusted to that corresponding to a water

DD FORM 1 JAN 73 1473 EDITION OF 1 NOV 65 IS OBSOLETE
S/N 0102-014-6601 |
(Page 1)

SECURITY CLASSIFICATION OF THIS PAGE (When Data Entered)

speed of 40 m/min; wind speeds were measured at the samplers' mouths by a remote controlled hot-wire anemometer. Photographs were taken of the flow patterns through the use of a flow visualization system comprised of a liquid aerosol generator and tunnel injection system. A study of the photographs and the reduced data resulted in the discovery of an optimum design for a plankton collection system that is composed of a mouth reduction nose cone and two nets in series housed in a cylindrical casing.

Design and Wind Tunnel Testing of a Size Sampling in-situ Net System (SSISNET)

by

Robert Paul Mitchke
Lieutenant, United States Navy
B.S., University of Houston, 1967

Submitted in partial fulfillment of the
requirements for the degree of

MASTER OF SCIENCE IN OCEANOGRAPHY

from the

NAVAL POSTGRADUATE SCHOOL
September 1976

ABSTRACT

A number of plankton sampling devices have been designed and tested and their physical properties (filtration, efficiency, filtration pressure drop, net filtration ratio and mesh approach speed) have been calculated and compared. The data necessary to make these calculations were collected by mounting 1/4 scale sampler models in a wind tunnel, the wind speed having been adjusted to that corresponding to a water speed of 40 m/min; wind speeds were measured at the samplers' mouths by a remote controlled hot-wire anemometer. Photographs were taken of the flow patterns through the use of a flow visualization system comprised of a liquid aerosol generator and tunnel injection system. A study of the photographs and the reduced data resulted in the discovery of an optimum design for a plankton collection system that is composed of a mouth reduction nose cone and two nets in series housed in a cylindrical casing.

TABLE OF CONTENTS

LIST OF FIGURES

LIST OF PLATES

ACKNOWLEDGEMENTS

The author wishes to express his appreciation to Dr. Eugene D. Traganza, the advisor, for allowing the author to participate in his project: Investigation of Biochemical Relationships for Determining Concentrations of Zooplankton Biomass and Its Correlation with Chemical and Acoustical Properties of the Ocean, sponsored by the Office of Naval Research, Code 482, Arlington, Virginia; for his perceptive guidance and suggestions; for his encouragement and experienced insight in the final preparation of the manuscript.

A sincere debt of gratitude is owed to Dr. T. Sarpkaya and Dr. T. M. Houlihan of the Department of Mechanical Engineering who so willingly donated their equipment, time, talent, suggestions and encouragement to this project.

A special acknowledgement is due the Mechanical Engineering Department laboratory personnel, whose technical assistance was priceless: Mr. Tom Christian, Mr. Kenneth Mothersell and Mr. James Selby.

The author is especially grateful to his family for their understanding, patience and support and for the many sacrifices they made while the research was being conducted and the manuscript prepared and completed.

I. INTRODUCTION

According to Aron (1965): "Problems associated with variation of time and space among pelagic organisms are already difficult enough to evaluate without imposing additional complexity through the inadequate understanding of the sampling tools." Plankton sampling by nets began about 150 years ago and in these early stages of collection one haul produced such a wealth of unknown organisms that a lifetime of work was involved in their description. Thus, it is not surprising that the concentration of effort was studying plankton rather than understanding the intrinsic details of the plankton sampler. Tranter (1968) states that when it became apparent that plankton "had such significance in the productivity of the sea and the food chains therein, planktologists wanted to know how to relate the number of organisms found to the volume of water filtered, their distribution in depth, space and time, and their daily, seasonal and annual variations. Development of the gear was gradual to begin with but its tempo increased, partly because of the increased realization of the importance of quantitative work, and partly because of the increase in the number of people studying the subject. The desire for so much comprehensive quantitative knowledge brought with it a host of sampling problems": escapement, avoidance, speed of tow, volume of water filtered, mesh size, drag and clogging. These problems have recently become more comprehensible with

the use of underwater diving and photography and wind and water test tunnels, along with the assistance of experts in hydrodynamics and engineering. Although these factors are giving the evolution of plankton sampling a new impetus, Tranter (1968) states that there has been a lack of experiments conducted to study the hydrodynamics associated with most contemporary samplers. Furthermore, a search of the literature published on the subject subsequent to 1968 has discovered no further attempts to empirically obtain this hydrodynamic data.

The foregoing clearly indicates the desirability and necessity for empirical flow pattern data characteristic of various sampler designs. And more specifically, as Tranter (1968) remarks, as far as encased plankton samplers are concerned there is insufficient data and information available for making any predictions or conclusions about their performance in relation to other sampler designs.

Consequently the subject of this investigation has been to study the relative entrance flow patterns associated with encased samplers, in particular a type that includes a mouth reduction nose cone and two nets in series housed in a cylindrical casing. This sampler type can aptly be termed as a "size sampling in-situ net" (SSISNET) system. An analysis of the flow patterns produced by several SSISNETS of different design has resulted in the discovery of an optimum combination of sampler parameters that can be used in the ultimate construction of a single SISSNET system.

II. THEORETICAL BACKGROUND

A. FILTRATION PERFORMANCE

Four physical properties associated with plankton net filtration that are of significant consequence when sampling plankton are (Tranter, 1968):

(1) filtration efficiency

(2) filtration pressure drop

(3) net filtration ratio

(4) mesh approach speed

Filtration efficiency (F) primarily affects the volume of water filtered, but also has an influence on plankton escapement and avoidance, both of which increase as F decreases. Filtration efficiency is defined by Tranter (1968) as the ratio of the volume of water filtered by a plankton sampler to the volume swept by the sampler mouth. That is,

$$F = \frac{W}{A \cdot D} \qquad (1)$$

where W is the volume of water filtered, A is the area of the sampler mouth and D is the distance traveled. The relation may also be expressed as,

$$F = \frac{A}{A} \cdot \frac{V'}{V} = \frac{V'}{V} \qquad (2)$$

where V is the tow speed and V' is the mean speed of the flow through the mouth of the sampler.

Filtration pressure drop (ΔP) influences the ultimate condition of the catch; it is determined by the speed at which the water approaches the net gauze (approach speed). According to Tranter (1968)

$$\Delta P = K \cdot \frac{1}{2} \rho v^2 \qquad (3)$$

where v is mesh approach speed, ρ is sea water density; K (resistance coefficient) is a function of the gauze porosity (β) and Reynolds number (Re) and has been shown by Wieghardt (1953) to be:

$$K \doteq \frac{1-\beta}{\beta^2} \cdot 6\ Re^{-1/3} \qquad (4)$$

Reynolds number is given by the equation

$$Re = \frac{V}{\beta} \cdot \frac{d}{k} \qquad (5)$$

where d is the diameter of the gauze strands, k is the kinematic viscosity of the water. The porosity is the open area fraction of the gauze comprising the filtering surface and is calculated from the equation:

$$\beta = \frac{m^2}{(d+m)^2} \qquad (6)$$

where m is the mesh width and d is the diameter of the strands in the meshwork. The effective Reynolds number becomes Re cos θ when the flow strikes the gauze at the angle θ to the

normal, thus the maximum possible values of filtration pressure are obtainable by setting $\theta=0$.

If a mouth reduction nose cone is added to a conical net, as in Figure 1, the filtration efficiency increases. The nose cone also has the effect of creating a low pressure area which

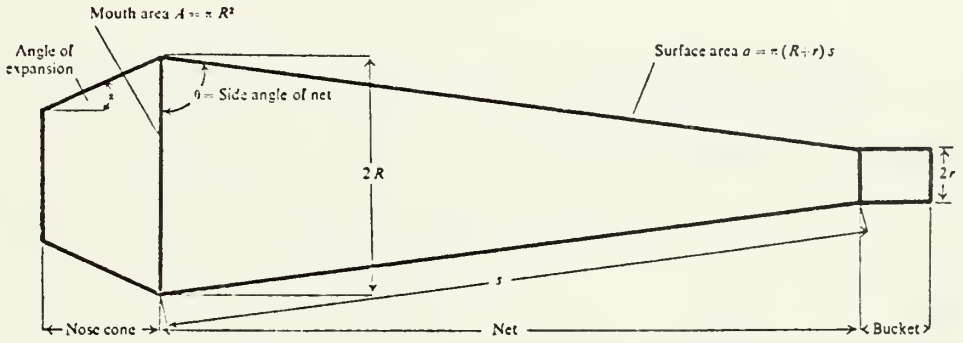

Figure 1. Generalized geometry of a plankton net with a mouth reduction nose cone (From Tranter and Heron, 1967).

draws a column of water wider than the reduced mouth through the sampler (Figure 4c). The angle of expansion and the length of the nose cone are critical because they actually control the filtration efficiency, which depends upon the mean flow velocity through mouth and the mouth area. Reduction cones are most efficient when their angle of expansion (α) is less than 3 1/2° (Pankhurst and Holder, 1952), and their length is greater than the diameter of the net mouth. Increase of length is restricted by physical practicality and by the reduction of the mouth area, which would decrease the volume accepted.

Another important limitation on dimensions is a result of the filtration efficiency decreasing sharply when the net side angle (θ) is reduced below 75° or the ratio $\frac{A}{a}$ rises above approximately 0.2 (Tranter and Heron, 1967; Smith et al., 1965). This ratio can be calculated from

$$\frac{\text{mouth area}}{\text{porous area}} = \frac{A}{a} = \frac{\pi R^2}{\pi R s} = \cos \theta \qquad (7)$$

where R is the mouth radius and s is net slant length.

A factor closely related to this area ratio is the net filtration ratio (FR) and is given by

$$FR = \frac{a\beta}{A} \qquad (8)$$

where β is the net porosity. As the length of the net decreases the filtration ratio decreases; this condition promotes clogging which, in turn, reduces the filtration efficiency. Therefore the net must be long enough to minimize clogging; however it also has to be restricted to that length which is physically manageable.

The mesh approach speed (v) is a parameter that can be obtained from the equation (Tranter, 1968)

$$v = V \cdot F \cdot \frac{A}{a} \qquad (9)$$

and then used to calculate the filtration pressure drop by equation (3). This approach speed alone does not cause damage to organisms; but it is primarily the associated

pressure drop across the net that would be responsible for any damage. It is also likely that this pressure drop influences the selectivity or organisms by the meshes (Vannucci, 1968). That is, a high ΔP could cause organisms to be pulled through the mesh, distorting any selectivity data. Because ΔP varies as the square of the approach speed (equation (3)), small changes in this speed will lead to relatively large changes in ΔP. Therefore approach speed should be restricted to an optimum value, one that would create a ΔP large enough to insure a continuous fluid flow, but not great enough to be destructive to the organisms.

B. FLOW PATTERNS

The interaction between a plankton net and the water through which it is towed produces for each type of sampler a unique flow pattern which is closely related to its filtration performance. This interaction significantly affects the entire sampling process because of the many other factors involved. For example, an approaching net causes disturbances that may result in avoidance by motile zooplankton; the volume of water filtered is directly related to the shape of the net; and clogging of the net can seriously reduce filtration. The following discussion will closely examine these and other water-net interactions with a description of the various flow patterns produced.

"The pressures on both sides of the gauze are equal for a stationary net; however, for a moving net the inside pressure is higher than that on the outside and the resulting flow

pattern is dependent upon the distribution of these pressures" (Tranter, 1968). Also Tranter (1968) states that the conical net has the most evenly distributed pressures, thereby resulting in a uniform flow rate over the entire filtering area of the net which is important when attempting to maximize filtration efficiency.

The entrance area of the net displays flow patterns that are influenced both by the resistance of the net and by towing structures ahead or near the mouth. Most of the disturbances created ahead of the net by the tow cable and bridle can be alleviated by towing with the cable attached to the top of the forward section of the sampler casing or by attaching the cable to the rear of the casing and sampling during a guided vertical fall. Upstream accelerations caused by various towing appratus are shown in Figure 2. This disturbance, coupled with any upstream pressure variation when nets are attached, can have a severe adverse impact upon results of collection efforts due to the belief that plankton sense and move away from foreign objects (Tranter, 1968).

"The sampler mouth, or at least the shape of its mouth, can play an important role in reducing or even alleviating upstream disturbances that may cause avoidance by plankton" (Tranter, 1968). It has been shown by Tranter (1968) that the addition of a mouth-reduction cone increases filtration efficiency by creating a low pressure area which results in a larger cross-section of the water column being drawn into the net. Figure 3 is a comparison of streamline patterns

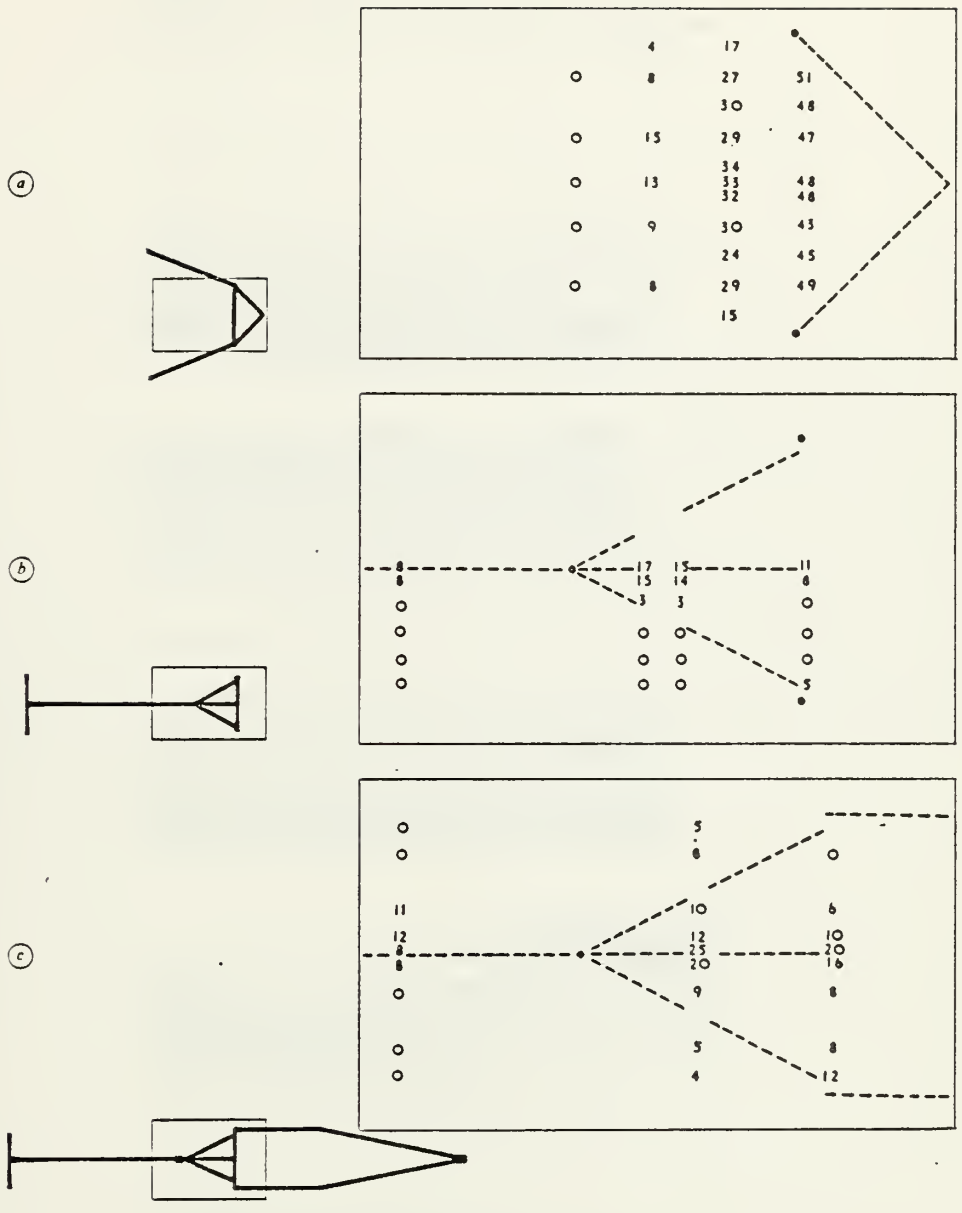

Figure 2. The accelerations (cm/sec) ahead of plankton nets.
a. Linear accelerations ahead of a non-filtering cone 1 m in diameter without a bridle preceding the entrance. The tow speed is 77 cm/sec (44 m/min).
b. Linear accelerations ahead of a ring with bridle and lead line. The tow speed is 129 cm/sec (77 m/min).
c. Linear accelerations ahead of a plankton net ring, bridle and lead line. The tow speed is 129 cm/sec (77 m/min). (from Tranter, 1968).

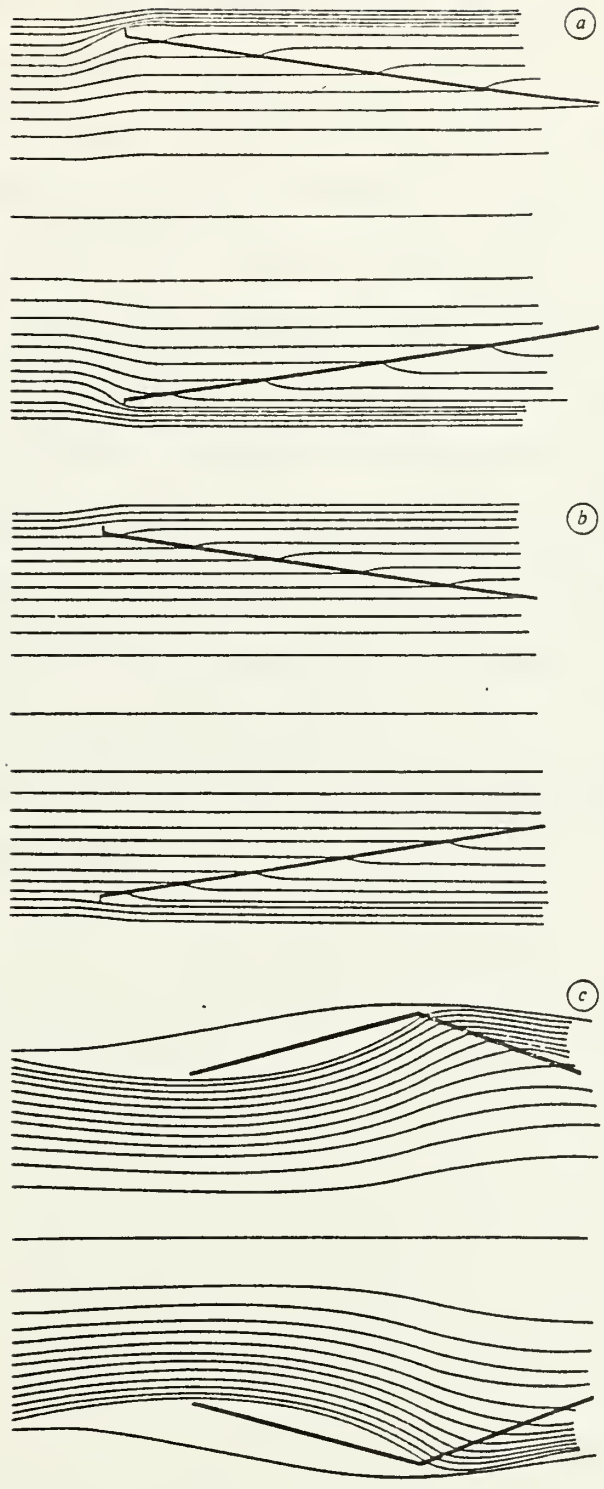

Figure 3. Streamlines ahead of nets. Each streamline encloses 10 percent of the water entering a circular net.
a. A conical net which is accepting 75 percent of the water presented to it.
b. A conical net which is accepting 95 percent of the water presented to it.
c. A conical net, with a mouth-reduction cone, which is accepting 125 percent of the water presented to it (from Tranter, 1968).

associated with conical nets with and without a reduction cone. The advantage gained in filtration efficiency through the use of the mouth reduction cone can be seen by examining that figure and noting the increase in percentage of water accepted when using the cone with the net.

Tranter (1968) also offered a series of figures depicting probable flow patterns associated with some basic forms of plankton samplers. These are shown in Figure 4; however, they are based on theory rather than actual observance. Plankton sampler type f was selected for study in this thesis because it would allow stacking different size nets within the casing for separating plankton by size. This type sampler also has the filtration control advantages of a mouth reduction nose cone.

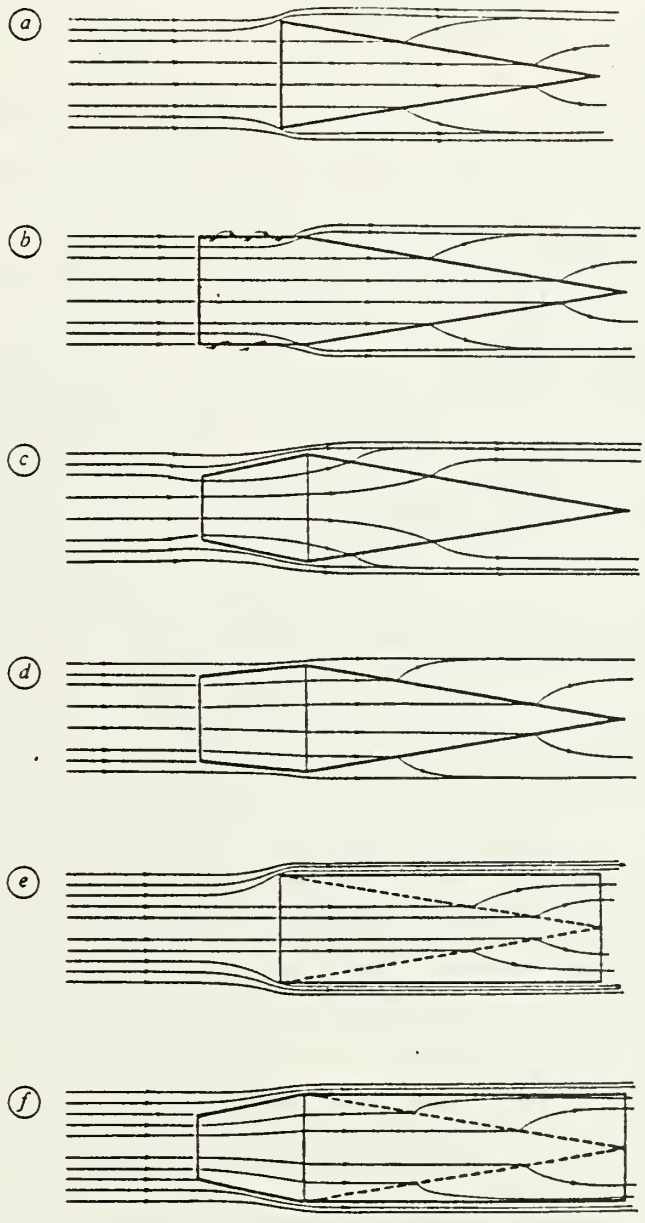

Figure 4. Probable flow pattern associated with some basic forms of plankton sampler.
a. Simple conical net ($F < 1$).
b. Conical net with porous collar ($F \doteq 1$).
c. Conical net with nonporous mouth-reducing cone ($F > 1$).
d. Conical net with nonporous mouth-reducing cone ($F = 1$).
e. Conical net with nonporous casing ($F < 1$).
f. Conical net with nonporous casing and nonporous mouth-reducing cone ($F = 1$). (from Tranter, 1968)

III. METHODS

A. WIND TUNNEL TESTING

One method of measuring the hydrodynamic characteristics of plankton nets is to construct scale models and to test them in wind or water tunnels. The wind tunnels are particularly suited for this purpose becasue of ease of experimentation, flow visualization, and measurement of the forces acting on the nets. It is for this reason that it was decided to carry out a series of experiments in the low speed wind tunnel of the Mechanical Engineering Department of the Naval Postgraduate School (Plate 1).

The tunnel is of open circuit design with its intake inside the building and exhausting outside. The test section is 51 cm by 71 cm at the center and is 2.4 meters long. The prime mover is a six blade axial fan, located at the downstream end, and driven by a variable speed 75 horsepower electric motor. The wind speed is continuously variable from 548 m/min to 5486 m/min when the test section is clean, and from about 914 to 4572 m/min (equivalent to 15 and 75 m/min water speed) when the model is installed. The freestream turbulence intensity is controlled at the plenum entrance, followed by up to five interchangeable graded screens and an area contraction ratio of ten to one.

The tunnel was equipped with a flow visualization system comprised of a liquid aerosol generator and injection system

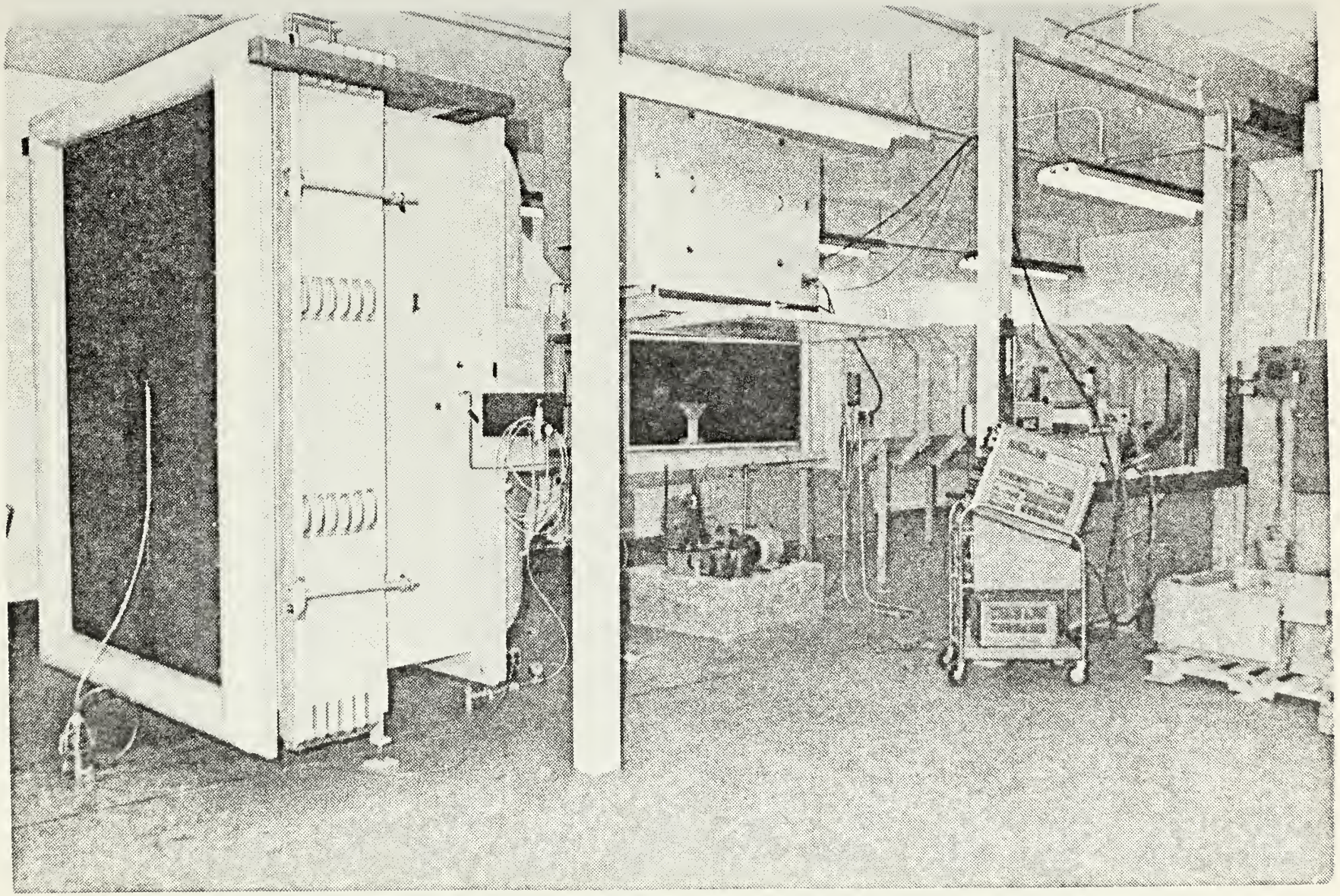

Plate 1. Low speed wind tunnel.

(Plate 2). The flow of the aerosol particles in front of and around the models have been used to study the flow patterns. This will be described in greater detail later.

Evidently, model tests in general and the use of different fluids (e.g. air and water) for the model and prototype require the establishment of model laws in order to be able to correctly interpret the results and to transfer them from one model to another. Fundamentals of fluid mechanics show that (see for example Streeter, 1958) complete similarity requires geometric, kinematic and dynamic similarity of the models. In other words, for the present investigation, this requires that the model and the prototype be geometrically similar and that the model and prototype Reynolds numbers and Mach numbers be identical. It is assumed that there are no free surface effects and the Froude number is excluded from further consideration. Reynolds similarity establishes the correct ratio of the inertial forces to viscous forces in the model and prototype at the corresponding points. Mach similarity, on the other hand, brings into the tests the possible effects of the fluid compressibility and expresses the ratio of the inertial forces to elastic forces. In the present study, the compressibilities of the fluids involved, that is of air and water, are quite negligible. Air shows compressibility effects for body speeds corresponding to Mach numbers of about 0.4 or greater. Water shows compressibility effects for speeds of sound in water or close to it. This, in fact, corresponds to a sound speed of about 4000 feet/sec. Cavitation

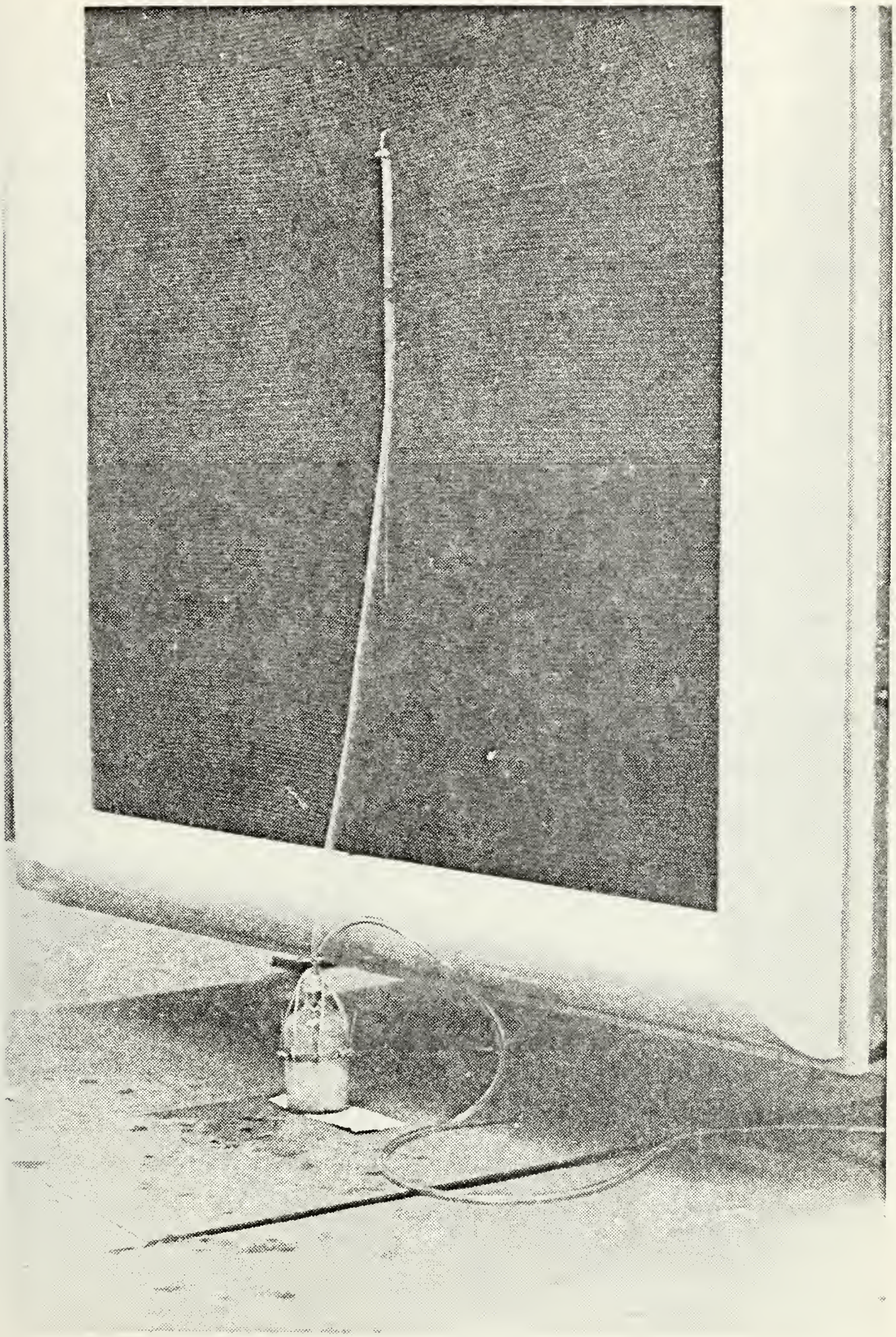

Plate 2. Liquid aerosol generator and tunnel injection system.

and other effects take place long before the compressibility effects come into the picture in collecting plankton (if the collector were ever to travel at such high speeds). Further discussion of the compressibility effects is meaningless and the Mach similarity need not be considered.

According to Reynolds similarity, Streeter (1958) used the equation

$$\frac{U_a D_a}{\nu_a} = \frac{V D_w}{\nu_w} = \text{Reynolds number} \qquad (10)$$

in which U and V are wind and water speeds relative to the collector, D the diameter, and ν the kinematic viscosity of the fluid (ν_{air} = 9000 X 10^{-7} m^2/min at room temperature and ν_{water} = 575 X 10^{-7} m^2/min at 20°C temperature). The indices "a" and "w" denote "air" and "water" respectively to indicate the Reynolds numbers for the model and prototype media. Solving for the speed of air in the wind tunnel, one has:

$$U_a = \frac{\nu_a}{\nu_w} \cdot \frac{D_w}{D_a} \cdot V \qquad (11)$$

The characteristic dimension is taken as the inlet diameter of the collector without a nose cone, for the prototype D_w = 31.6 cm, and for the model D_a = 7.9 cm, for a model scale of 1/4. The Reynolds numbers and the corresponding wind and water speeds for the model and prototype respectively are given in Table I.

TABLE I. Various wind tunnel air speeds (U_a) and the corresponding water speeds (V) required to match the Reynolds numbers.

U_a wind speed (m/min)	Reynolds number (dimensionless)	V water speed (m/min)
1560	137400	25
1870	164900	30
2190	192400	35
2505	219700	40
2815	247300	45
3130	275000	50
3440	302300	55
3760	330000	60
4070	357300	65
4380	385000	70

B. FLOW SPEED MEASUREMENTS

The desired model combination of nets, reduction cone and casing was assembled and mounted in the test section of the wind tunnel. The air speed was adjusted to that corresponding the water speed. Photographs were taken of the flow stream lines, i.e. aerosol particles (Plates 6 through 14).

A remote controlled hot-wire anemometer was used to measure voltages at various points in front of the different models (Plates 3 and 4). These voltages were recorded on an X-Y plotter (Plate 5), then converted to wind speeds (U_a) with the following equation, which is derived from the standard calibration procedure of a hot-wire anemometer probe:

$$U_a^{1/2} = \frac{E^2 - E_o^2}{y} \qquad (12)$$

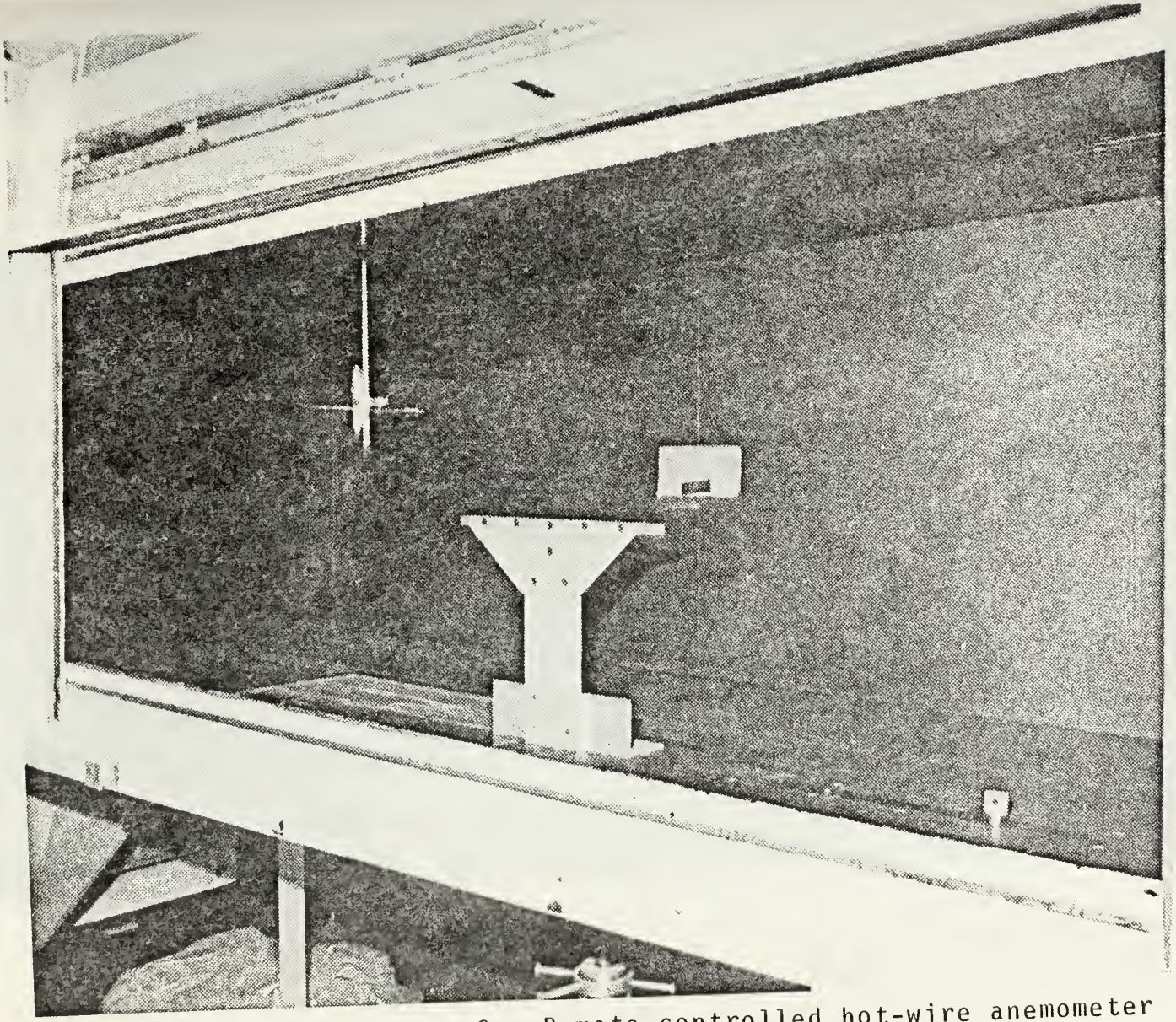

Plate 3. Remote controlled hot-wire anemometer probe.

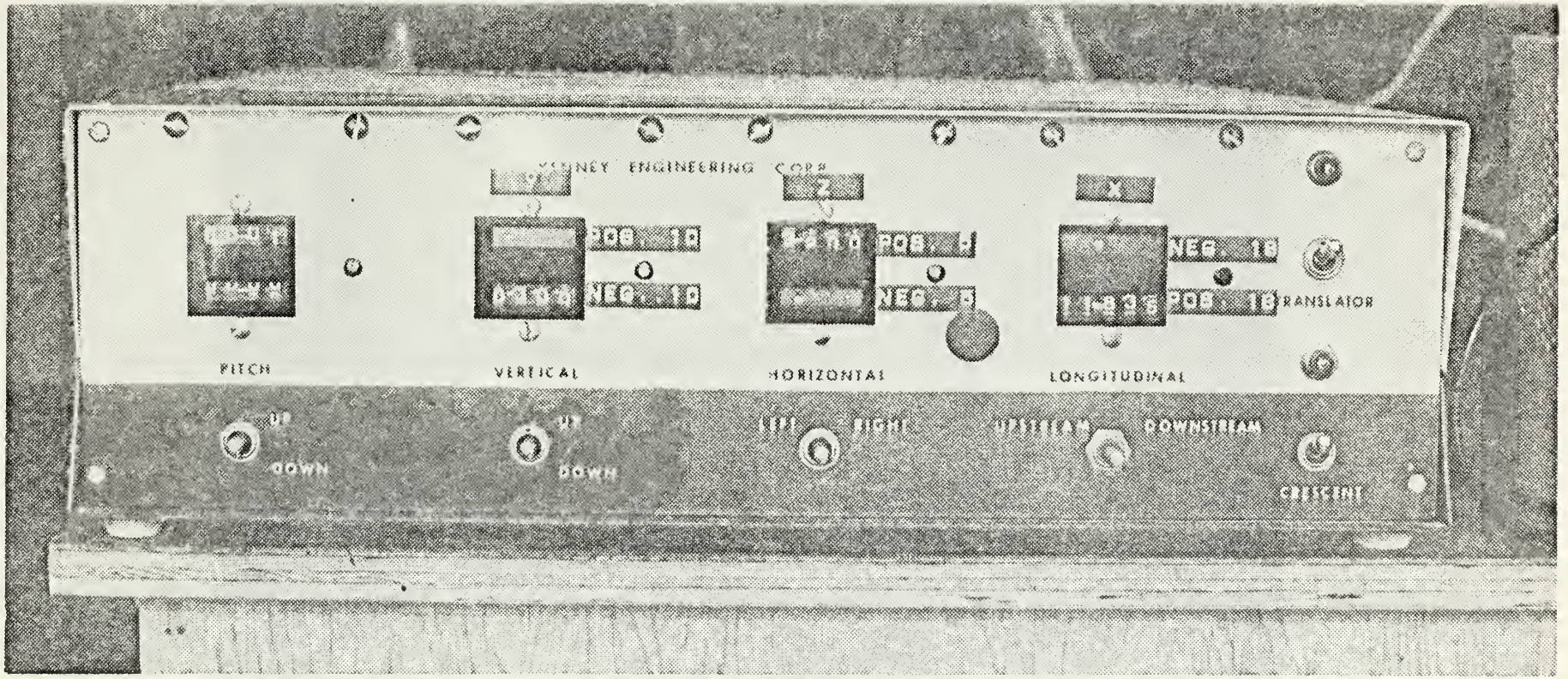

Plate 4. Servo-translater unit used to remotely position hot-wire anemometer probe.

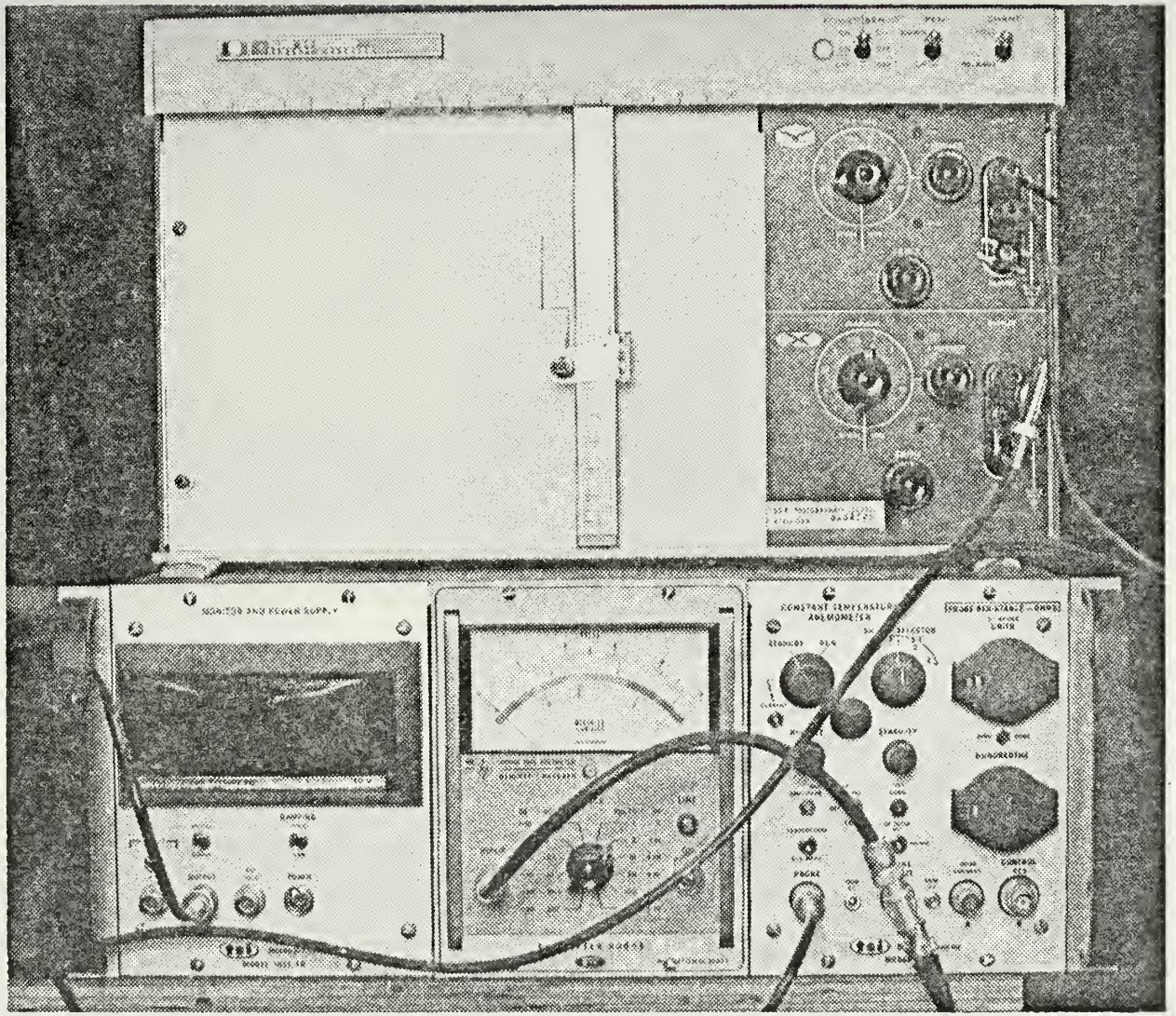

Plate 5. X-Y plotter and power supply.

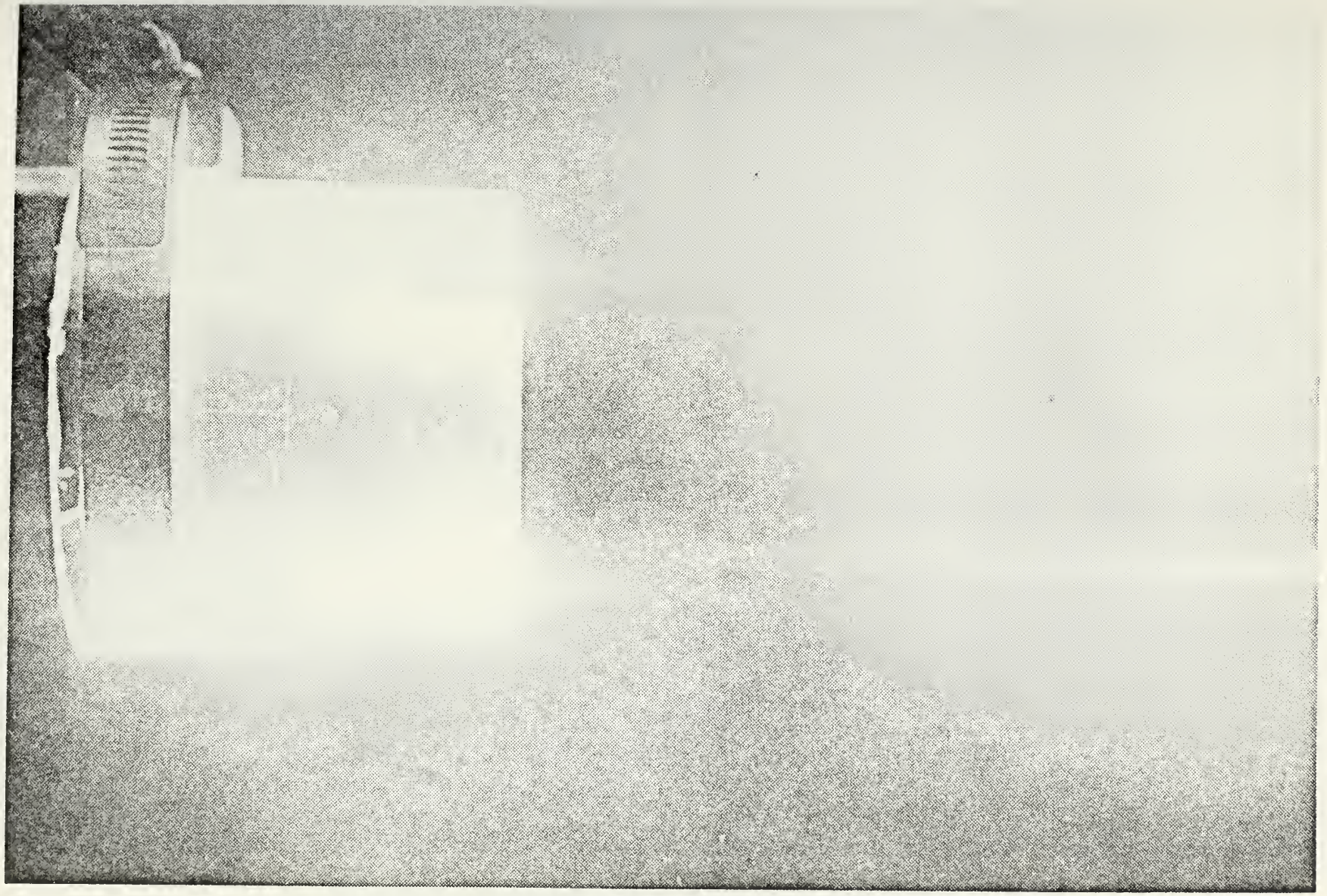

Plate 6. Mouth reduction nose cone model 1.

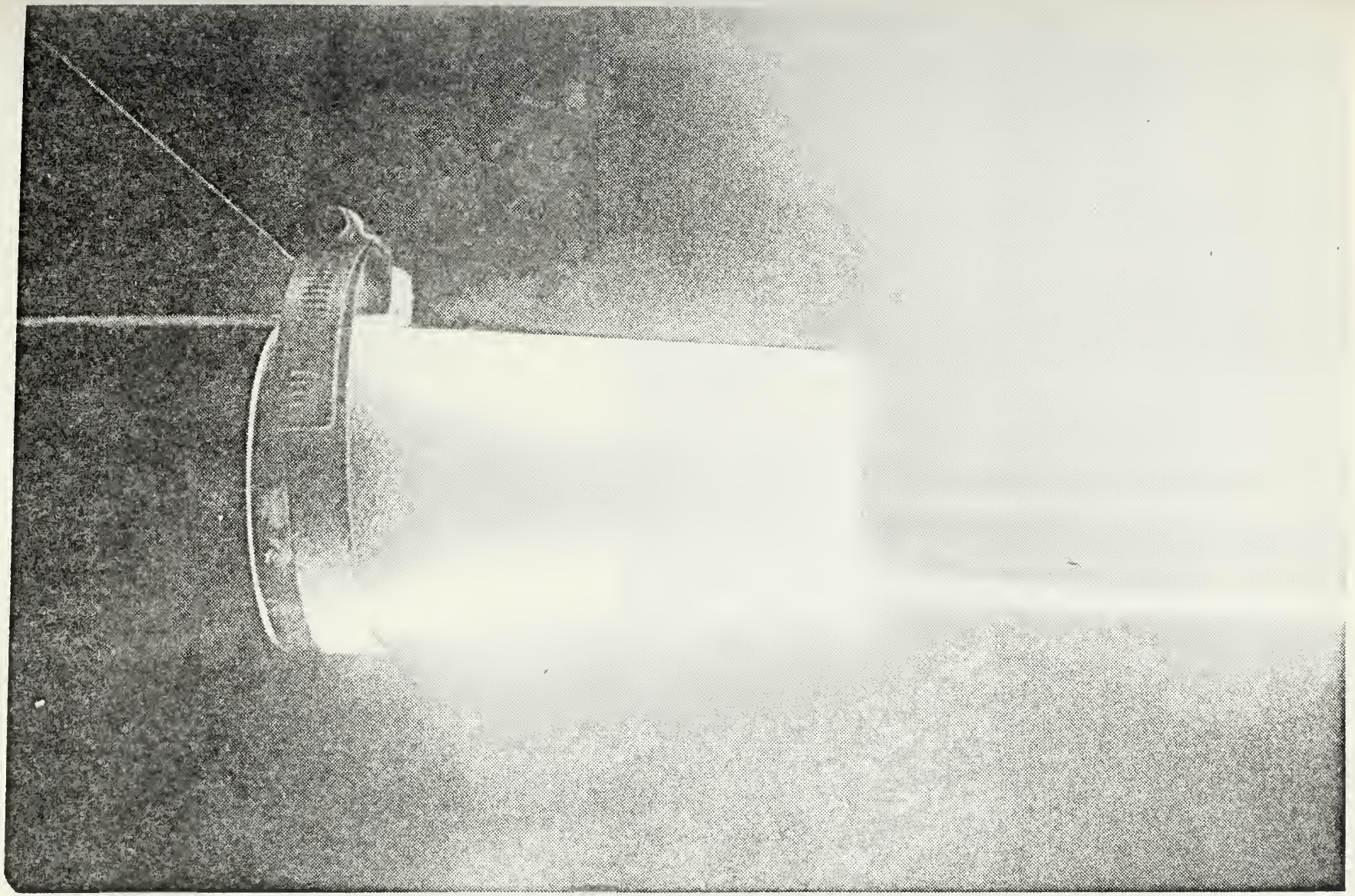

Plate 7. Mouth reduction nose cone model 2.

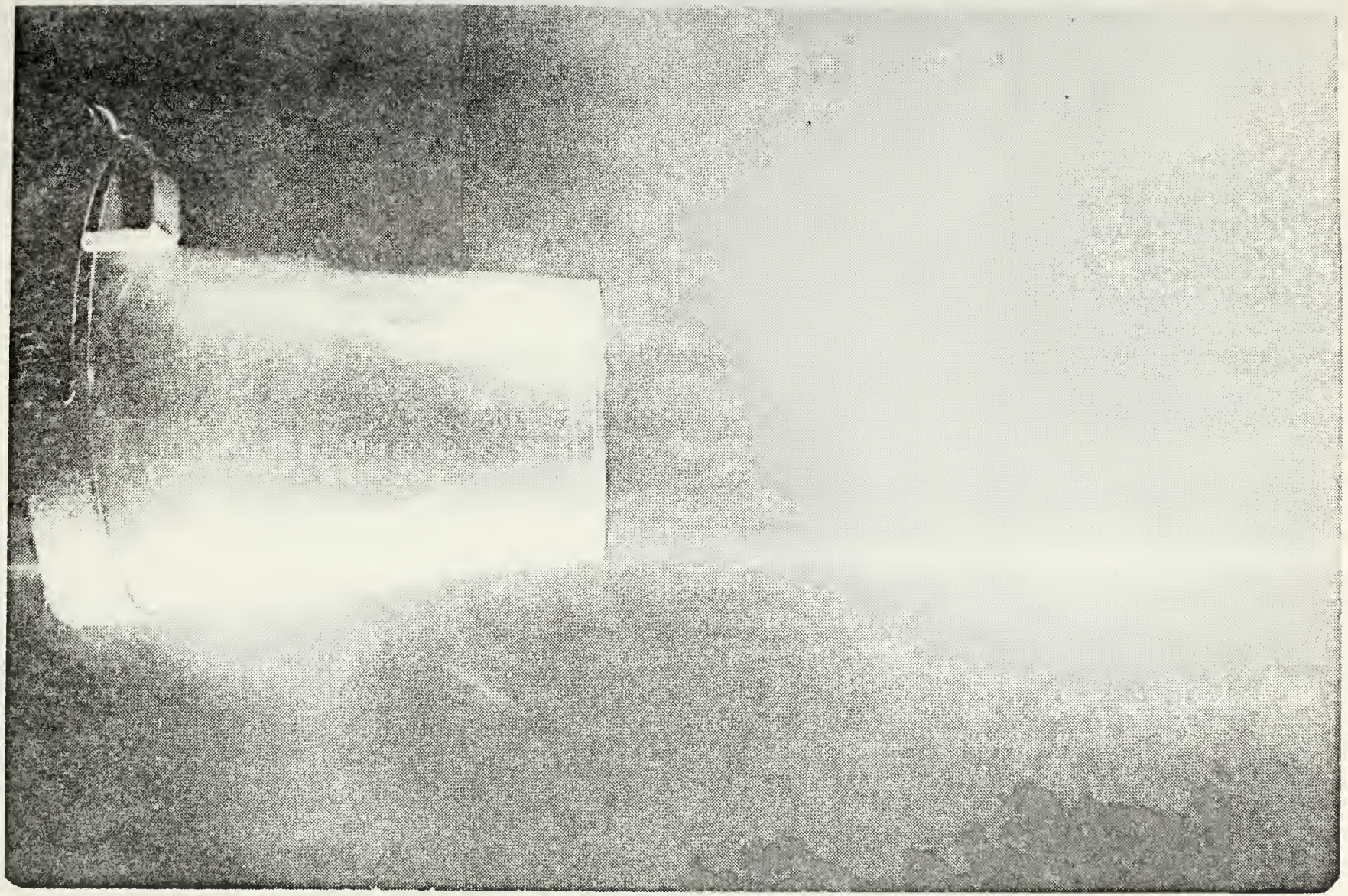

Plate 8. Mouth reduction nose cone model 3.

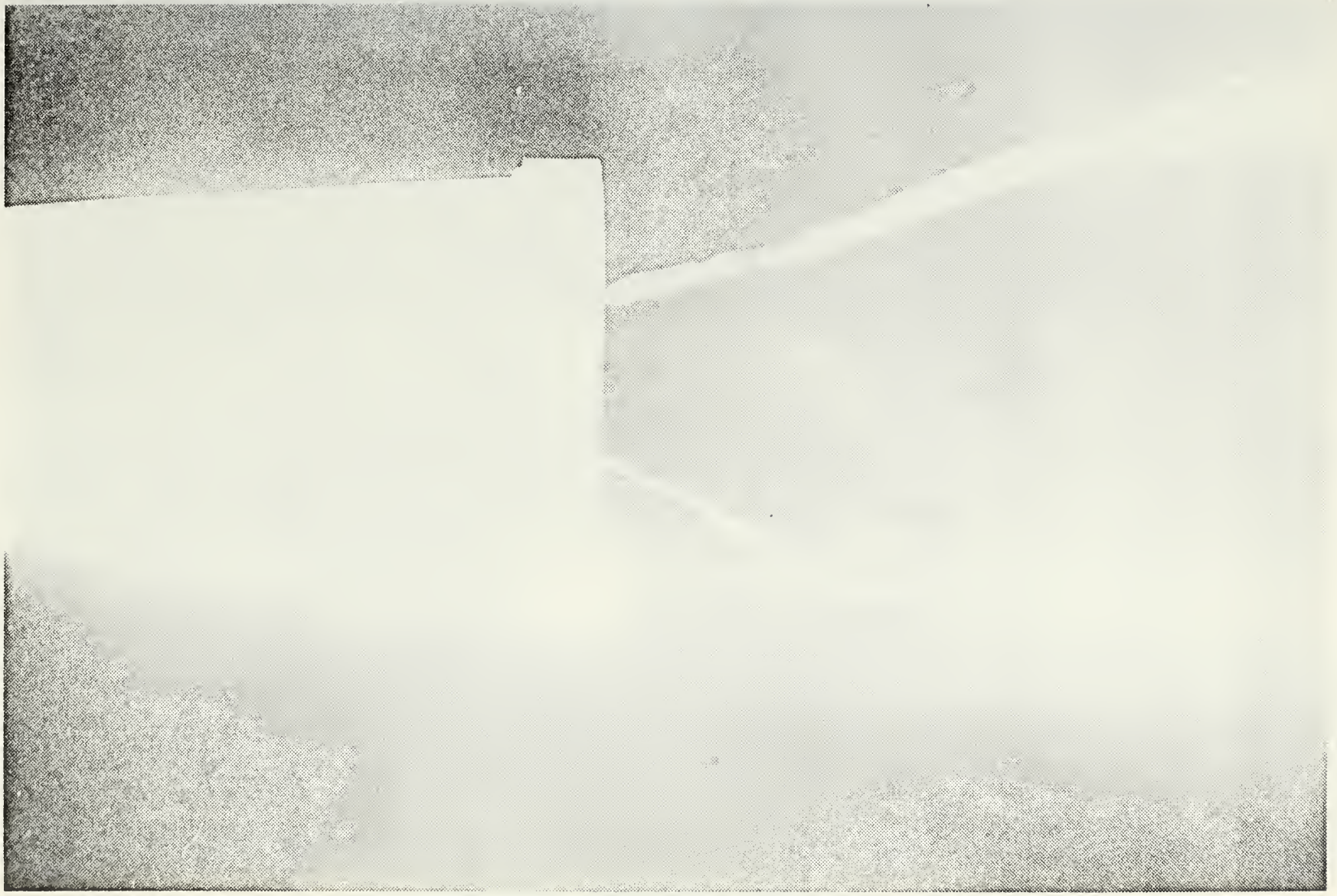

Plate 9. Sampler model A: simple conical net.

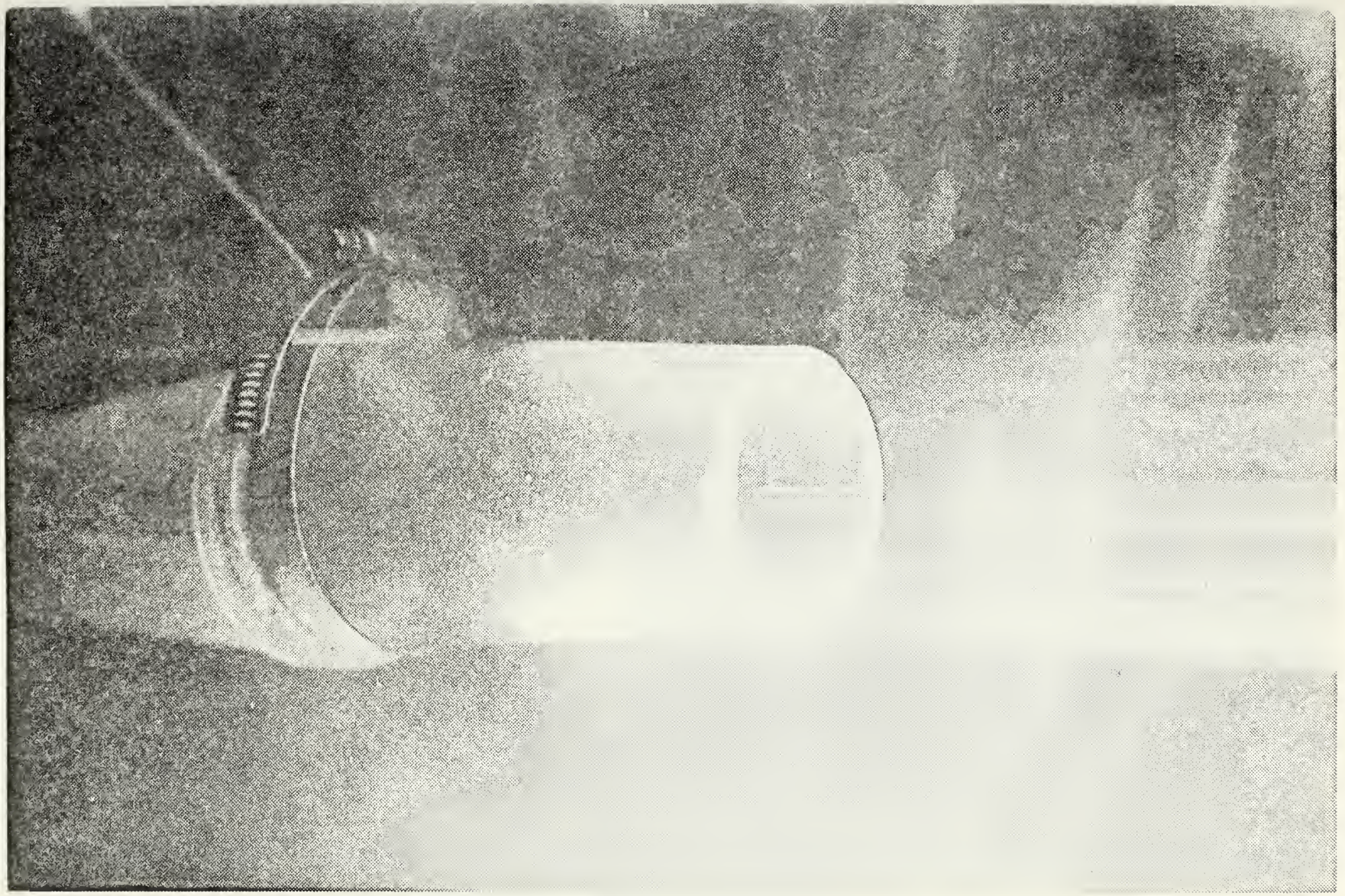

Plate 10. Sampler model C.

Plate 11. Sampler model H.

Plate 12. Sampler model J.

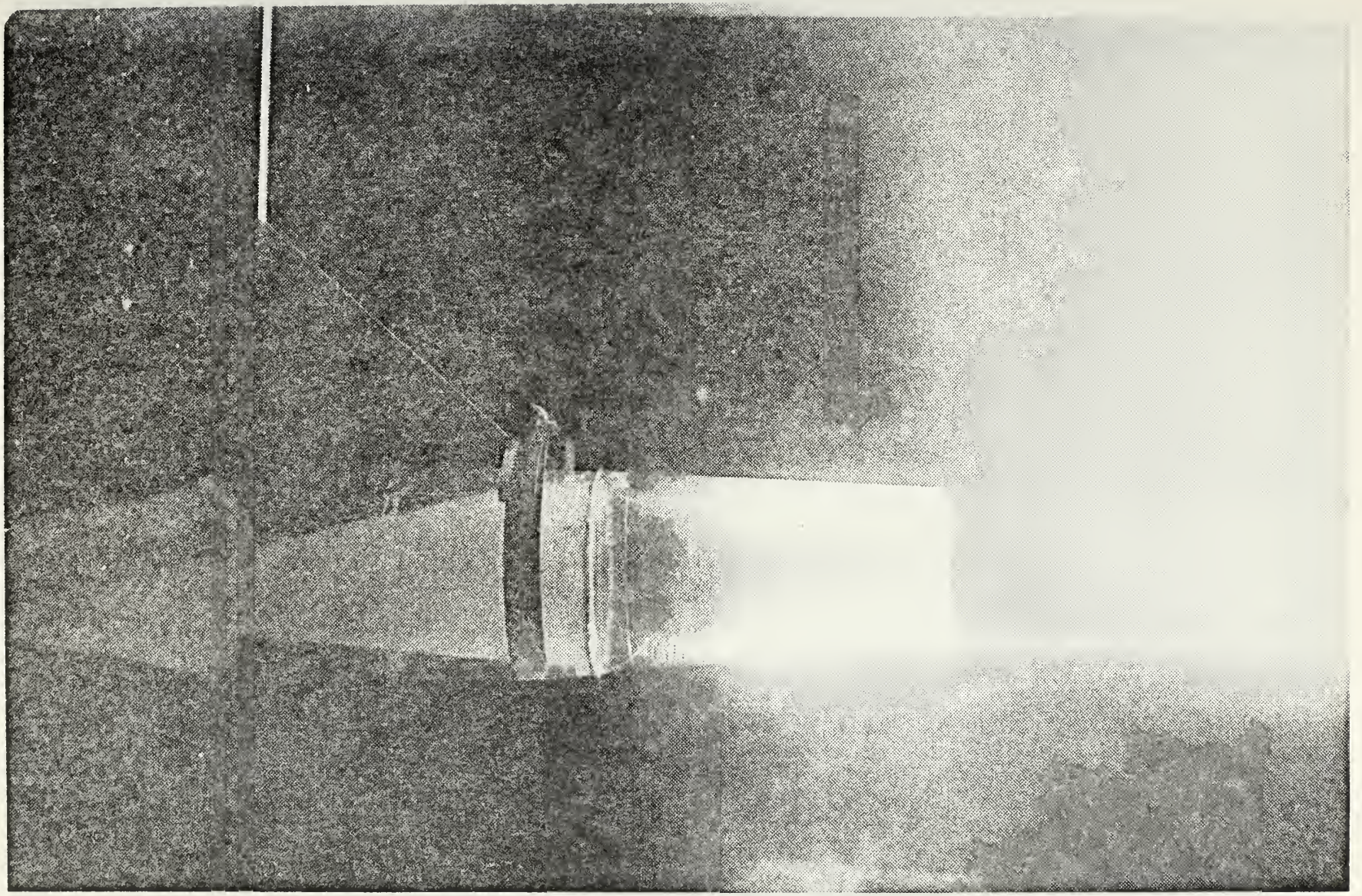

Plate 13. Sampler model K.

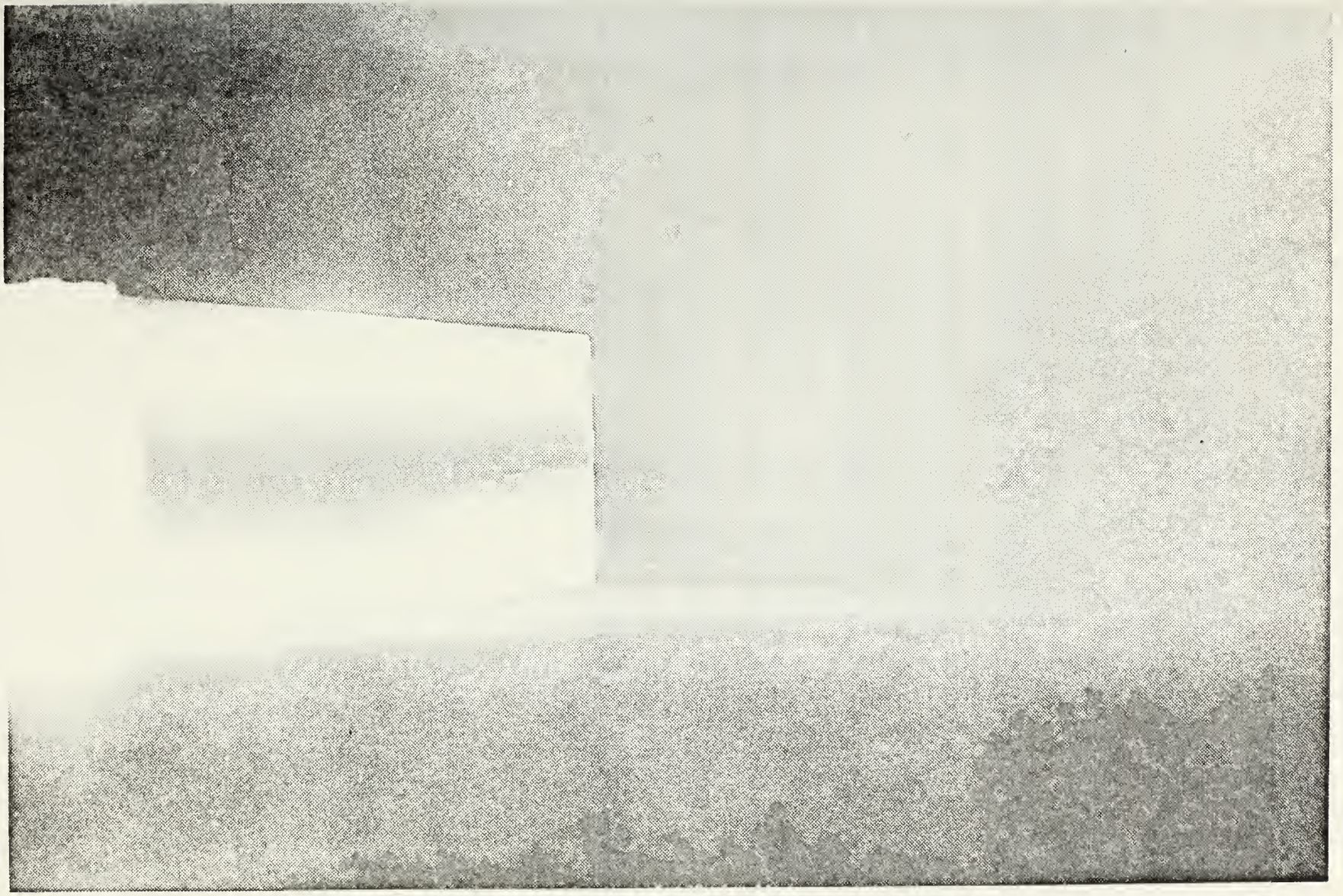

Plate 14. Sampler model L.

where E is the voltage recorded on the X-Y plotter, E_0 is the voltage registered by the anemometer at zero wind speed and y is the anemometer probe characteristic impedance. In the case of one probe E_0 was found to be 5.4 volts and y to be 0.79. A second probe had an E_0 of 3.27 and a y of 0.5. The wind speeds were then converted into corresponding water speeds (V) through the use of Table I. The voltage profile data and corresponding water speeds were tabulated for each system model in the Appendix. The water speed data were used in equation (2) to obtain the filtration efficiency and in equation (9) for mesh approach speed calculations, which in turn was used in equation (3) to obtain filtration pressure drop values. These results are tabulated for all models and are listed on the corresponding drawings (Figures 5 through 23). A comparison of the values were made for the purpose of choosing the model that had optimum characteristics.

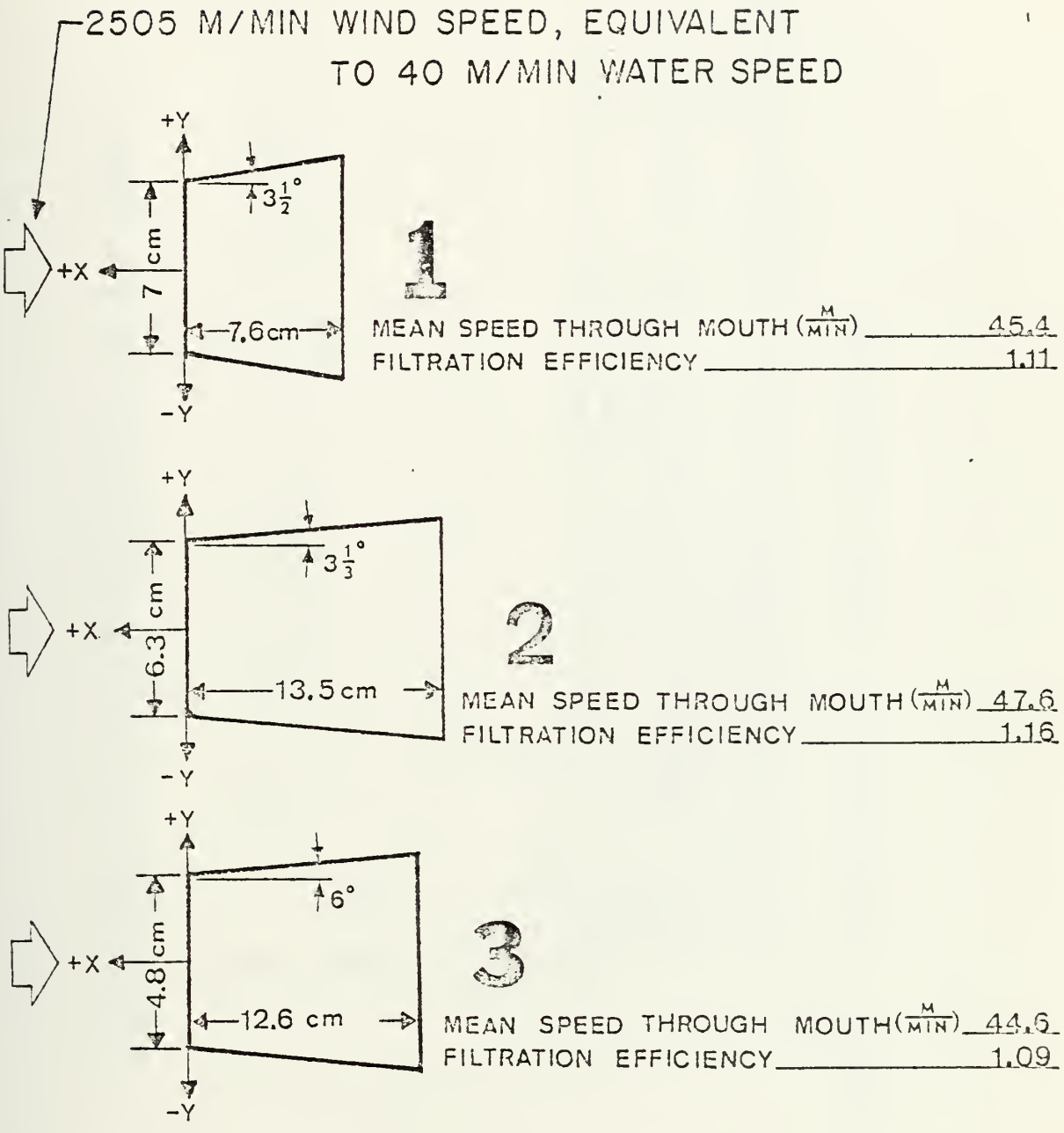

Figure 5. Mouth reduction nose cone models 1, 2 and 3.

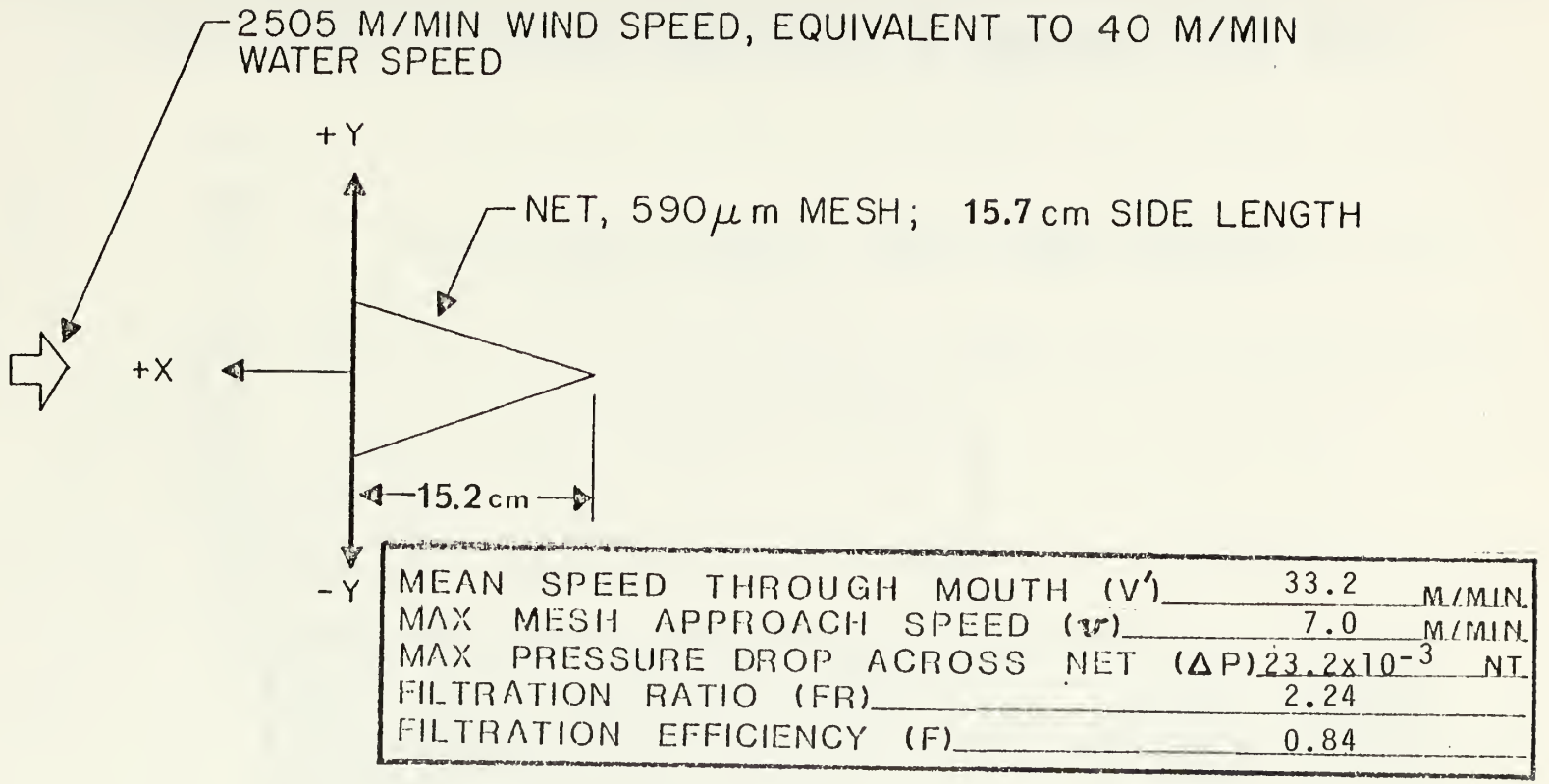

Figure 6. Sampler model A: simple conical net.

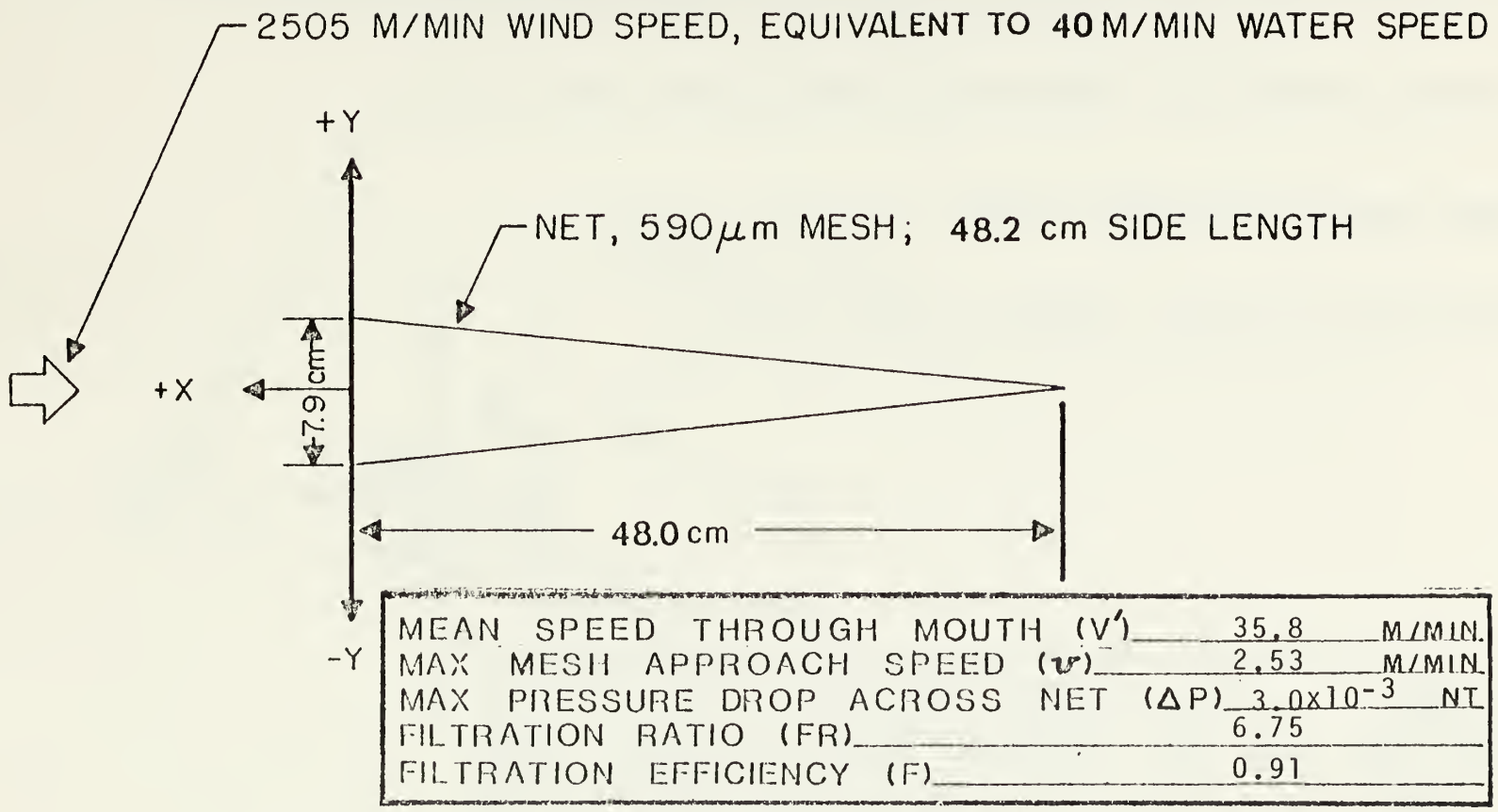

Figure 7. Sampler model B: simple conical net.

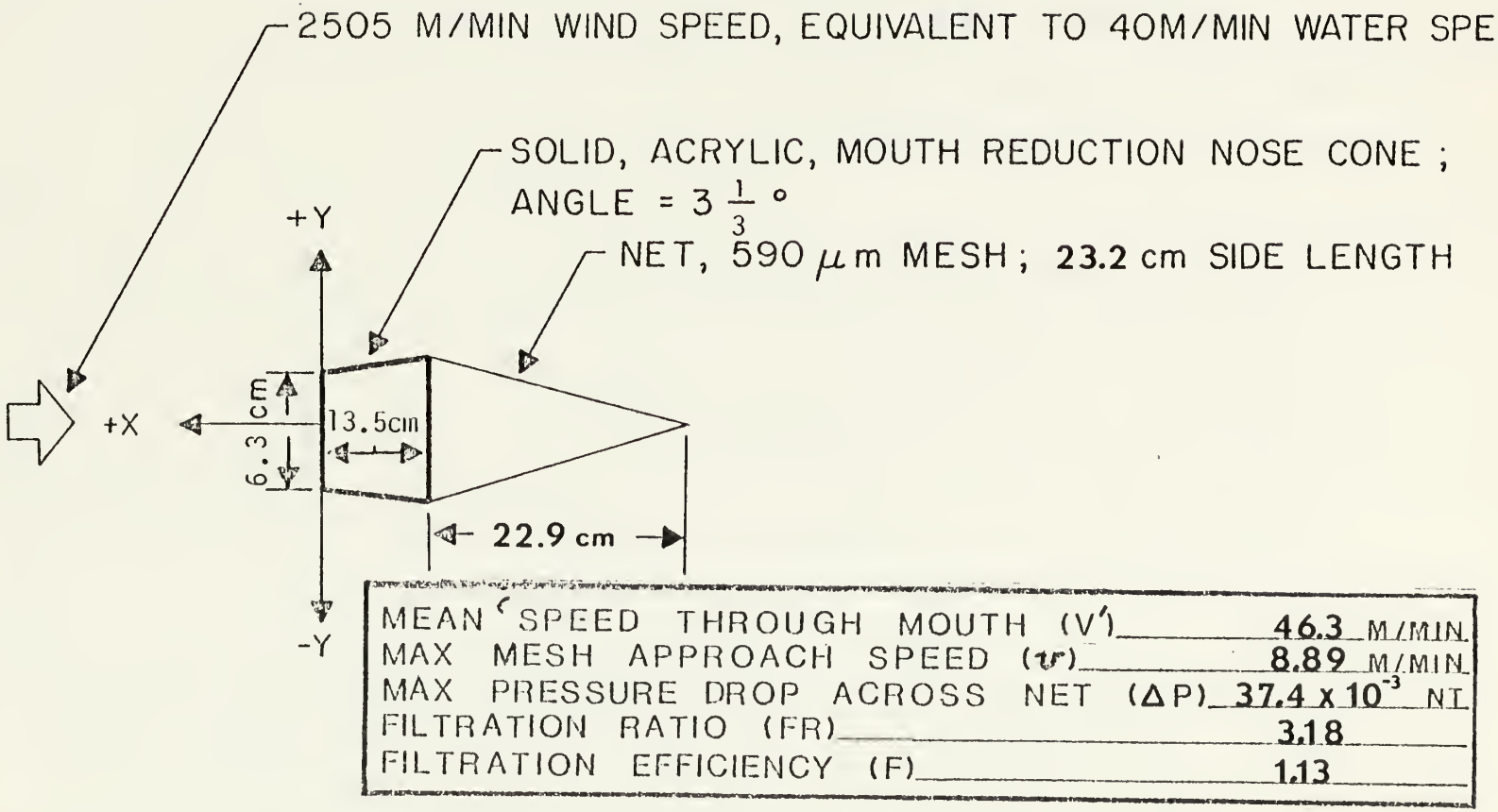

Figure 8. Sampler model C: nose cone model 2 and conical net.

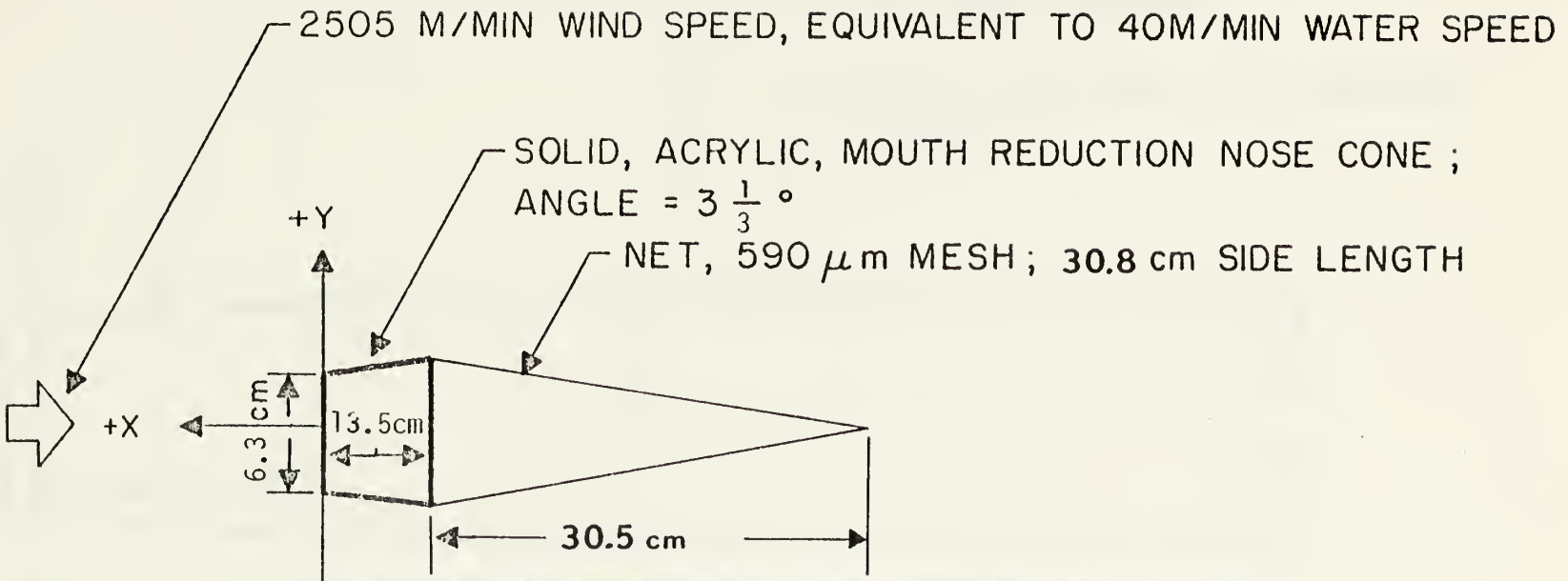

MEAN SPEED THROUGH MOUTH (V')	46.2 M/MIN.
MAX MESH APPROACH SPEED (v)	6.68 M/MIN.
MAX PRESSURE DROP ACROSS NET (ΔP)	21.1×10^{-3} NI.
FILTRATION RATIO (FR)	4.15
FILTRATION EFFICIENCY (F)	1.13

Figure 9. Sampler model D: nose cone model 2 and conical net.

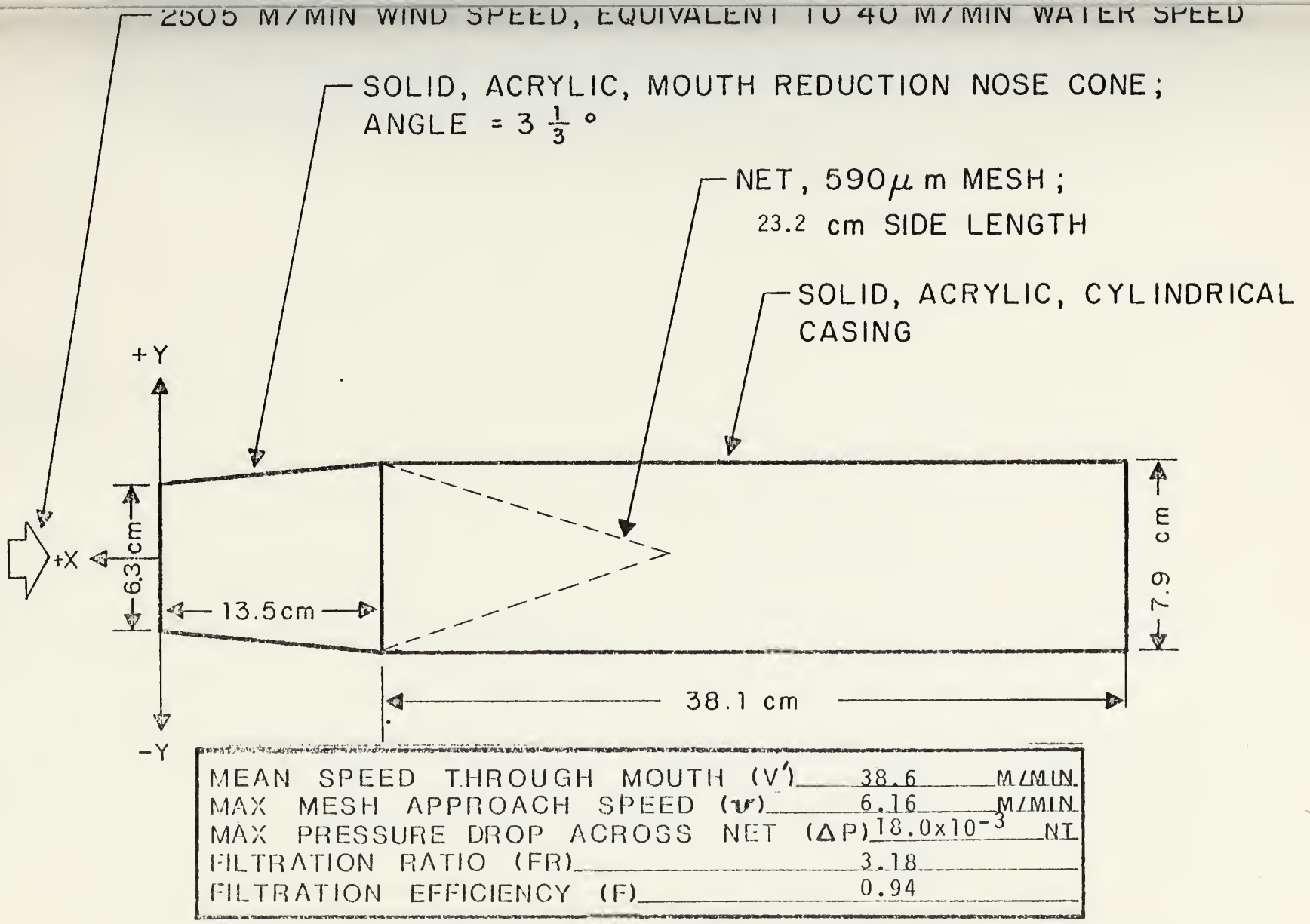

MEAN SPEED THROUGH MOUTH (V')	38.6	M/MIN.
MAX MESH APPROACH SPEED (v)	6.16	M/MIN.
MAX PRESSURE DROP ACROSS NET (ΔP)	18.0×10^{-3}	NI
FILTRATION RATIO (FR)	3.18	
FILTRATION EFFICIENCY (F)	0.94	

Figure 10. Sampler model E: nose cone model 2, conical net and casing.

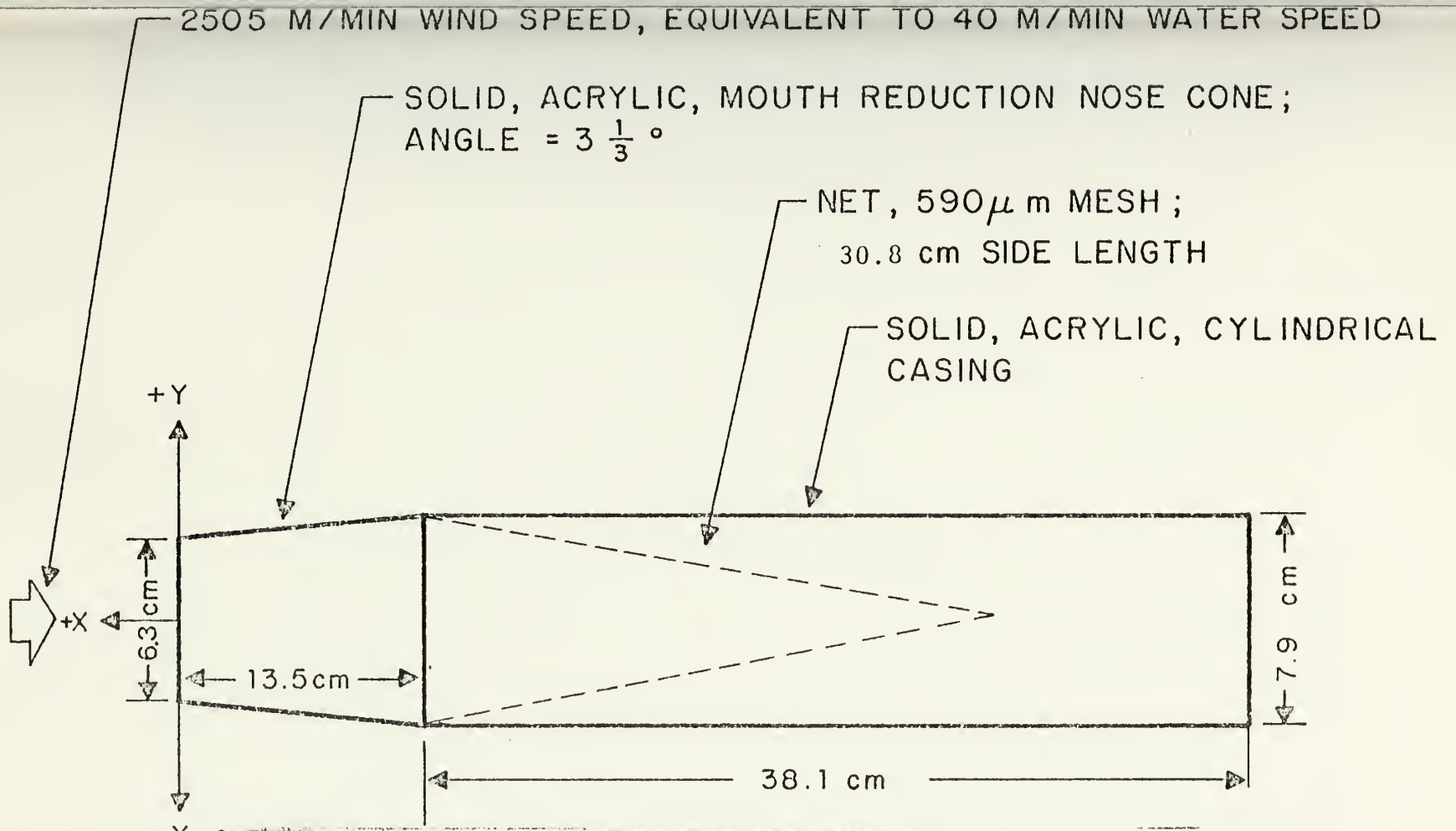

MEAN SPEED THROUGH MOUTH (V')	36.2	M/MIN.
MAX MESH APPROACH SPEED (v)	4.14	M/MIN.
MAX PRESSURE DROP ACROSS NET (ΔP)	8.1×10^{-3}	NT
FILTRATION RATIO (FR)	4.15	
FILTRATION EFFICIENCY (F)	0.88	

Figure 11. Sampler model F: nose cone model 2, conical net and casing.

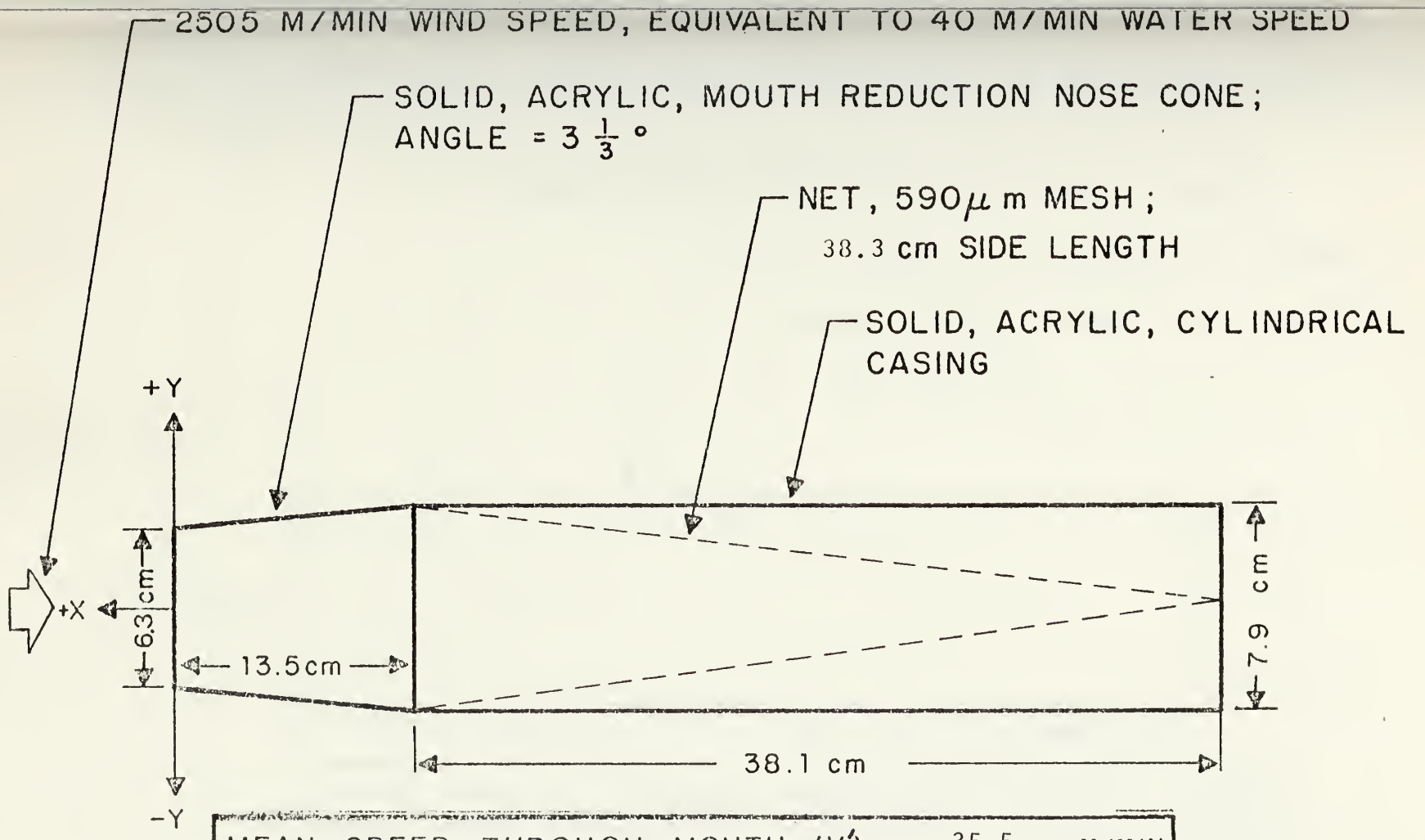

MEAN SPEED THROUGH MOUTH (V')	35.5	M/MIN.
MAX MESH APPROACH SPEED (v)	3.14	M/MIN.
MAX PRESSURE DROP ACROSS NET (ΔP)	4.7×10^{-3}	NT.
FILTRATION RATIO (FR)	5.4	
FILTRATION EFFICIENCY (F)	0.86	

Figure 12. Sampler model G: nose cone model 2, conical net and casing.

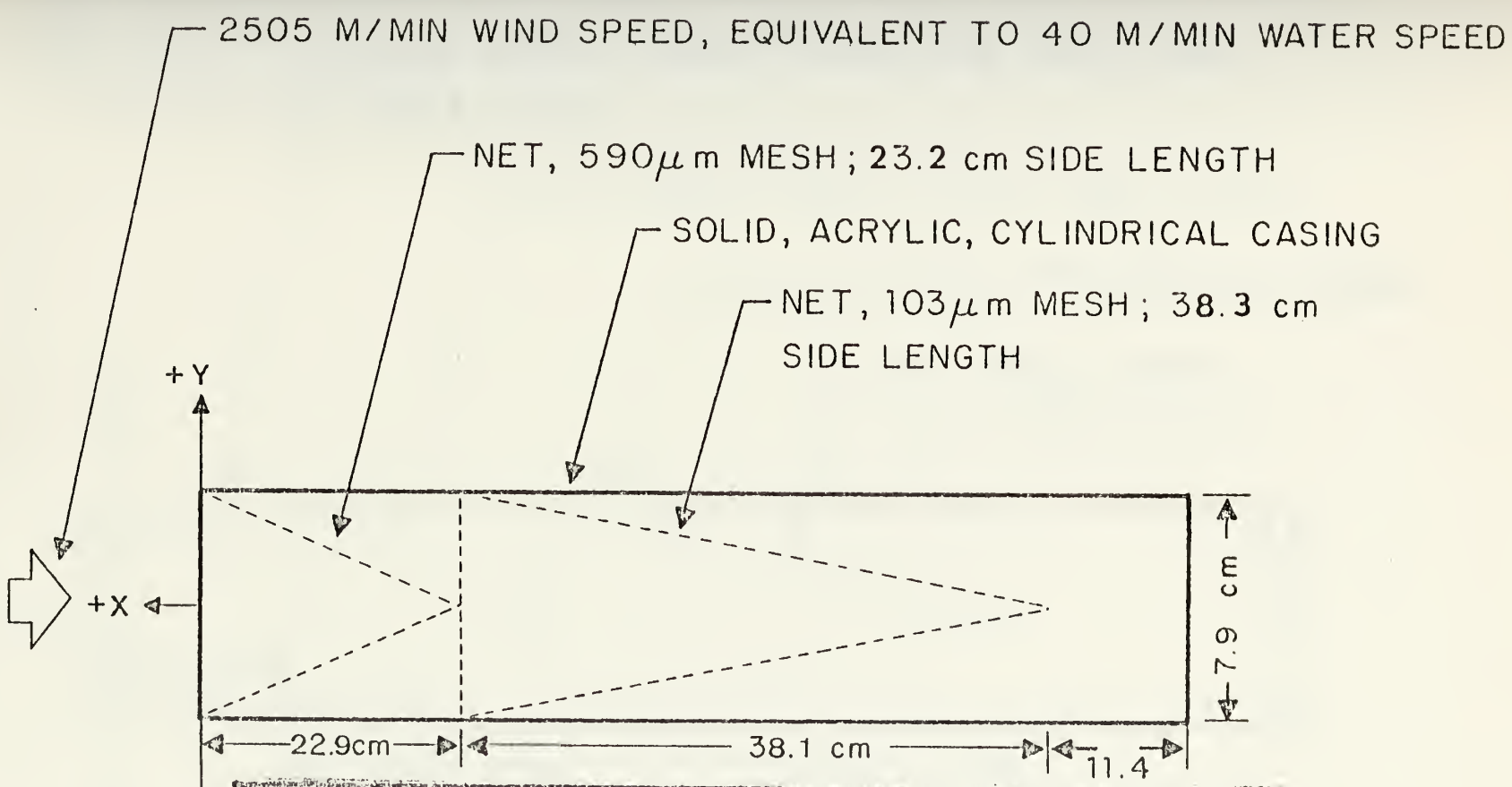

Figure 13. SSISNET sampler model H: two conical nets and casing.

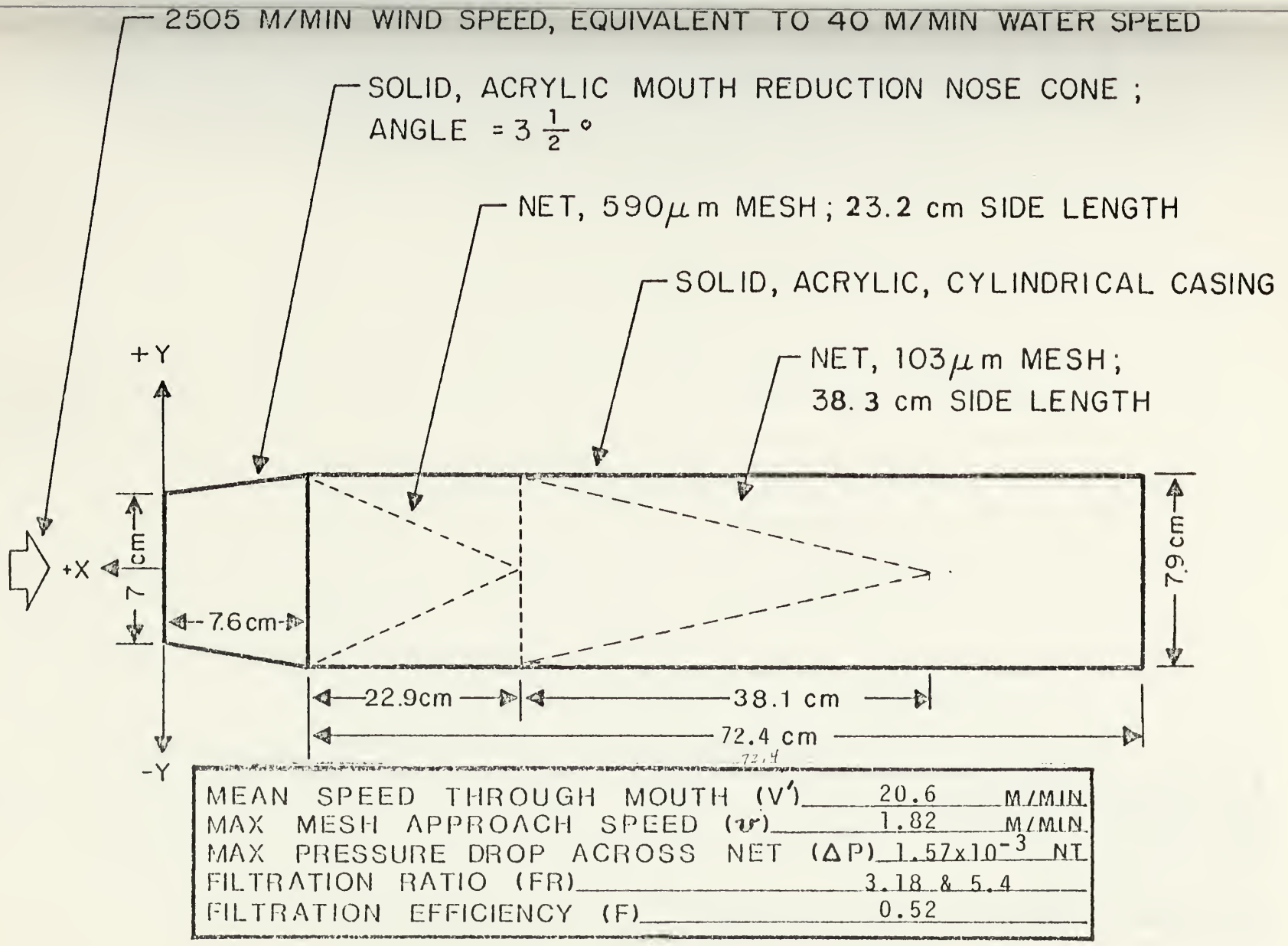

Figure 14. SSISNET sampler model I: nose cone model 1, two conical nets and casing.

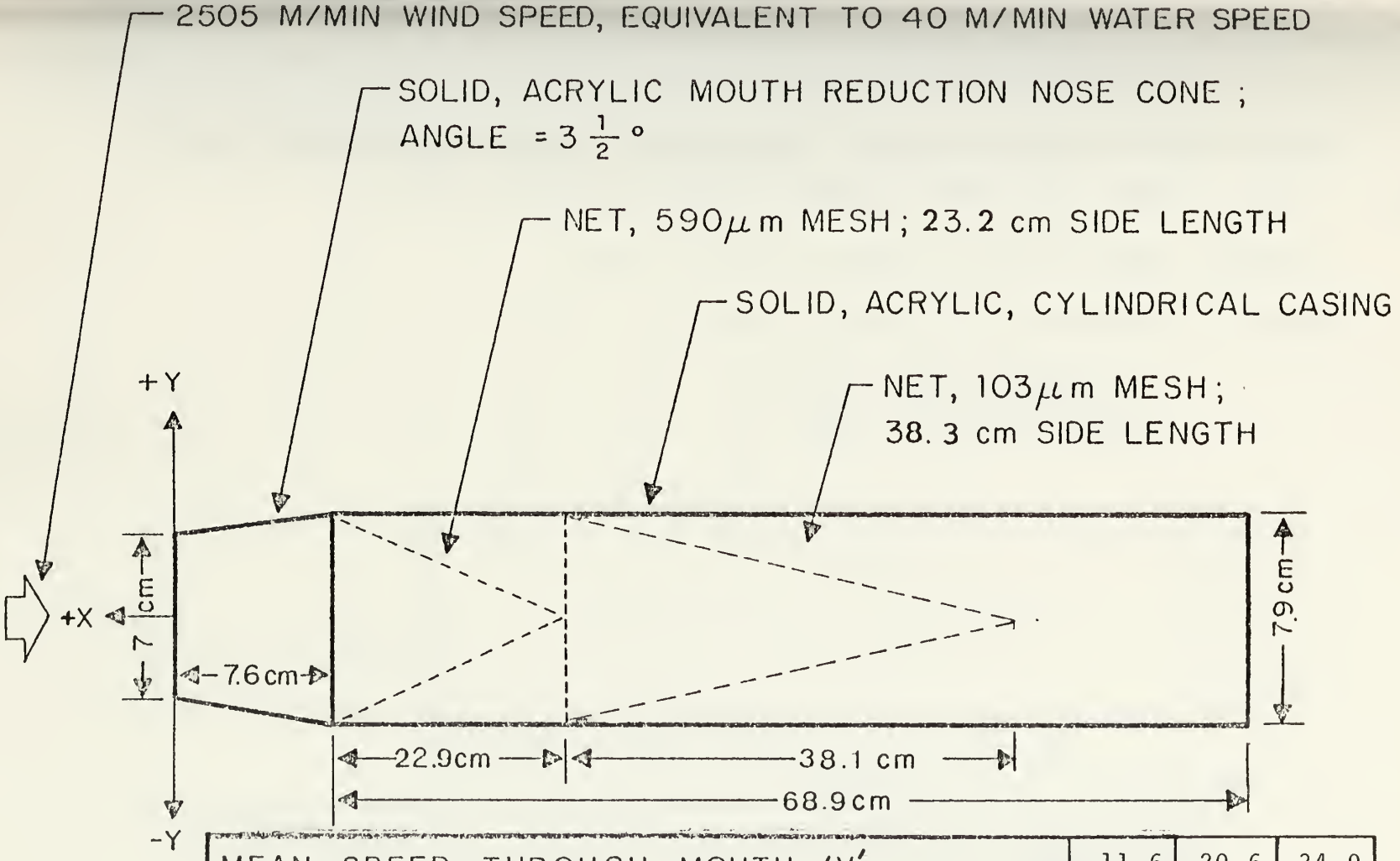

MEAN SPEED THROUGH MOUTH (V'	11.6	20.6	34.9
MAX MESH APPROACH SPEED (v	0.97	1.82	3.44
MAX PRESSURE DROP ACROSS NET (ΔP	0.44	1.57	5.60
FILTRATION RATIO (FR)	3.18 and 5.4		
FILTRATION EFFICIENCY (F)	0.49	0.52	0.58

Figure 15. SSISNET sampler model J: nose cone model 1, two conical nets and casing. Tests conducted at three different tow speeds: 23.7, 39.5 and 59.6 m/min.

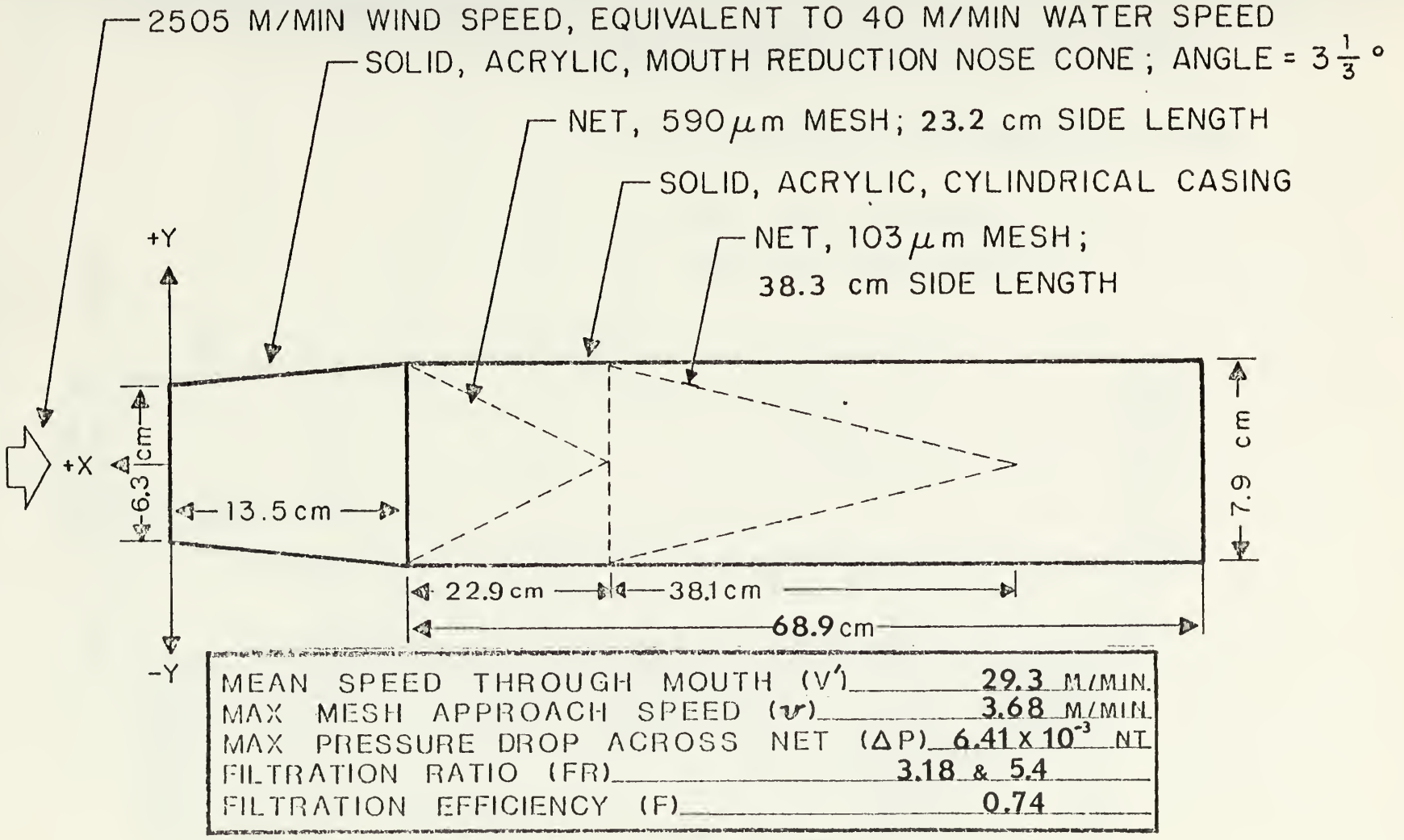

Figure 16. SSISNET sampler model K: nose cone model 2, two conical nets and casing.

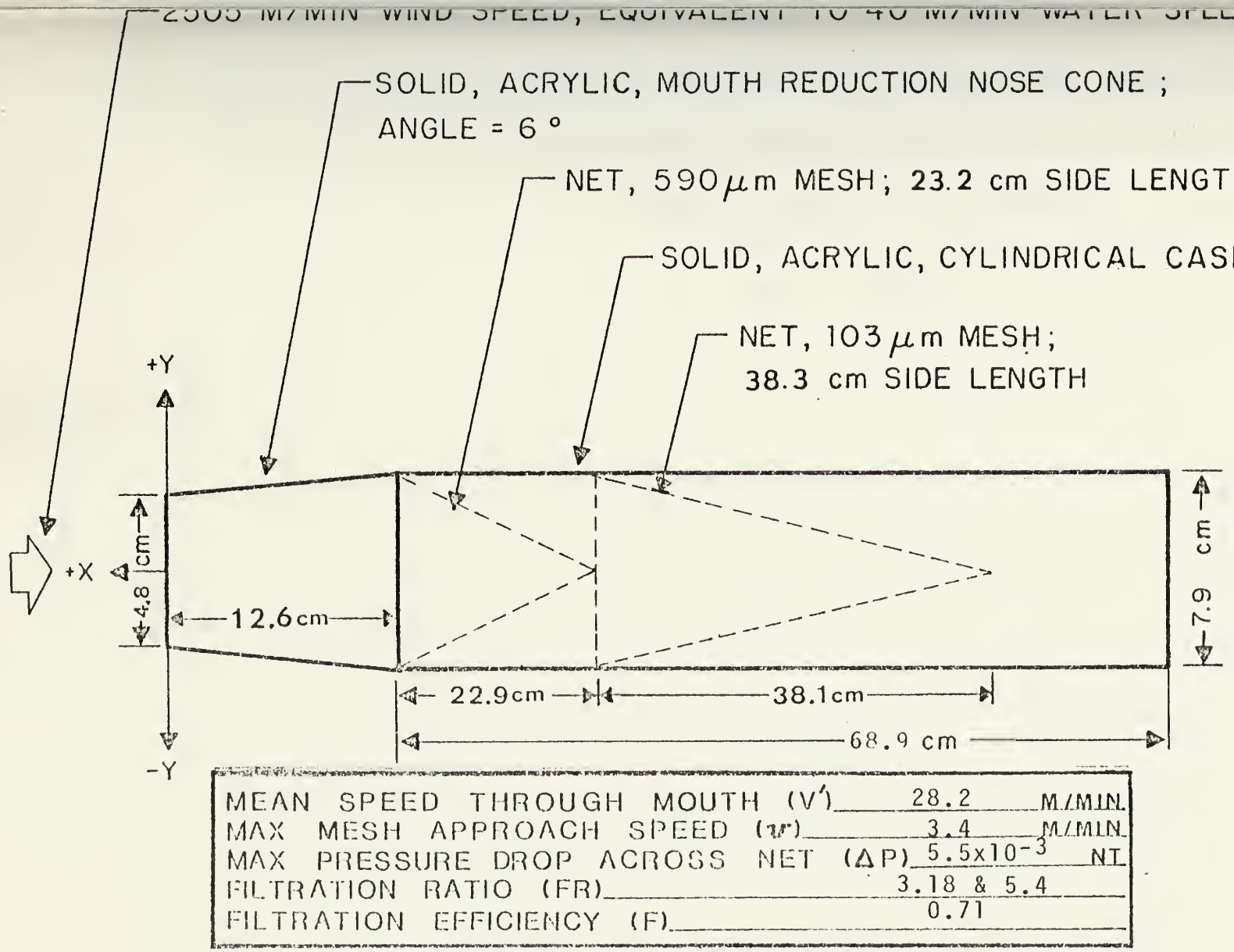

Figure 17. SSISNET sampler model L: nose cone model 3, two conical nets and casing.

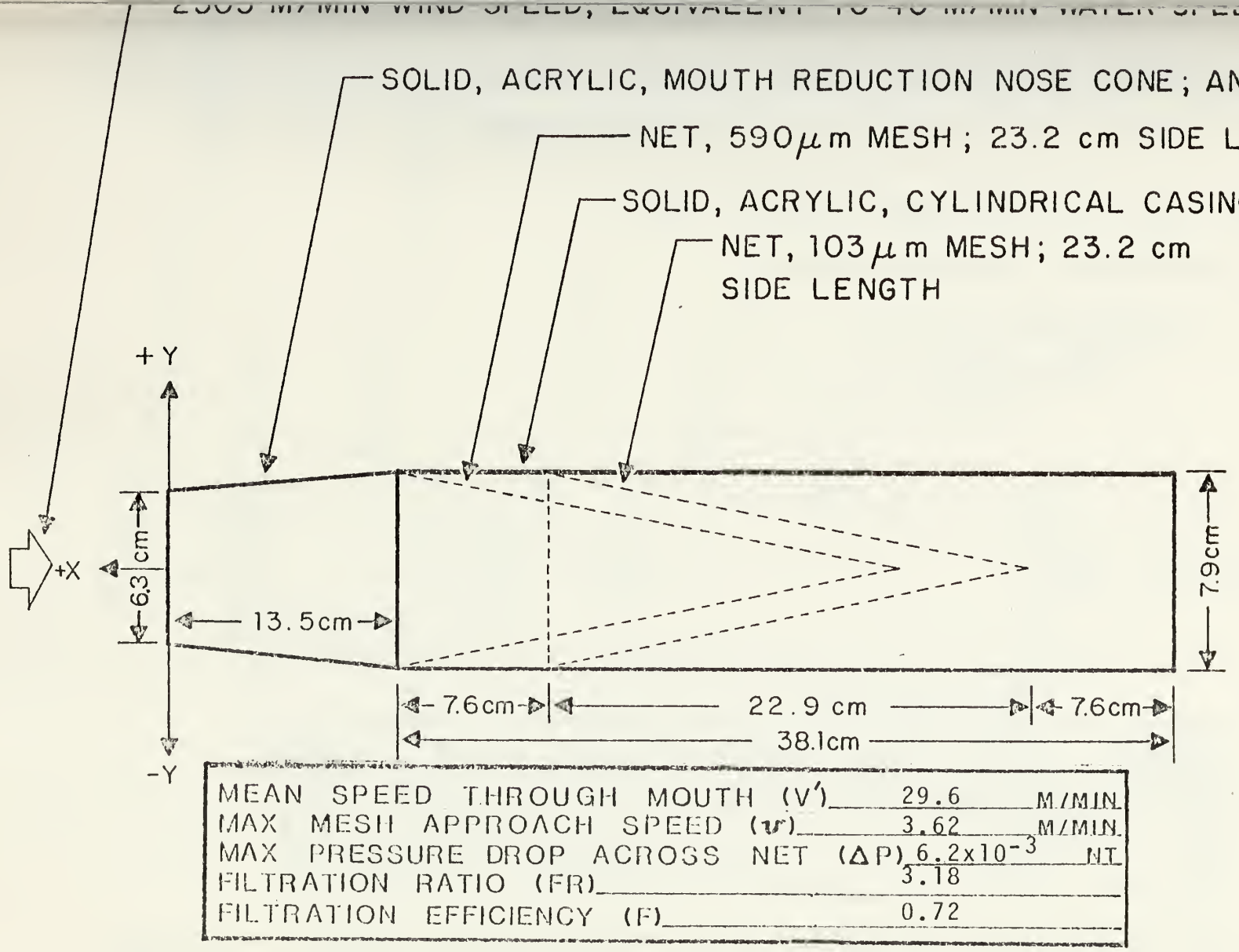

Figure 18. SSISNET sampler model M: nose cone model 2, two conical nets and casing.

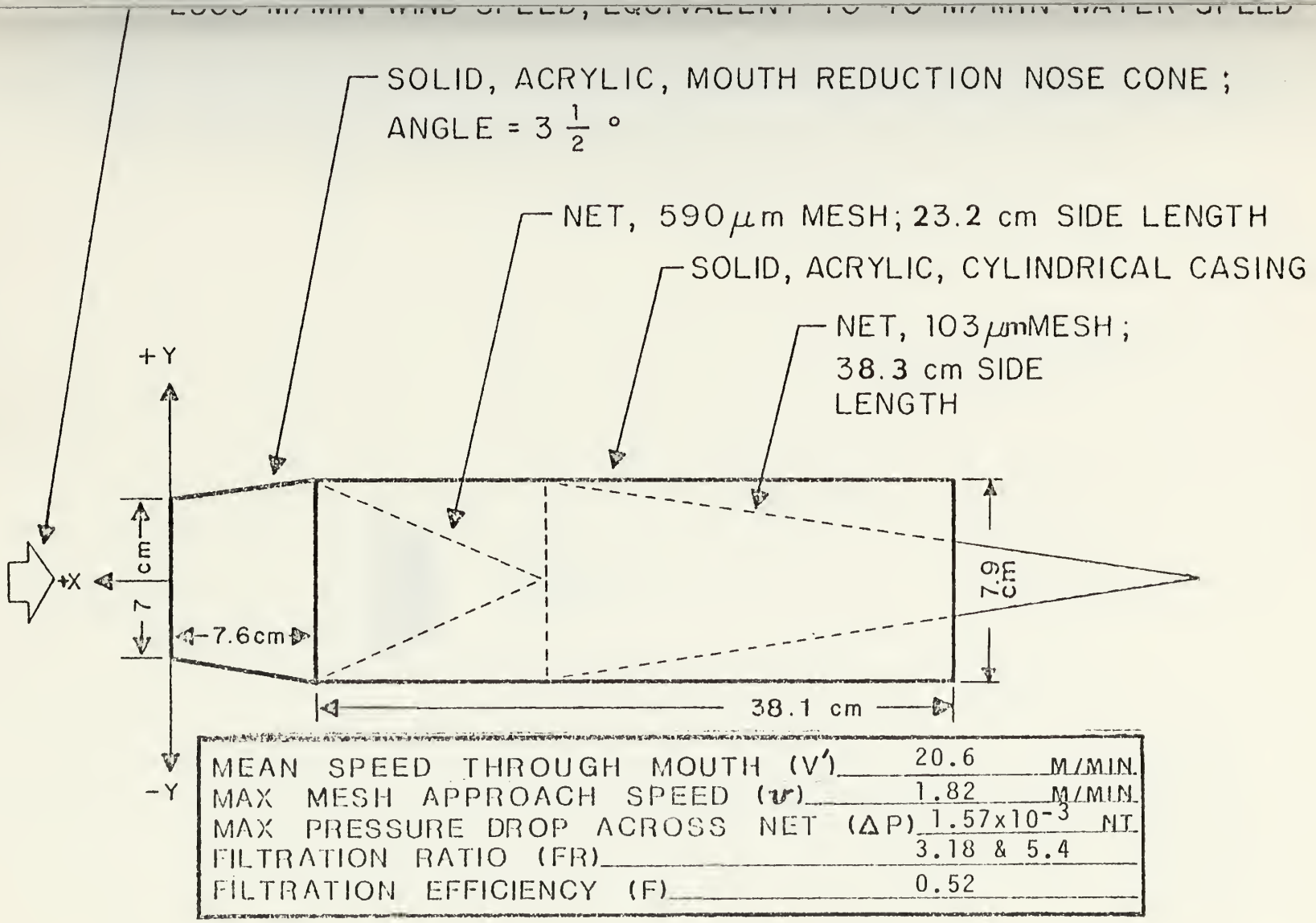

Figure 19. SSISNET sampler model N: nose cone model 1, two conical nets and casing.

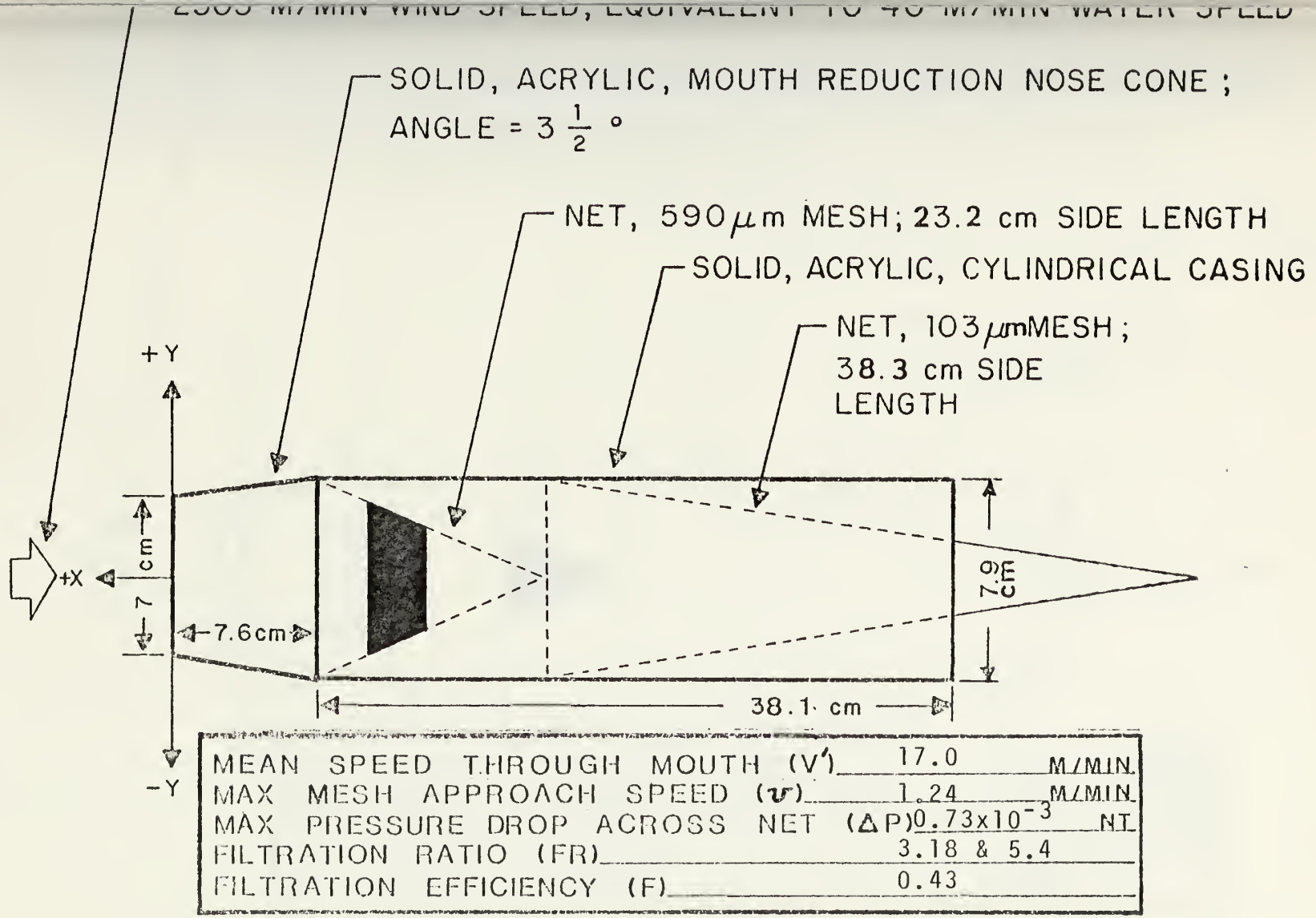

Figure 20. SSISNET sampler model 0: nose cone model 1, 590 μm conical net (one-third mesh area clogged), 103 μm conical net and casing.

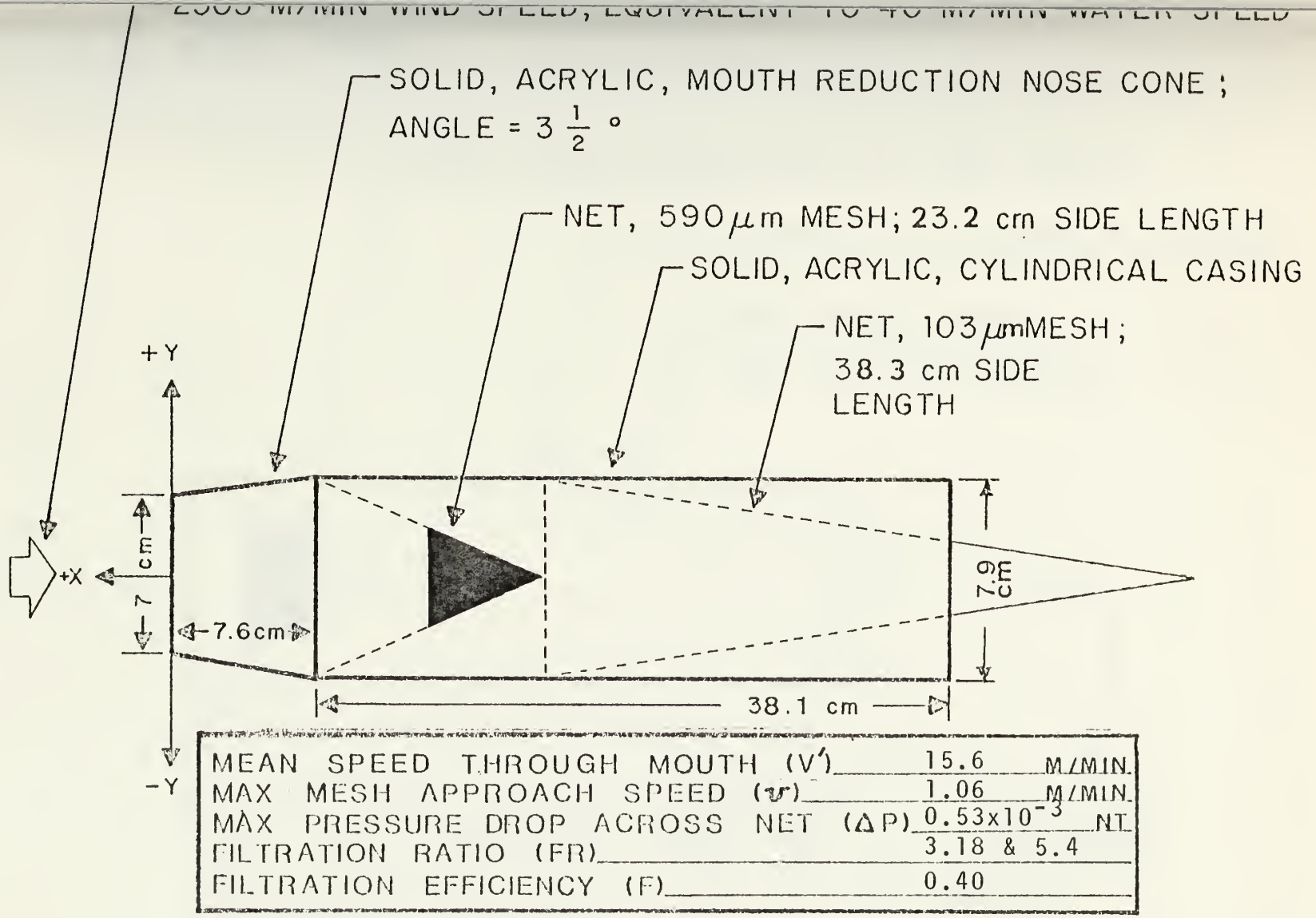

Figure 21. SSISNET sampler model P: nose cone model 1, 590 μm conical net (one-third mesh area clogged), 103 μm conical net and casing.

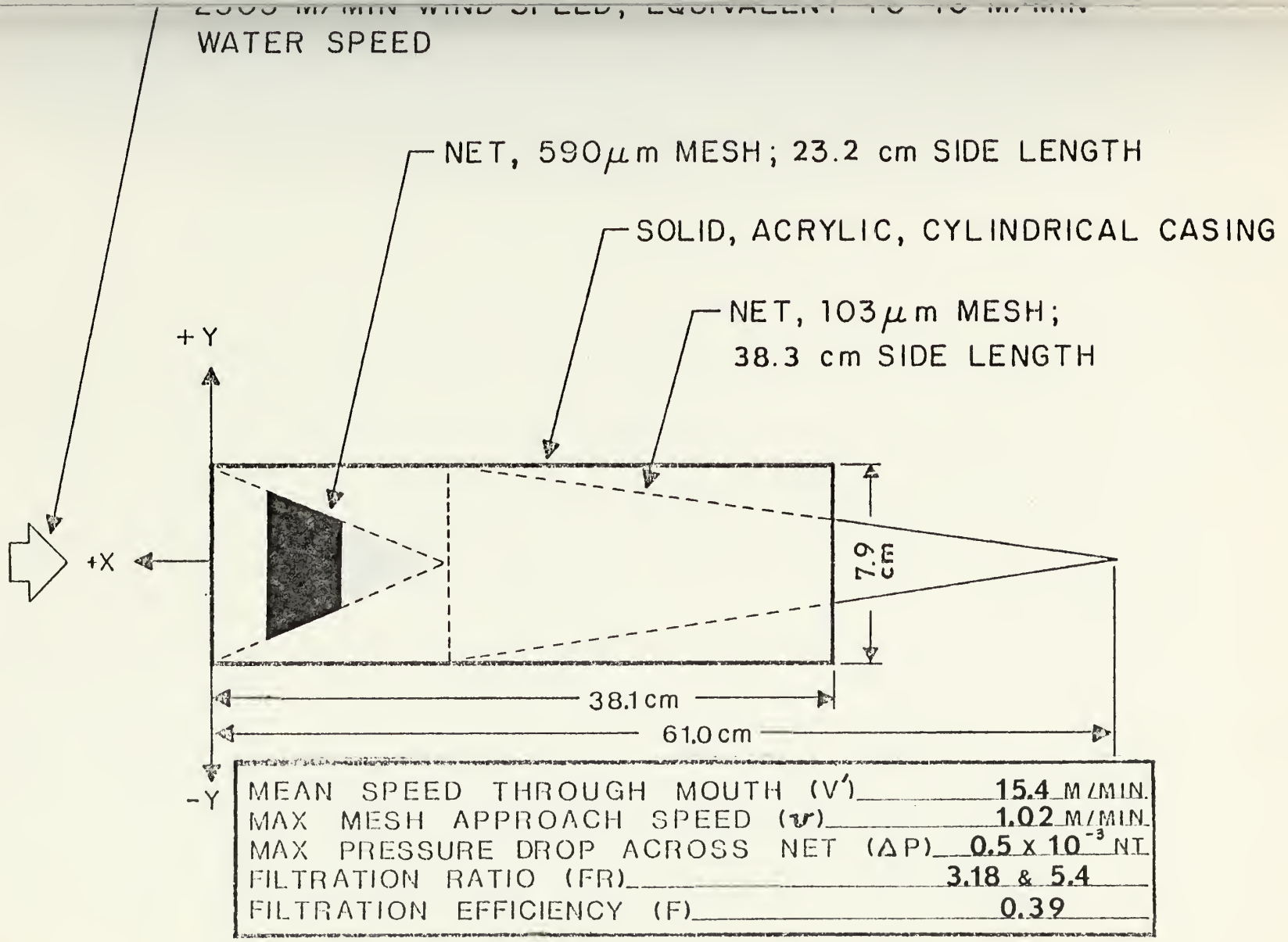

Figure 22. SSISNET sampler model Q: 590 μm conical net (one-third mesh area clogged), 103 μm conical net and casing.

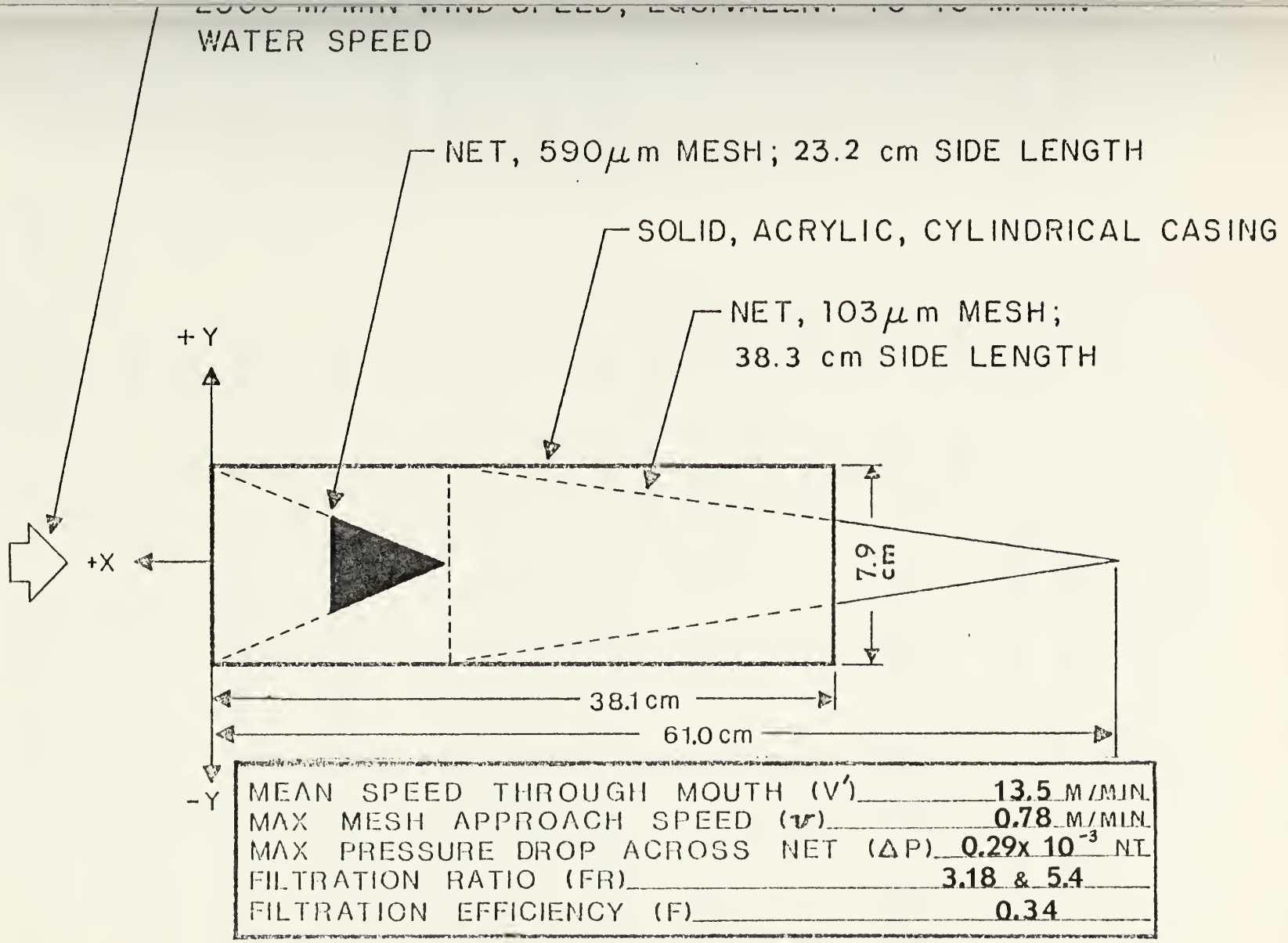

Figure 23. SSISNET sampler model R: 590 μm conical net (one-third mesh area clogged), 103 μm conical net and casing.

IV. TESTS

The effects of filtration efficiency, filtration pressure drop, net filtration ratio and mesh approach speed were investigated by varying the following sampler model parameters:

casing length

mouth reduction nose cone length and angle

speed of tow

number of nets

net mesh size

length of nets

clogging of nets

Each wind tunnel test, model description and corresponding figures and plates are listed below (data tabulated on figures are based upon prototype dimensions and water speed equivalences; the X-Y coordinate system is reference for the hot-wire anemometer probe positions):

1. Nose cone model 1 of 7.6 cm length and 3 1/2° angle (Figure 5 and Plate 6)
2. Nose cone model 2 of 13.5 cm length and 3 1/3° angle (Figure 5 and Plate 7)
3. Nose cone model 3 of 12.6 cm length and 6° angle (Figure 5 and Plate 8)
4. Sampler model A: 15.2 cm, 590 μm simple conical net (Figure 6)

5. Sampler model B: 48.0 cm, 590 µm simple conical net (Figure 7 and Plate 9)
6. Sampler model C: nose cone model 2 with 22.9 cm, 590 µm conical net attached (Figure 8 and Plate 10)
7. Sampler model D: nose cone model 2 with 30.5 cm, 590 µm conical net attached (Figure 9)
8. Sampler model E: nose cone model 2 with 22.9 cm, 590 µm conical net and 38.1 cm casing attached (Figure 10)
9. Sampler model F: nose cone model 2 with 30.5 cm, 590 µm conical net and 38.1 cm casing attached (Figure 11)
10. Sampler model G: nose cone model 2 with 38.1 cm, 590 µm conical net and 38.1 cm casing attached (Figure 12)
11. Sampler model H: 72.4 cm casing with a 22.9 cm, 590 µm conical net and a 38.1 cm, 103 µm conical net attached (Figure 13 and Plate 11)
12. Sampler model I: nose cone model 1 with a 22.9 cm, 590 µm conical net, a 38.1 cm, 103 µm conical net and a 72.4 cm casing attached (Figure 14)
13. Sampler model J: nose cone model 1 with a 22.9 cm, 590 µm conical net, a 38.1 cm, 103 µm conical net and a 68.9 cm casing attached (Figure 15 and Plate 12).
14. Sampler model K: nose cone model 2 with a 22.9 cm, 590 µm conical net, a 38.1 cm, 103 µm conical net and a 68.9 cm casing attached (Figure 16 and Plate 13)
15. Sampler model L: nose cone model 3 with a 22.9 cm, 590 µm conical net, a 38.1 cm, 103 µm conical net and a 68.9 cm casing attached (Figure 17 and Plate 14)

16. Sampler model M: nose cone model 2 with two 22.9 cm, 590 µm conical nets and a 38.1 cm casing attached (Figure 18)
17. Sampler model N: nose cone model 1 with a 22.9 cm, 590 µm conical net, a 38.1 cm, 103 µm conical net and a 38.1 cm casing attached (Figure 19)
18. Sampler model O: nose cone model 1 with a 22.9 cm, 590 µm conical net (one-third mesh area clogged between mouth and apex), a 38.1 cm, 103 µm conical net and a 38.1 cm casing attached (Figure 20)
19. Sampler model P: nose cone model 1 with a 22.9 cm, 590 µm conical net (one-third mesh area clogged at apex), a 38.1 cm, 103 µm conical net and a 38.1 cm casing attached (Figure 21)
20. Sampler model Q: 38.1 cm casing with a 22.9 cm, 590 µm conical net (one-third mesh area clogged between mouth and apex), a 38.1 cm, 103 µm conical net attached (Figure 22)
21. Sampler model R: 38.1 cm casing with a 22.9 cm, 590 µm conical net (one-third mesh area clogged at apex), a 38.1 cm, 103 µm conical net attached (Figure 23)

Figure 24 is a plot of all different sampler prototypes (vice models) with different combinations of mesh approach speed and pressure drop; the curve demonstrates that a slight increase in approach speed corresponds to a very drastic increase in pressure drop across the net. This large pressure variable is highly undesirable since the objective is to collect organisms that will be preserved by the sampler rather than possibly destroyed due to high pressure differential across the net.

The sampler prototypes at the lower end of the curve are those that were clogged (O, P, Q, R), illustrating the degradation in a system's performance as a result. Prototype H is a system with two nets and casing and has low speeds, pressure drop and filtration efficiency (0.37). Prototypes I, J and N are identical with the exception that the casing lengths are 2.9 m, 2.76 m and 1.52 m respectively, a factor that has no observed effect on any of the parameters; these three systems, however, utilized nose cone 1, which proves to be responsible for those systems' low filtration efficiencies (each were 0.52). A and B are simple conical nets of length 1.93 m and 0.60 m respectively. Prototypes E, F and G are all systems with reduction cone, casing and only one net (an undesirable feature).

Prototypes K, L and M are all systems with reduction cone, casing, and two nets; system K has the highest filtration efficiency (0.74) and it is located at a point just before the curve extends into the region of higher pressure drops.

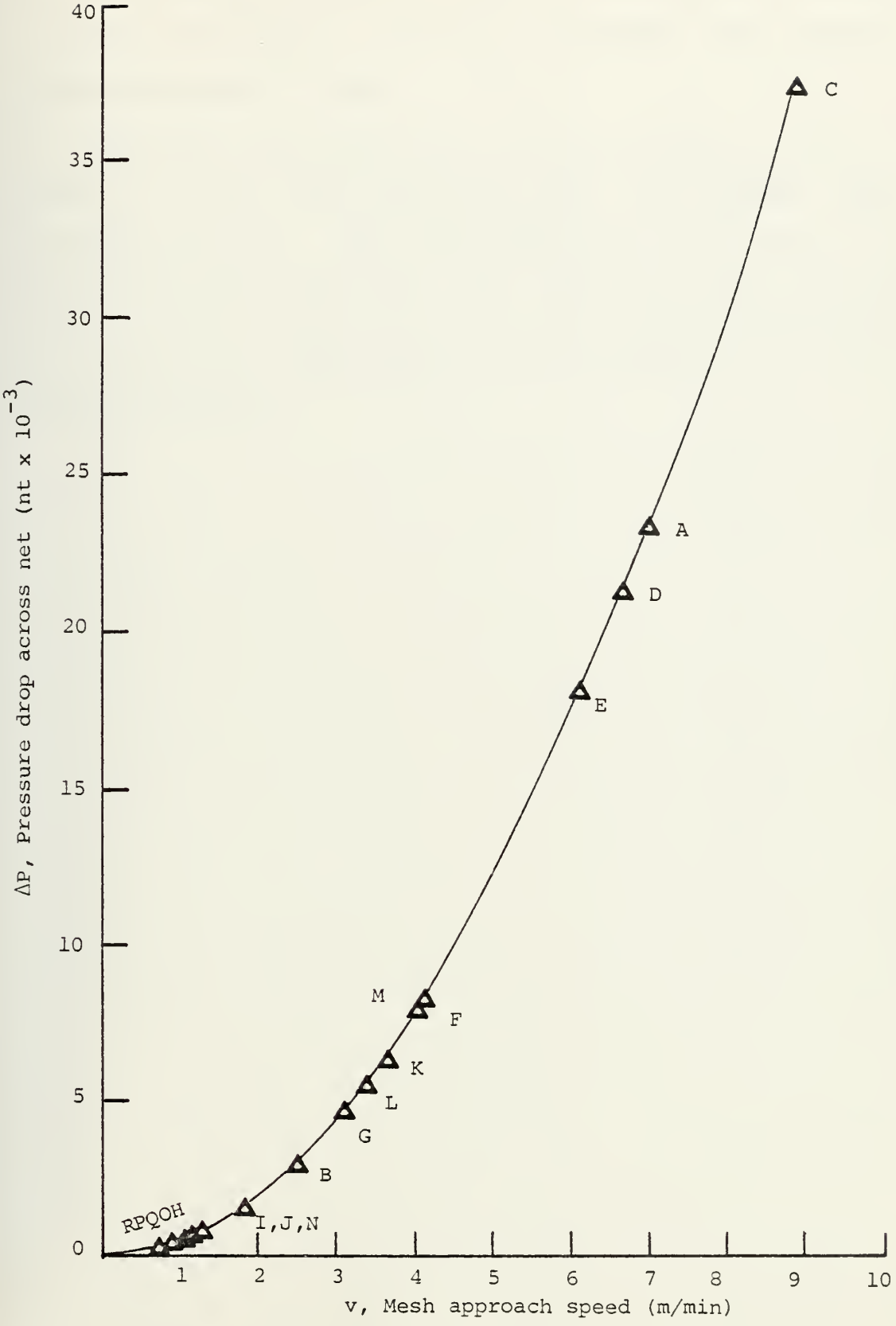

Figure 24. Pressure drop (ΔP) vs. mesh approach speed (v) for each sampling system prototype.

The two remaining systems (C and D) are those of a reduction cone and net assembly, which have extremely high approach speed and pressure drops.

Prototype K is clearly the optimum system. It has a relatively high filtration efficiency, low approach speed and pressure drop. Its casing houses two nets, both of which have area ratios below 0.2. The total length of the system can be varied by reducing the casing length provided the nets remain protected.

V. RESULTS

1. Figure 5 shows that the mouth reduction nose cone model 2 has a higher filtration efficiency than models 1 and 3.
2. Figures 6 and 7 show that an increase in the net length increases filtration ratio, and filtration efficiency but reduces the pressure drop across the net.
3. Figures 8 and 9 show that increasing net length when a nose cone is attached results in an increase in filtration ratio, no change in filtration efficiency and a decrease in pressure drop.
4. The reduction cones and net assemblies shown in Figures 10 and 11 have higher filtration efficiencies than the corresponding reduction cone, net and casing assemblies shown in Figures 11 and 12. However, the addition of the casing results in a much lower pressure drop.
5. The model shown in Figure 10 has a greater filtration efficiency than those shown in Figures 11 and 12; however clogging rapidly diminishes the filtration efficiencies of nets with lower filtration ratios.
6. The model shown in Figure 18 has a lower filtration efficiency than that shown in Figure 10 due to the additional net; however the pressure drop is reduced.
7. The net and casing assembly shown in Figure 13 has a lower filtration efficiency than the same assembly with a mouth reduction nose cone attached as shown in Figure 14.

8. Figures 15, 16 and 17 show that the net and casing assembly with the reduction cone model 2 attached has a higher filtration efficiency than with either cone model 1 or 3 attached.
9. Figure 15 shows that an increase in tow speed increases filtration efficiency; however the increase is not a proportional one. An increase in tow speed from 23.7 m/min to 59.6 m/min resulted in an increase of filtration efficiency of only .09.
10. Figures 15 and 19 show that decreasing the model casing length from 68.9 cm to 38.1 cm has no effect on filtration efficiency.
11. A comparison of Figures 20, 21, 22 and 23 with Figure 19 shows that net clogging results in a lower filtration efficiency. Furthermore, if clogging is concentrated at the apex of the nets the result is a lower filtration efficiency than if the same percentage of clogging occurred nearer the mouth of the nets.

VI. DISCUSSION

A plankton collection device has been designed and tested that is a combination of relatively optimum physical characteristics, including a high filtration efficiency (0.74), a low filtration pressure drop (6.41×10^{-3} nt), high net filtration ratios (3.18 and 5.40) and a low maximum mesh approach speed (3.68 m/min).

The research was initiated by investigating these physical properties associated with the basic conical plankton net and was completed with the study of complex sampling systems. A simple conical net has a filtration efficiency less than 1.0; however with the attachment of a mouth reduction nose cone this figure was increased to greater than 1.0. The nose cone model that was found to result in the highest filtration efficiency was one of 13.5 cm in length with an angle of expansion of 3 1/3°. According to Pankhurst and Holder (1952) the best results are obtained by using a cone with an angle less than 3 1/2°.

The length of the nose cone, nets and casing were restricted so the scaled-up prototype would be of suitable size. Tranter (1968) points out that the filtration efficiency of a net decreases rapidly beyond an area ratio (A/a) of 0.2, which converts into a net minimum side length (for the model) of 19.5 cm or 78 cm for the prototype. Increasing the net length beyond this value increases the filtration

efficiency and reduces clogging; however, physical restraints have to be imposed due to handling, stowage and weight problems. In the optimum model net, side lengths of 22.9 cm and 38.1 cm were used for the 590 μm and 103 μm nets respectively. So that a size sampling *in situ* net (SSISNET) system could be realized, two nets had to be utilized in series. The mesh size of the front net would be such that all larger plankton would be collected there but the desired sized plankton would pass through and be collected by the rear net for removal and analysis. No more than two nets were tested because the system becomes cumbersome; a system that utilizes more than two nets increases resistance to flow (back pressure) and thus leads to a reduction in filtration efficiency.

Aside from the fact that a casing was needed to house the two nets, the casing was found to have several desirable effects on the overall performance of the system, although it did cause a reduction in filtration efficiency. The casing protects the catch and nets and minimizes turbulence; it lends hydrodynamic stability to the system, a factor that could perhaps be further conveniently improved with the addition of fins. The casing also causes a lower pressure drop across the nets. Thus, sampler model K, the encased net system shown in Figure 16 was chosen because it had the most desirable combination of characteristics, i.e. a high filtration efficiency (0.74), high filtration ratios (3.18 and 5.40), and a mesh approach speed that results in a low pressure differential across the nets (6.41×10^{-3} nt).

A P P E N D I X

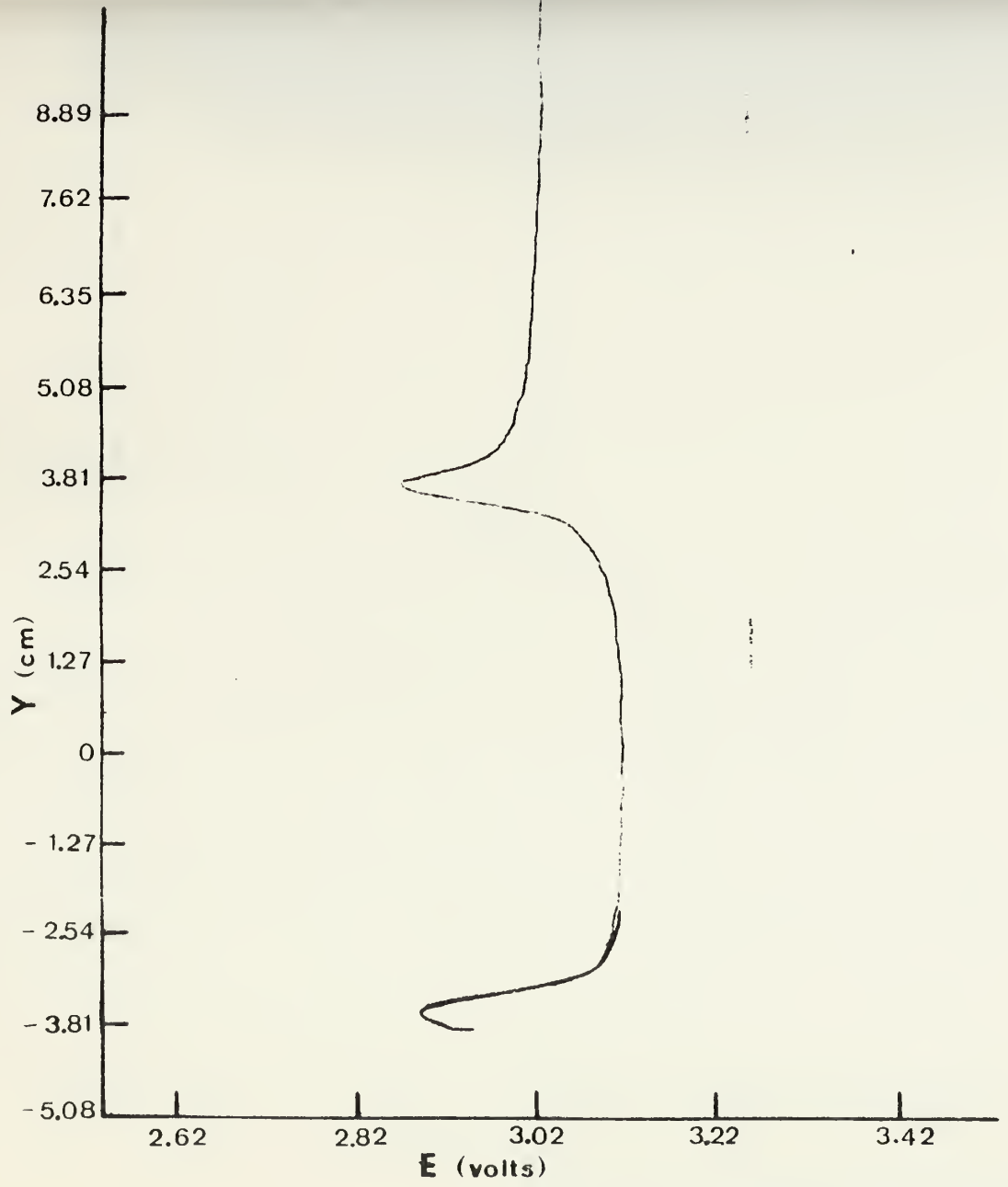

X = 0+ (at mouth of cone)

Y (cm)	V (m/min)	E (volts)
10.16	40.9	3.02
7.62	40.9	3.02
5.08	40.0	3.01
4.45	38.5	2.99
3.81	33.3	2.92
3.68	29.6	2.87
3.18	42.7	3.04
2.54	47.0	3.09
1.91	49.0	3.11
1.27	50.0	3.12
.635	50.0	3.12
0	50.0	3.12
- .635	50.0	3.12
-1.27	50.0	3.12
-1.91	49.0	3.11
-2.54	47.3	3.10
-3.18	44.5	3.06
-3.68	31.7	2.90

$V' =$ 45.4 m/min

Profile A. Mouth reduction nose cone model 1.

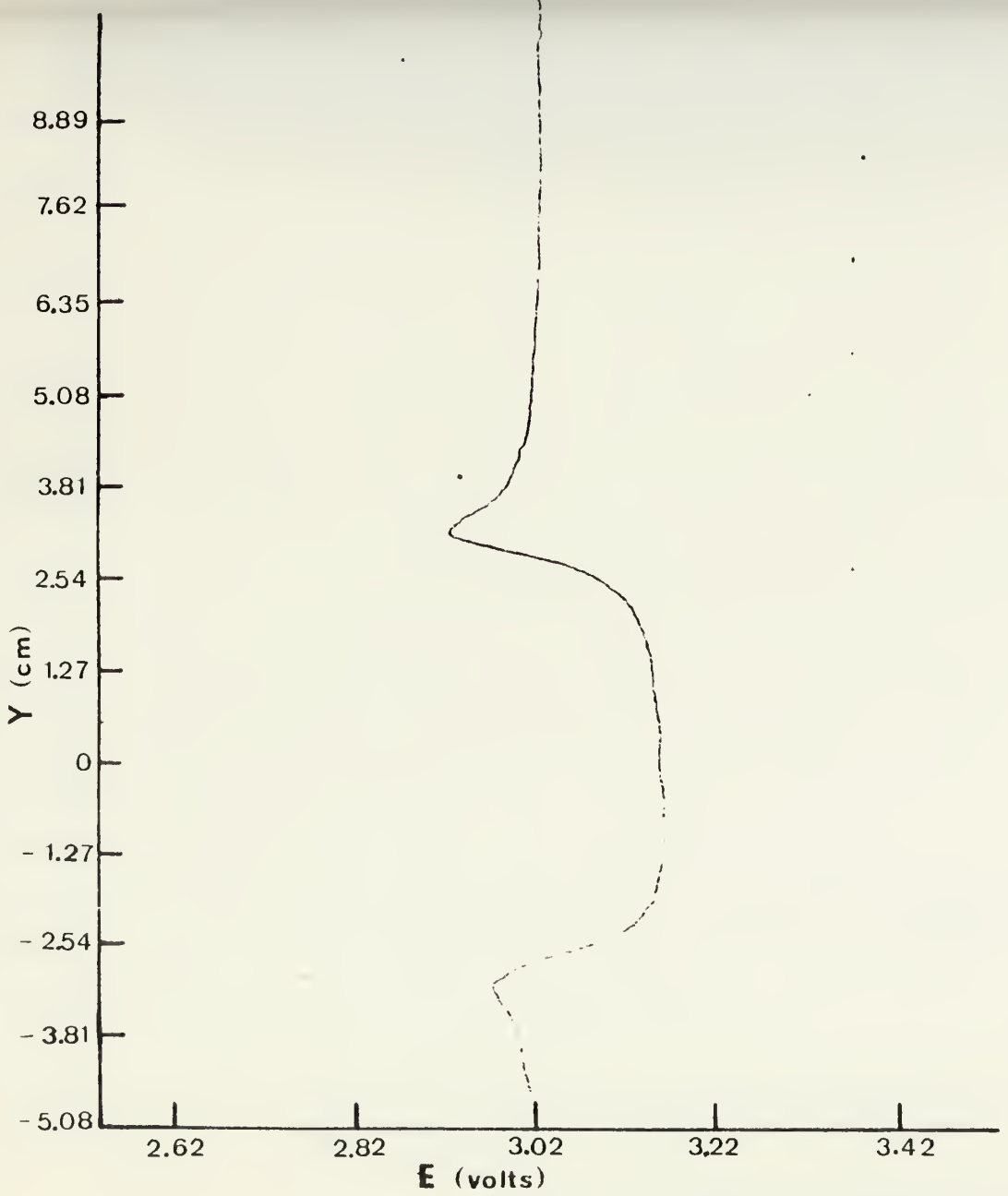

$X = 0^+$ (at mouth of cone)

Y (cm)	V (m/min)	E (volts)
10.16	40.9	3.02
6.35	40.9	3.02
4.45	40.0	3.01
3.81	37.7	2.98
3.18	33.3	2.92
2.54	45.3	3.07
1.91	50.0	3.12
1.27	52.0	3.14
.635	52.0	3.14
0	53.0	3.15
- .635	53.0	3.15
-1.27	53.0	3.15
-1.91	52.0	3.14
-2.54	43.5	3.05
-3.18	36.3	2.96
-3.81	38.0	2.99

$V' =$ 47.6 m/min

Profile B. Mouth reduction nose cone model 2.

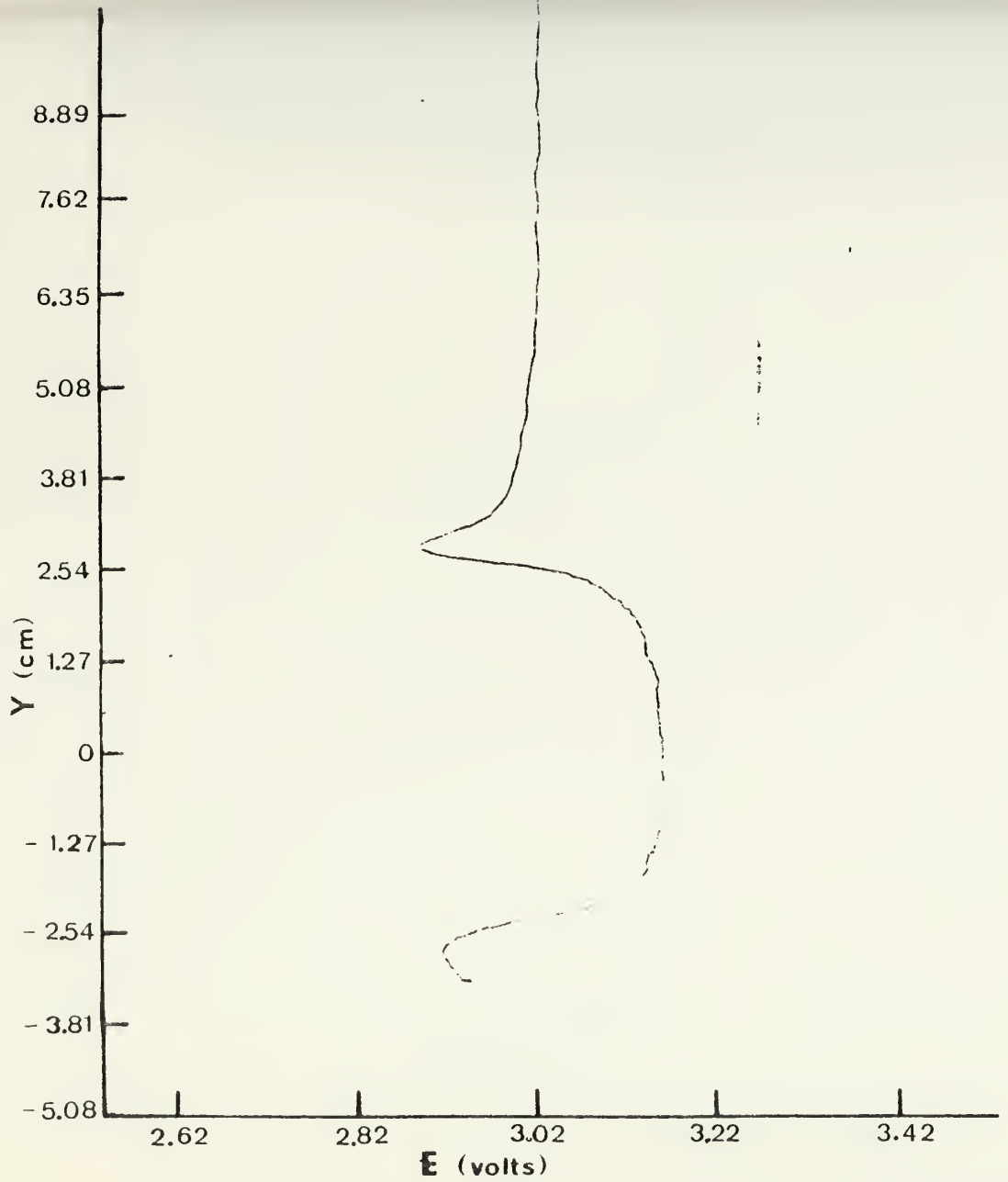

X = 0+ (at mouth of cone)

Y (cm)	V (m/min)	E (volts)
10.16	40.9	3.02
8.30	40.9	3.02
5.70	40.0	3.01
4.45	39.2	3.00
3.81	38.5	2.99
3.18	35.5	2.95
2.79	30.1	2.88
2.54	38.5	2.99
1.91	49.0	3.11
1.27	51.0	3.13
.635	52.0	3.14
0	52.0	3.14
- .635	52.0	3.14
-1.27	51.0	3.13
-1.91	50.0	3.12
-2.54	34.0	2.93
-2.79	31.7	2.90
-3.18	33.3	2.92

$V' =$ 44.6 m/min

Profile C. Mouth reduction nose cone model 3.

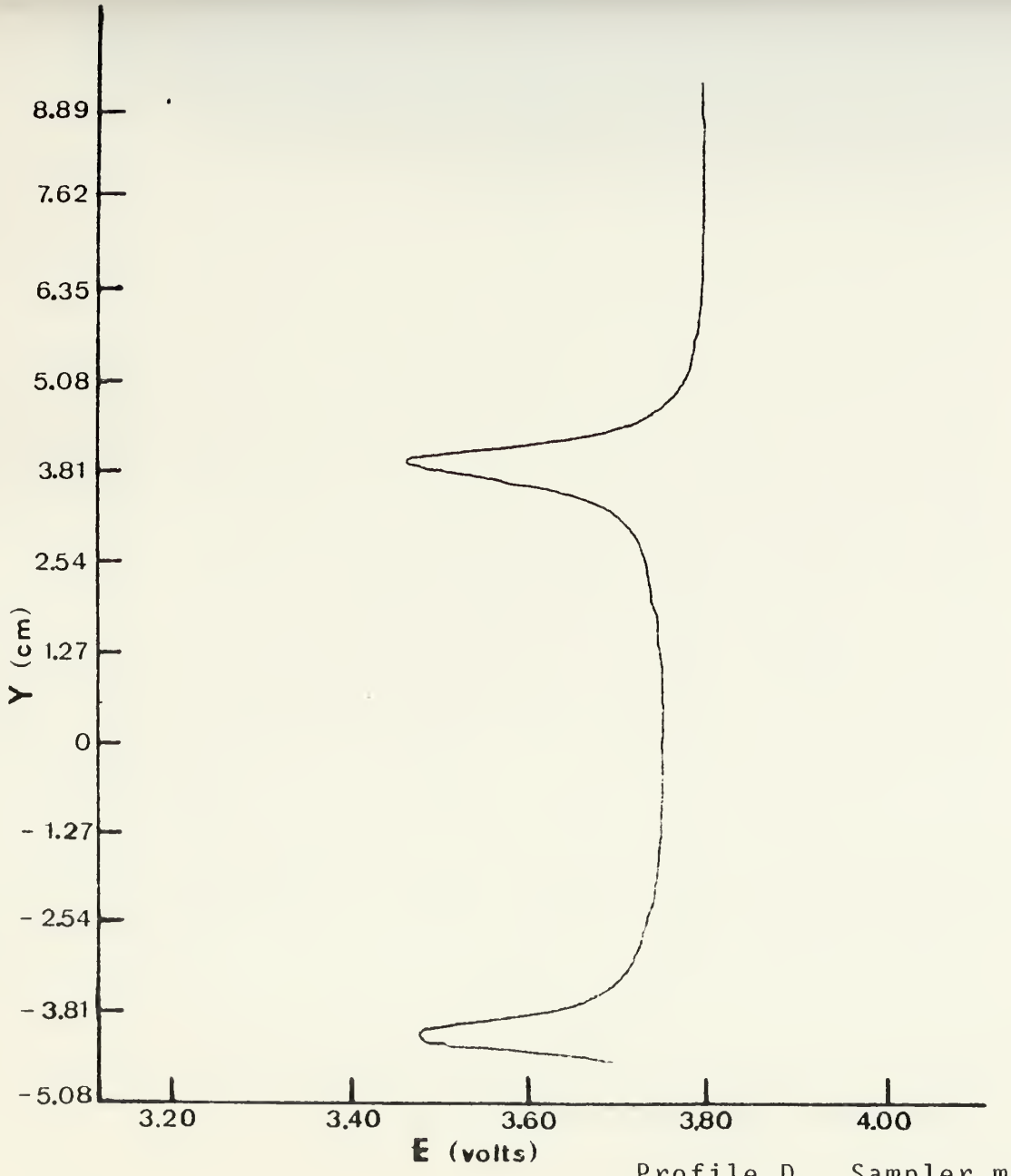

X=0+ (at mouth of sampler)

Y (cm)	V (m/min)	E (volts)
7.62	39.5	3.8
6.35	39.5	3.8
5.72	39.5	3.8
5.08	38.5	3.78
4.45	34.0	3.71
3.94	21.2	3.47
3.81	23.0	3.51
3.18	34.5	3.72
2.54	36.4	3.75
1.91	37.0	3.76
1.27	37.7	3.77
.635	37.7	3.77
0	37.7	3.77
- .635	37.7	3.77
-1.27	37.7	3.77
-1.91	37.0	3.76
-2.54	36.4	3.75
-3.18	35.1	3.73
-3.81	27.1	3.59
-3.94	22.1	3.49
-4.45	32.7	3.69
-5.08	38.5	3.78

V′= 33.2 m/min

Profile D. Sampler model A.

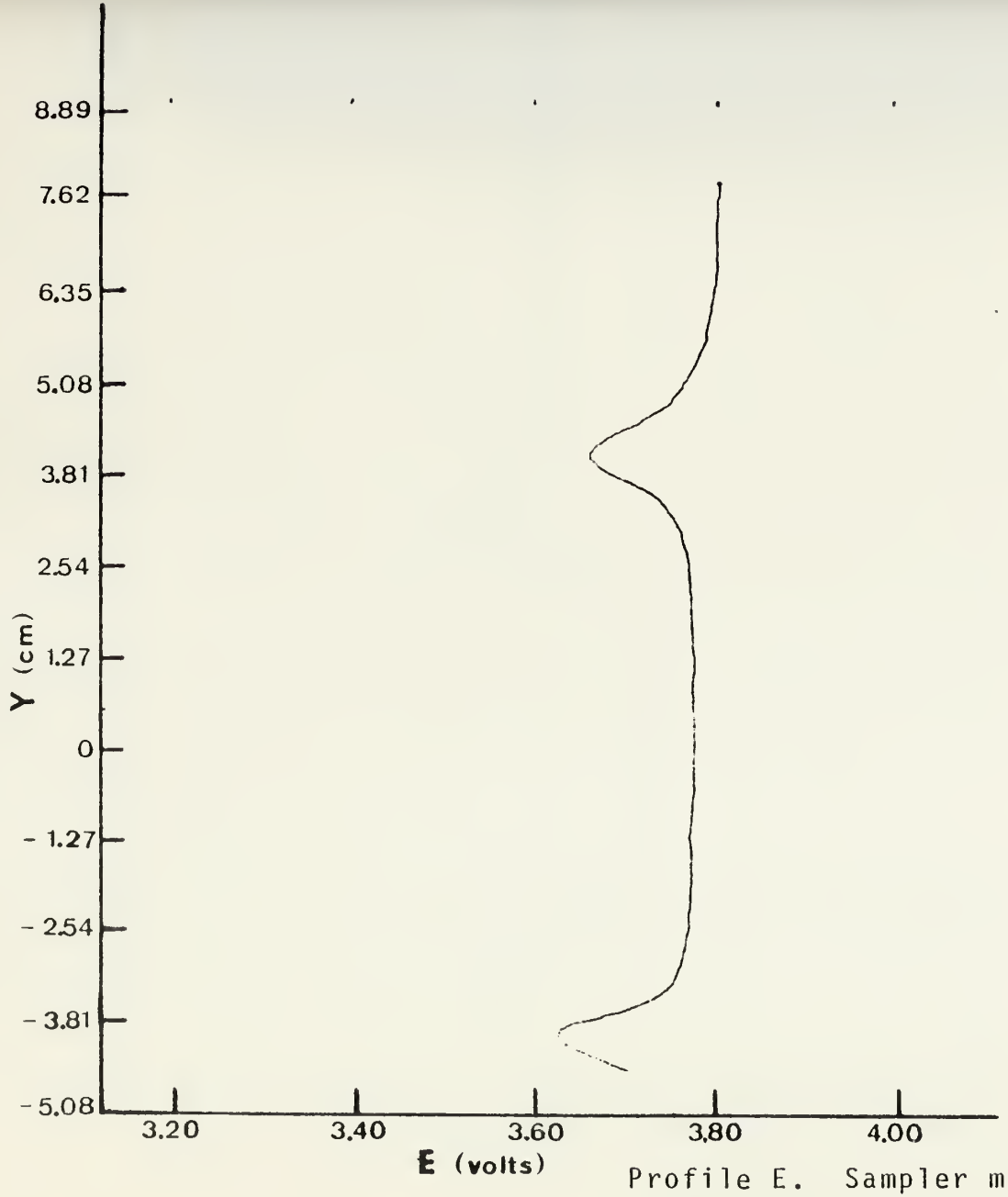

$X = 0^+$ (at mouth of sampler)

Y (cm)	V (m/min)	E (volts)
7.62	39.5	3.8
6.99	39.5	3.8
6.35	39.0	3.79
5.72	39.0	3.79
5.08	38.5	3.78
4.45	35.1	3.73
3.94	31.0	3.66
3.81	31.6	3.67
3.18	36.4	3.75
2.54	37.0	3.76
1.91	37.7	3.77
1.27	37.7	3.77
.635	37.7	3.77
0	37.7	3.77
- .635	37.7	3.77
-1.27	37.7	3.77
-1.91	37.7	3.77
-2.54	37.7	3.77
-3.18	37.0	3.76
-3.81	32.2	3.68
-3.94	29.9	3.64
-4.45	32.7	3.69
-5.08	37.0	3.76

$V' =$ 35.8 m/min

Profile E. Sampler model B.

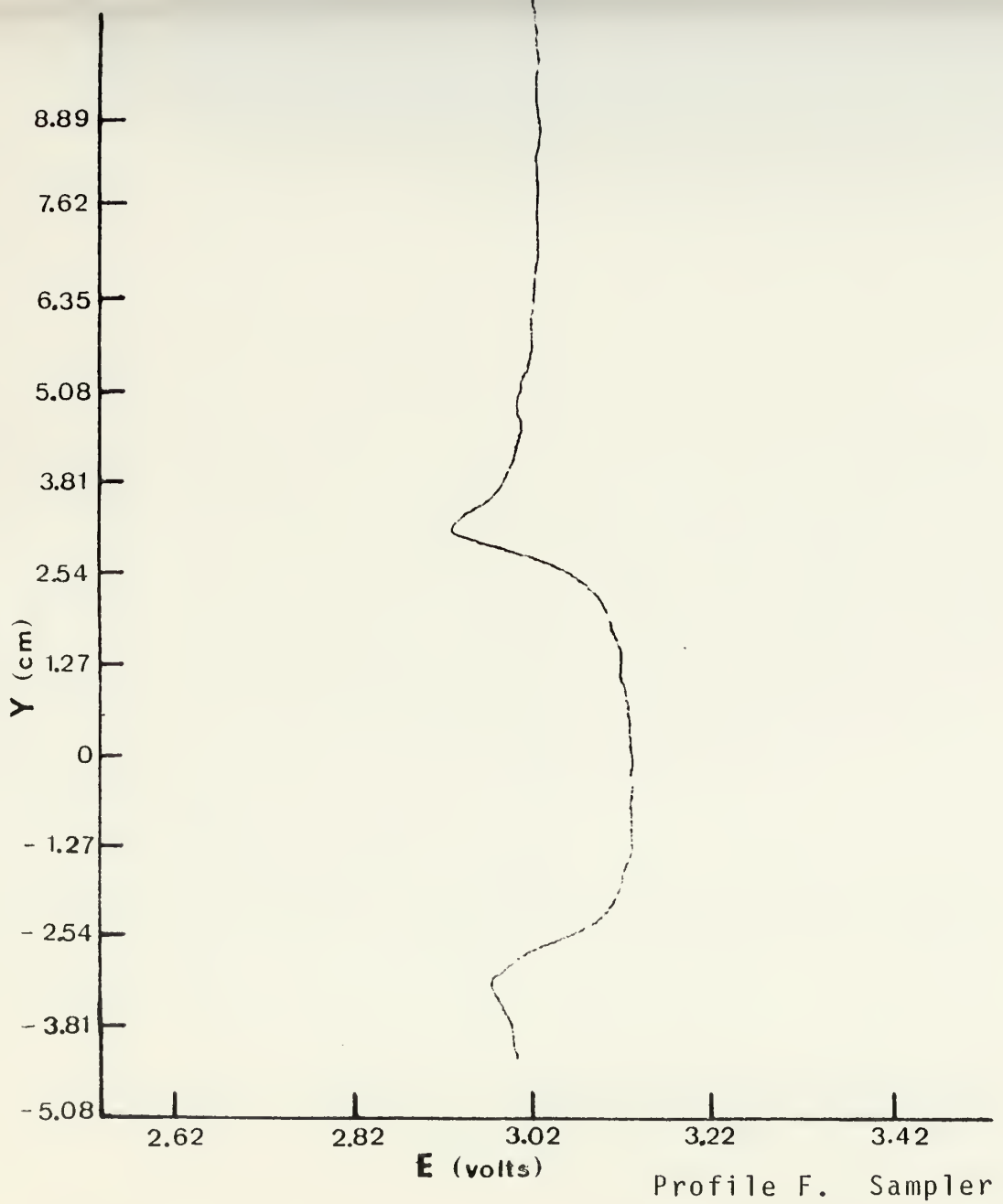

$X = 0^+$ (at mouth of sampler)

Y (cm)	V (m/min)	E (volts)
10.16	40.9	3.02
7.62	40.9	3.02
5.08	40.9	3.02
4.45	39.3	3.00
3.81	39.3	3.00
3.18	34.0	2.93
2.54	43.5	3.05
1.91	48.1	3.10
1.27	49.0	3.11
.635	51.0	3.13
0	51.0	3.13
- .635	51.0	3.13
-1.27	51.0	3.13
-1.91	50.0	3.12
-2.54	44.4	3.06
-3.18	36.8	2.97
-3.81	38.5	2.99

$V' =$ 46.3 m/min

Profile F. Sampler model C.

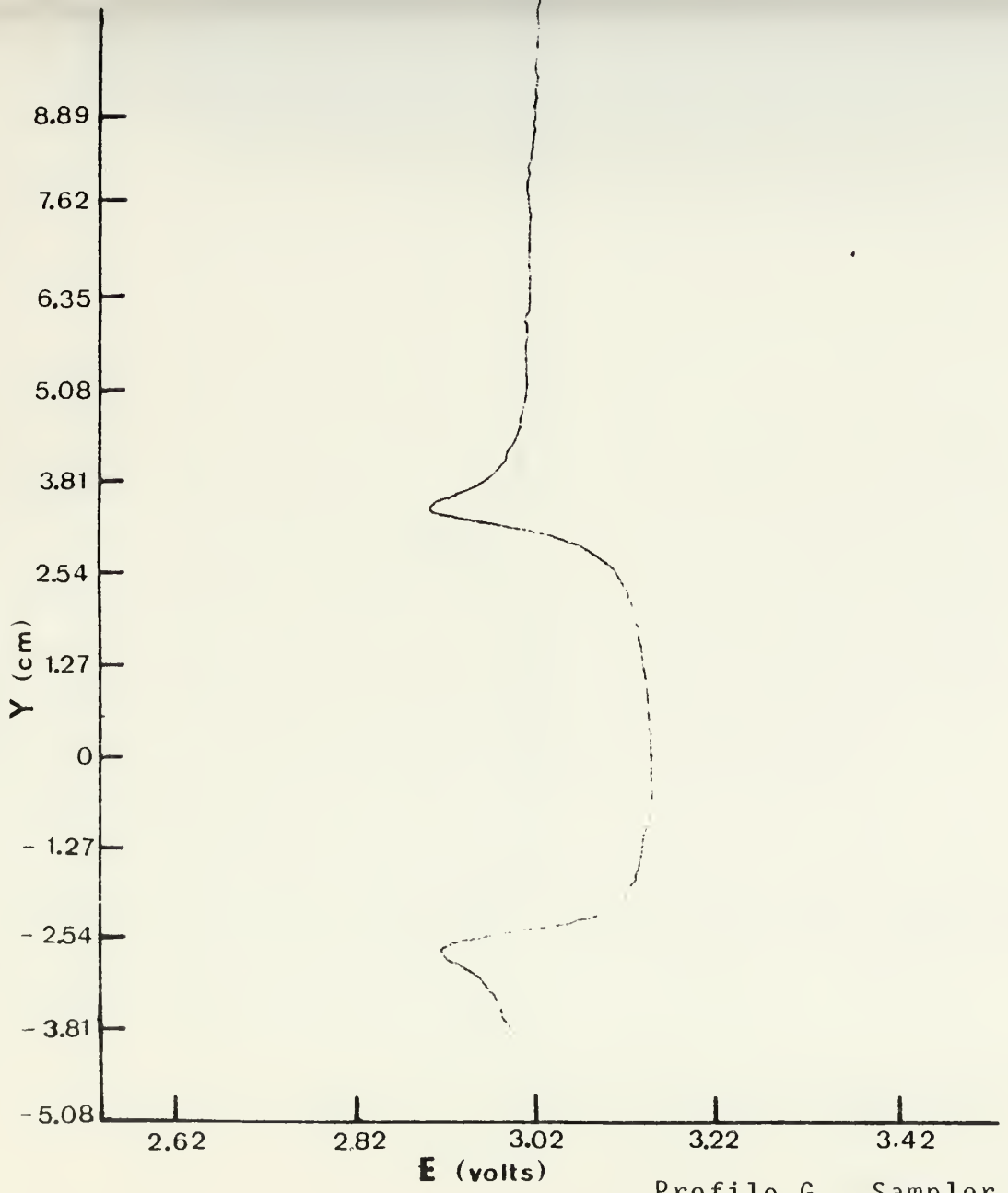

$X = 0^+$ (at mouth of sampler)

Y (cm)	V (m/min)	E (volts)
10.16	40.9	3.02
7.62	40.0	3.01
5.08	39.3	3.00
4.45	39.3	3.00
3.81	37.7	2.98
3.18	32.6	2.91
3.05	30.8	2.89
2.54	43.5	3.05
1.91	49.0	3.11
1.27	50.0	3.12
.635	51.0	3.13
0	52.0	3.14
- .635	52.0	3.14
-1.27	52.0	3.14
-1.91	50.0	3.12
-2.54	47.2	3.09
-3.05	30.8	2.89
-3.18	32.6	2.91
-3.81	37.7	2.98

$V' =$ 46.2 m/min

Profile G. Sampler model D.

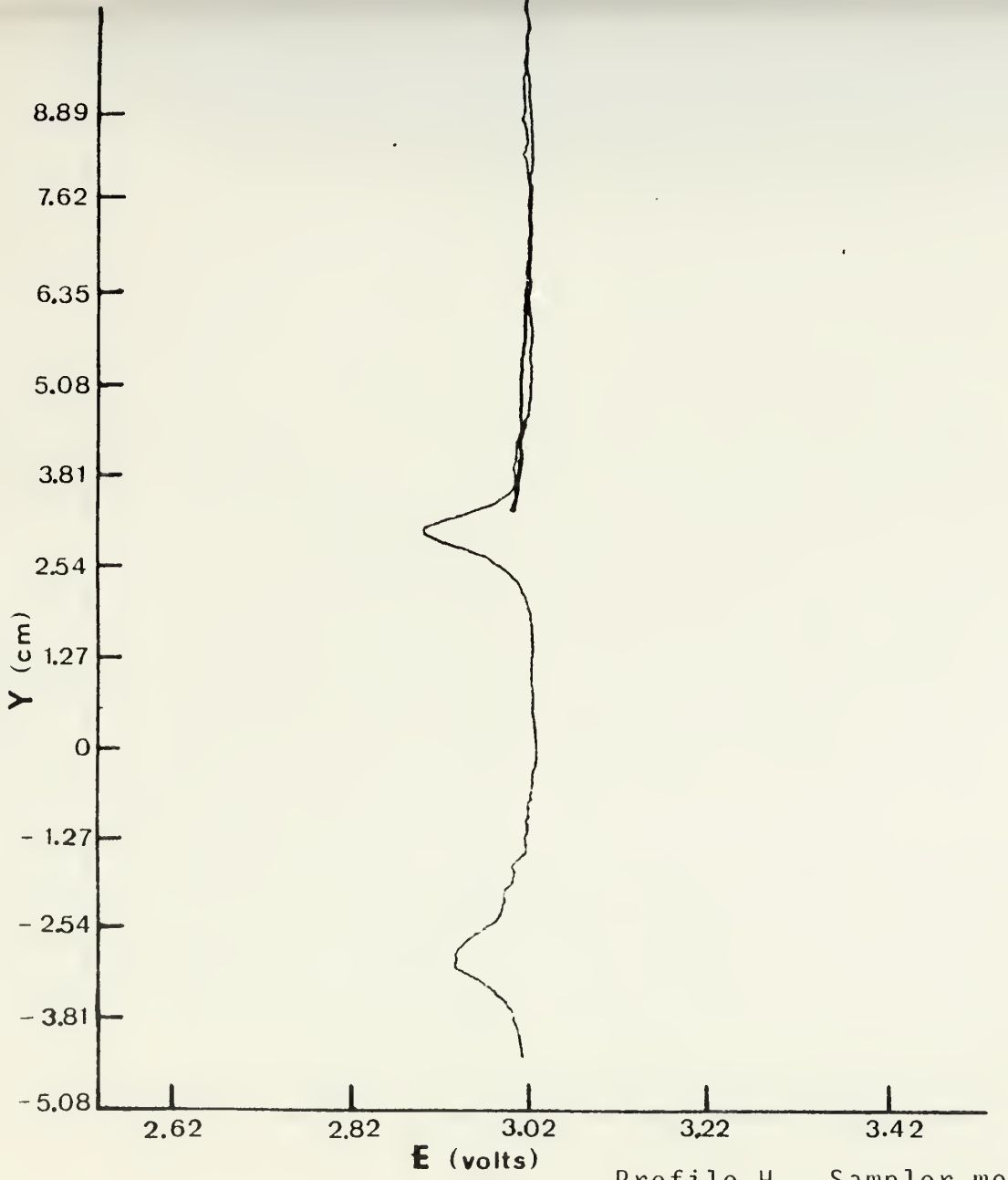

$X = 0^+$ (at mouth of sampler)

Y (cm)	V (m/min)	E (volts)
7.62	40.9	3.02
5.08	40.9	3.02
4.45	40.0	3.01
3.81	39.2	3.00
3.18	34.5	2.94
3.05	31.6	2.90
2.54	37.8	2.98
1.91	40.9	3.02
1.27	40.9	3.02
.635	40.9	3.02
0	40.9	3.02
- .635	40.9	3.02
-1.27	40.0	3.01
-1.91	39.2	3.00
-2.54	36.8	2.97
-3.05	34.5	2.94
-3.18	34.5	2.94
-3.81	39.2	3.00

$V' =$ 38.6 m/min

Profile H. Sampler model E.

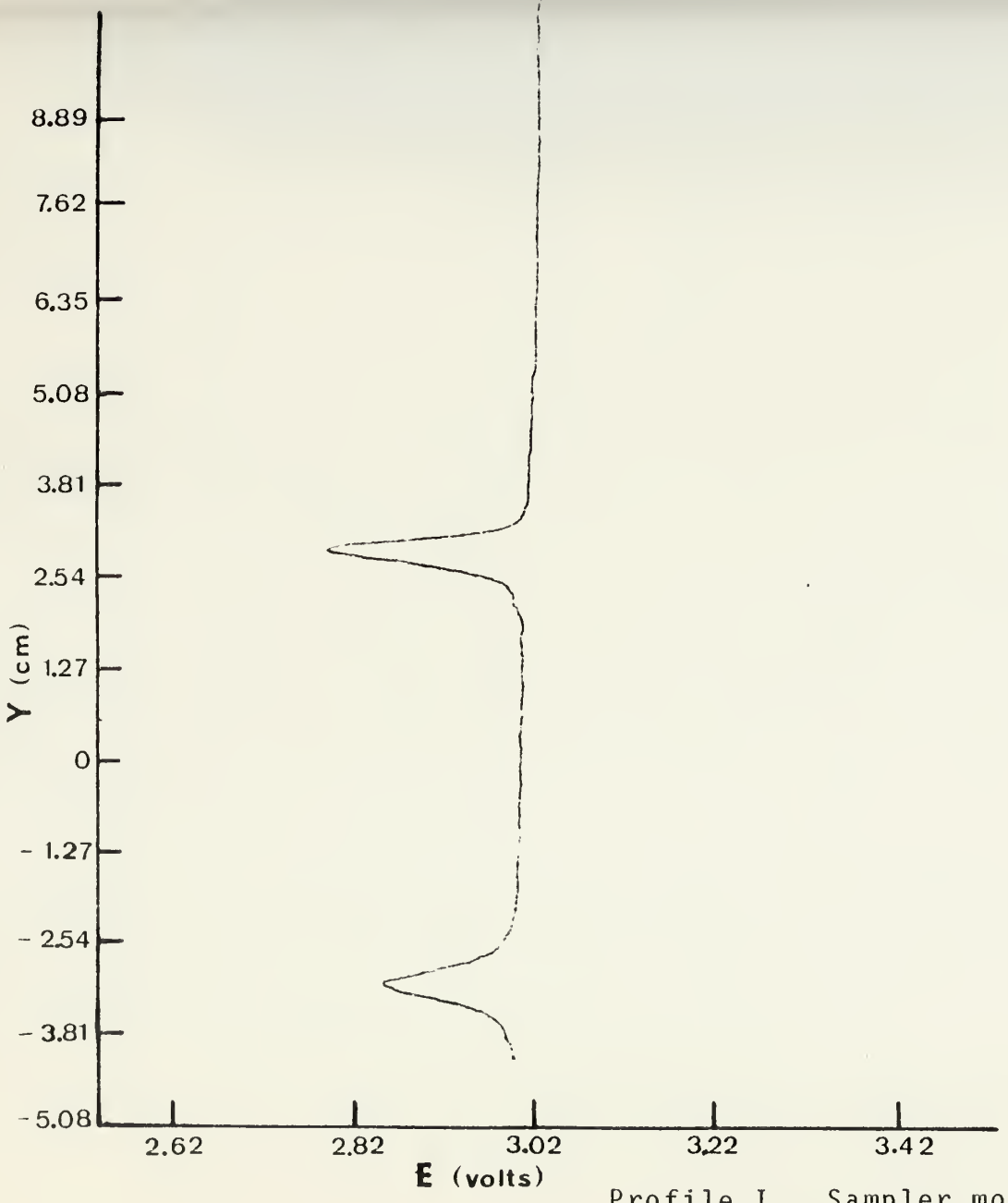

$X = 0^+$ (at mouth of sampler)

Y (cm)	V (m/min)	E (volts)
10.16	40.9	3.02
7.62	40.9	3.02
4.45	40.0	3.01
3.81	40.0	3.01
3.18	37.0	2.97
3.05	24.4	2.79
2.54	35.3	2.95
1.91	39.3	3.00
1.27	39.3	3.00
.635	39.3	3.00
0	39.3	3.00
- .635	39.3	3.00
-1.27	39.3	3.00
-1.91	38.0	2.99
-2.54	37.0	2.97
-3.05	28.2	2.85
-3.18	29.5	2.87
-3.81	37.7	2.98

$V' =$ 36.2 m/min

Profile I. Sampler model F.

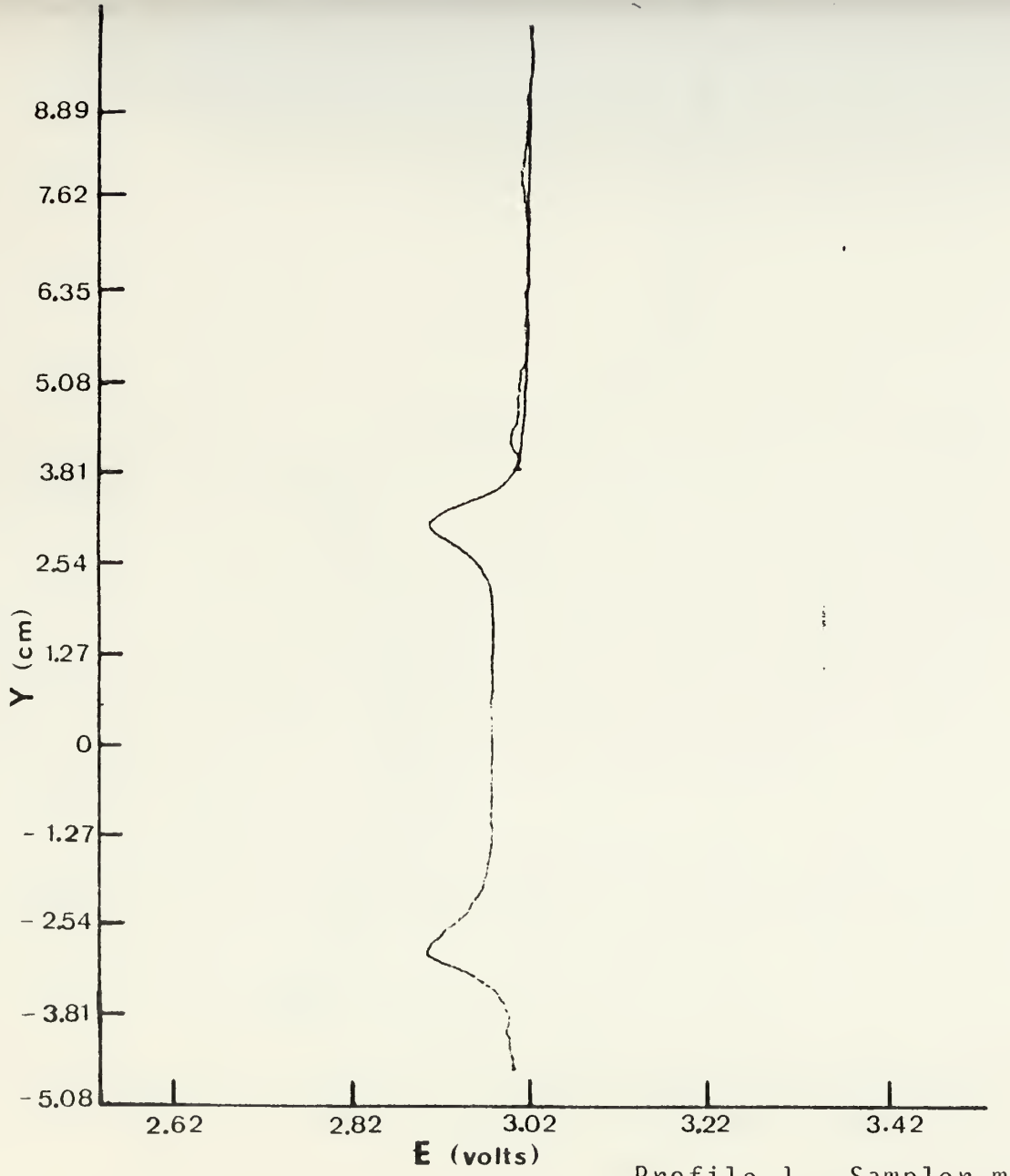

X = 0+ (at mouth of sampler)

Y (cm)	V (m/min)	E (volts)
12.70	40.9	3.02
11.43	40.9	3.02
7.62	40.5	3.015
3.81	39.6	3.005
3.56	38.5	2.99
3.18	34.5	2.94
3.05	31.6	2.90
2.79	33.5	2.92
2.54	35.3	2.95
1.91	37.0	2.97
1.27	37.3	2.975
.635	37.3	2.975
0	37.3	2.975
- .635	37.3	2.975
-1.27	37.3	2.975
-1.91	37.0	2.97
-2.54	35.3	2.95
-2.79	33.5	2.92
-3.05	31.6	2.90
-3.18	34.5	2.94
-3.81	39.6	3.005

$V' =$ 35.5 m/min

Profile J. Sampler model G.

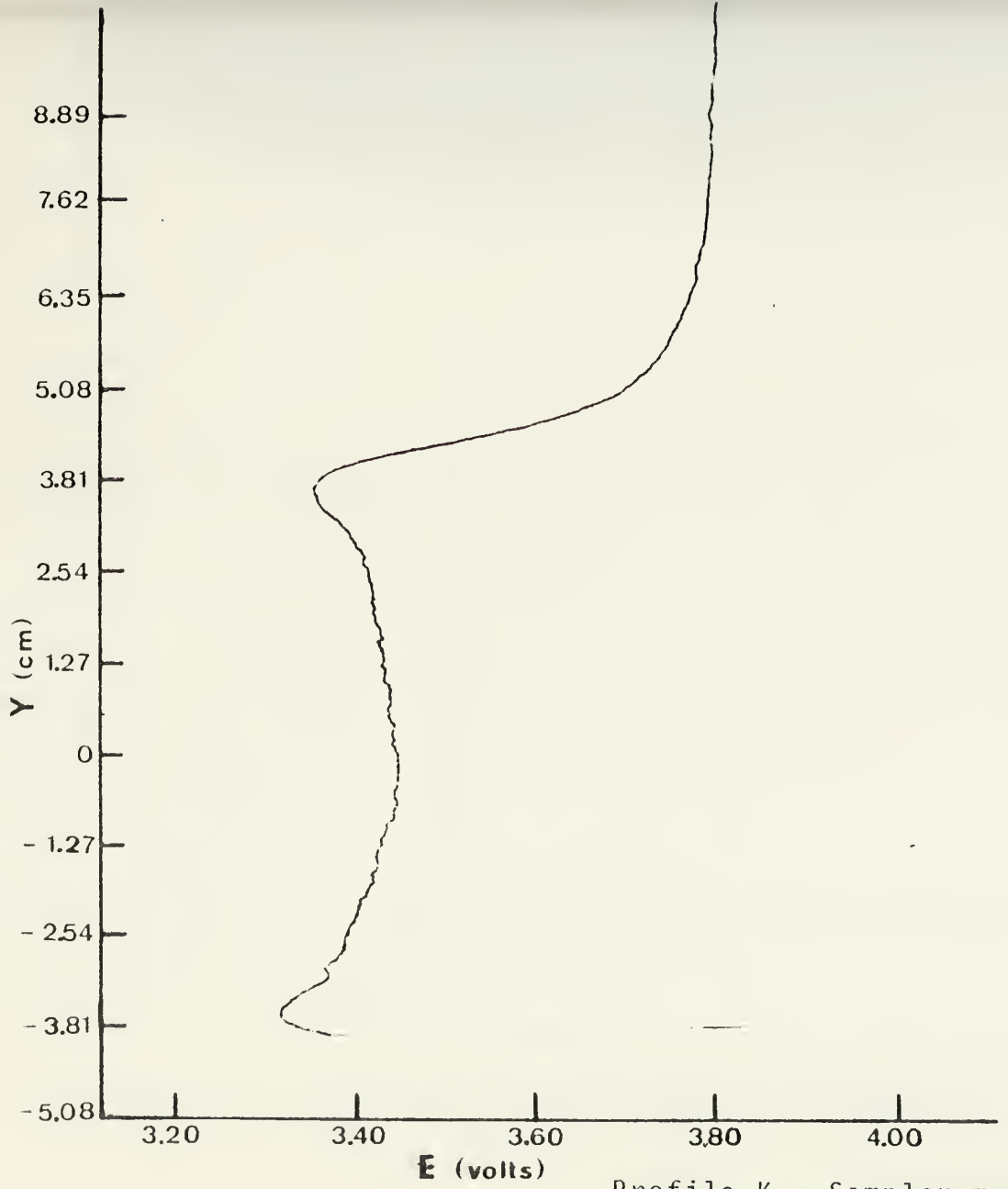

$X = 0^+$ (at mouth of sampler)

Y (cm)	V (m/min)	E (volts)
10.80	39.5	3.80
10.16	39.5	3.80
7.62	39.0	3.79
6.35	37.5	3.77
5.08	33.2	3.70
4.45	25.5	3.56
3.81	16.8	3.36
3.56	16.4	3.35
3.18	17.1	3.37
2.54	18.3	3.40
1.91	18.7	3.41
1.27	19.2	3.42
.635	19.6	3.43
0	20.0	3.44
- .635	20.0	3.44
-1.27	19.6	3.43
-1.91	18.7	3.41
-2.54	18.0	3.39
-3.18	16.8	3.36
-3.68	15.0	3.31
-3.81	15.6	3.33
-4.45	27.1	3.59

$V' =$ 18.3 m/min

Profile K. Sampler model H.

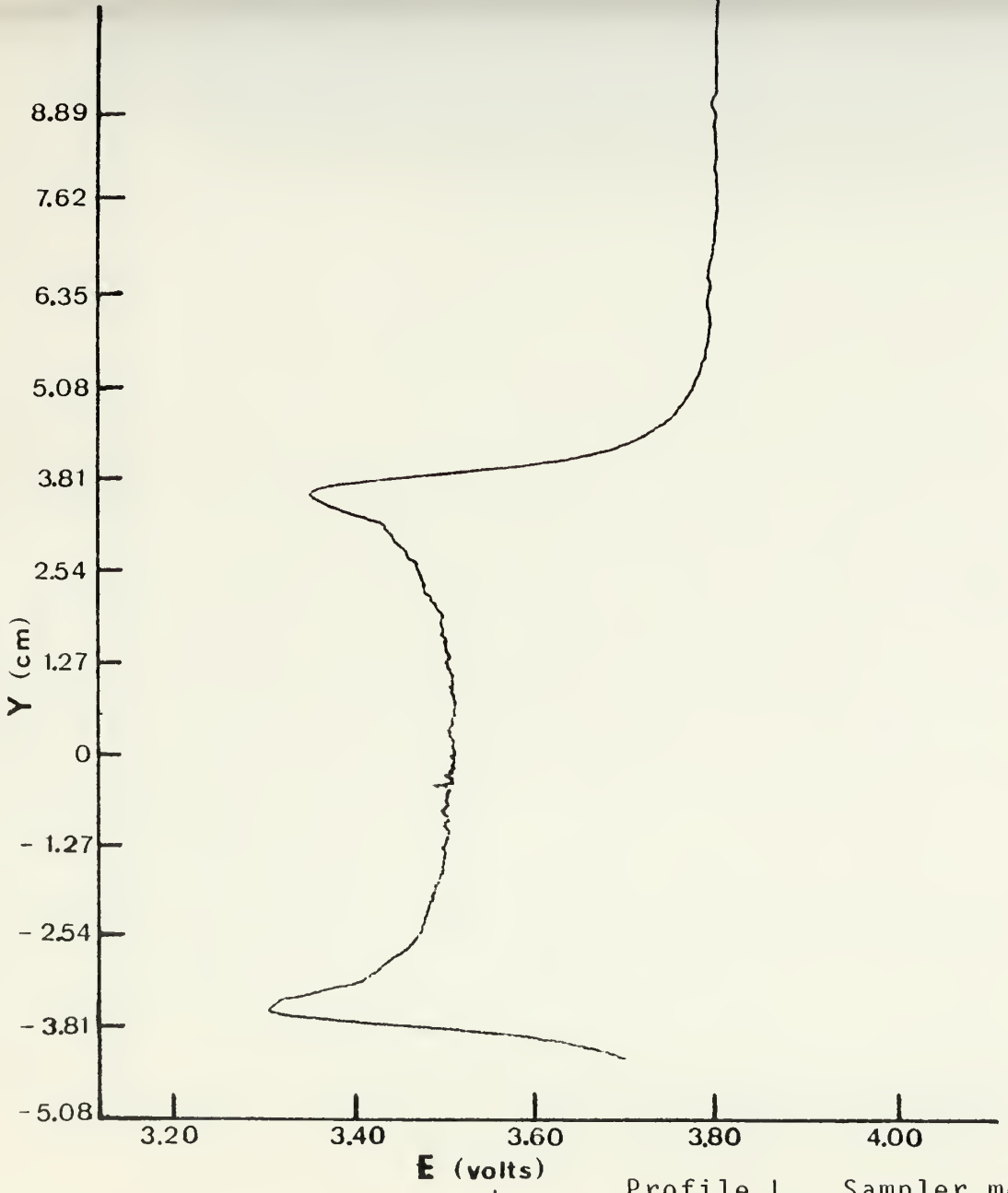

$X = 0^+$ (at mouth of sampler)

Y (cm)	V (m/min)	E (volts)
10.80	39.5	3.80
10.16	39.5	3.80
7.62	39.0	3.79
6.35	38.5	3.78
5.72	38.5	3.78
5.08	37.7	3.77
4.45	35.1	3.73
3.81	23.2	3.51
3.56	16.0	3.34
3.18	19.2	3.42
2.54	21.0	3.46
1.91	22.3	3.49
1.27	22.8	3.50
.635	23.2	3.51
0	23.2	3.51
- .635	22.8	3.50
-1.27	22.8	3.50
-1.91	21.8	3.48
-2.54	21.0	3.46
-3.18	18.4	3.40
-3.56	14.3	3.29
-3.81	21.0	3.46
-5.08	34.0	3.71

$V' =$ 20.6 m/min

Profile L. Sampler model I.

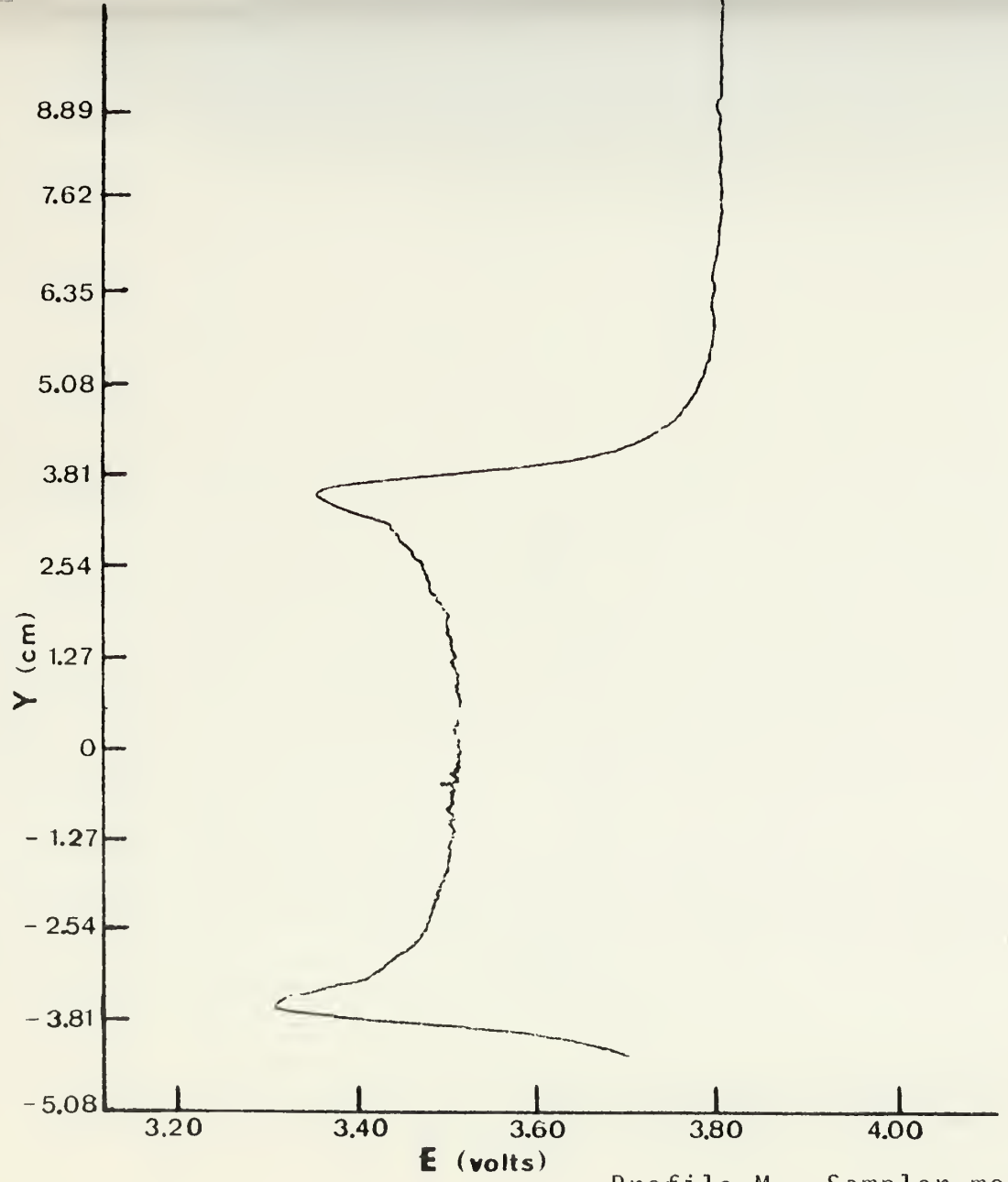

$X = 0^+$ (at mouth of sampler)

Y (cm)	V (m/min)	E (volts)
10.80	39.5	3.80
10.16	39.5	3.80
7.62	39.0	3.79
6.35	38.5	3.78
5.72	38.5	3.78
5.08	37.7	3.77
4.45	35.1	3.73
3.81	23.2	3.51
3.56	16.0	3.34
3.18	19.2	3.42
2.54	21.0	3.46
1.91	22.3	3.49
1.27	22.8	3.50
.635	23.2	3.51
0	23.2	3.51
- .635	22.8	3.50
-1.27	22.8	3.50
-1.91	21.8	3.48
-2.54	21.0	3.46
-3.18	18.4	3.40
-3.56	14.3	3.29
-3.81	21.0	3.46
-5.08	34.0	3.71

$V' = 20.6$ m/min

Profile M. Sampler model J.

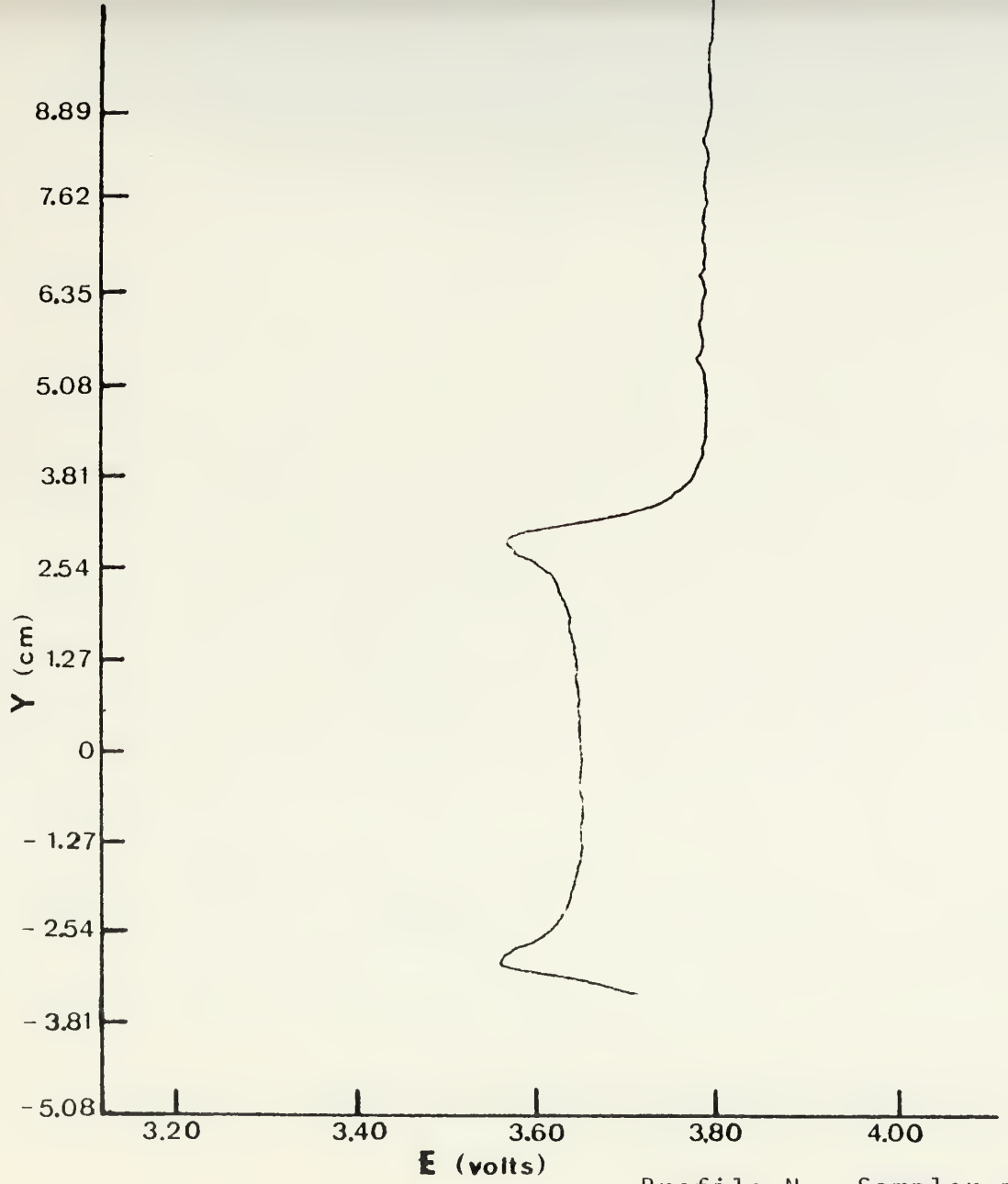

$X = 0^+$ (at mouth of sampler)

Y (cm)	V (m/min)	E (volts)
10.80	39.5	3.80
8.26	39.5	3.80
6.35	39.0	3.79
4.45	39.0	3.79
3.81	38.5	3.78
3.18	32.2	3.68
2.92	26.2	3.57
2.54	28.0	3.61
1.91	29.9	3.64
1.27	30.4	3.65
.635	30.4	3.65
0	31.0	3.66
- .635	31.0	3.66
-1.27	31.0	3.66
-1.91	29.9	3.64
-2.54	28.5	3.62
-2.92	25.7	3.56
-3.18	32.2	3.68
-3.81	37.7	3.77

$V' =$ 29.3 m/min

Profile N. Sampler model K.

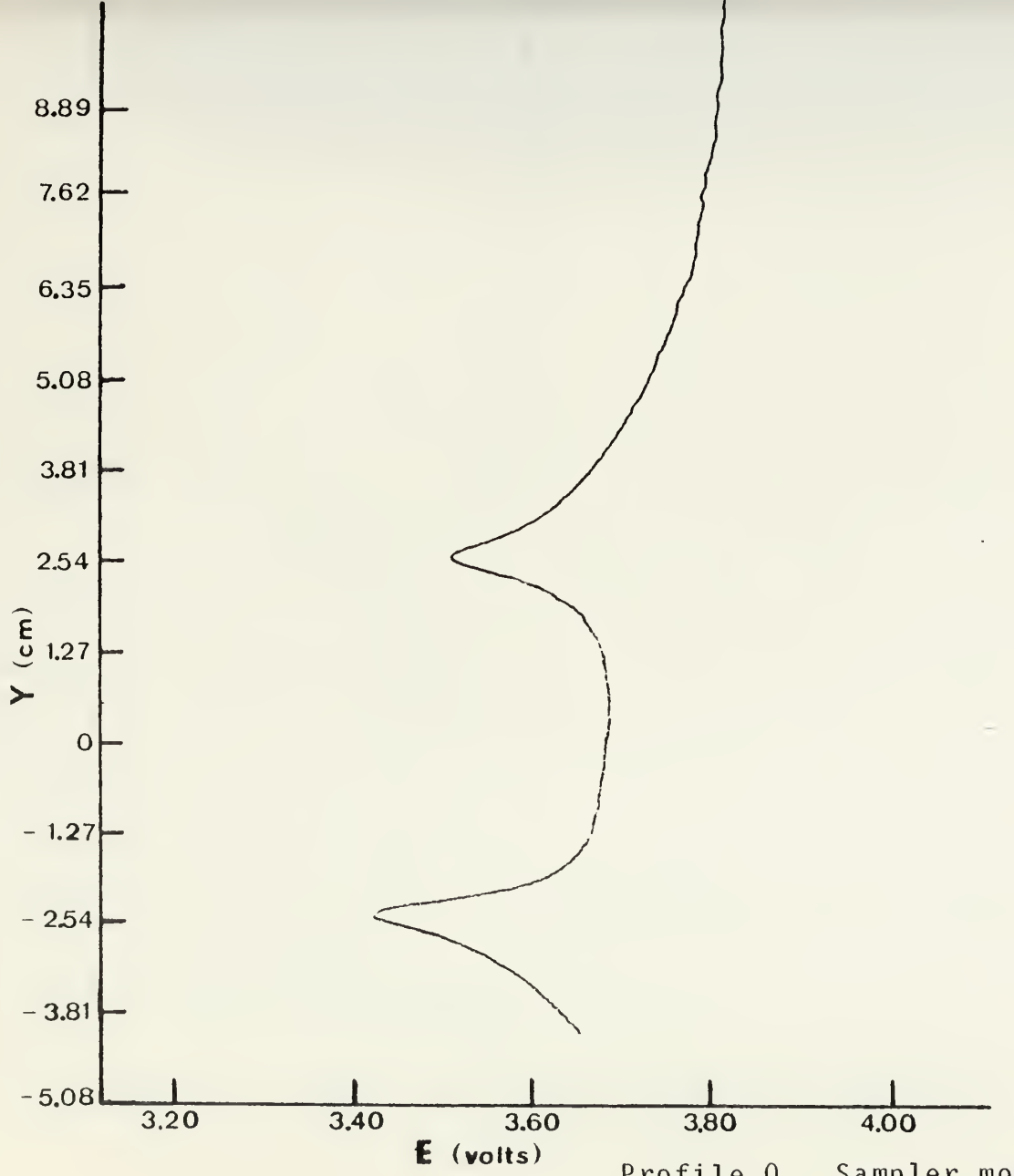

$X = 0^+$ (at mouth of sampler)

Y (cm)	V (m/min)	E (volts)
10.16	39.5	3.80
7.62	38.5	3.78
6.35	37.0	3.76
5.08	34.5	3.72
4.45	33.2	3.70
3.81	31.0	3.66
3.18	28.5	3.62
2.54	23.0	3.51
2.41	22.8	3.50
1.91	28.0	3.61
1.27	31.0	3.66
.635	31.6	3.67
0	31.6	3.67
- .635	31.0	3.66
-1.27	30.4	3.65
-1.91	28.8	3.62
-2.41	18.8	3.41
-2.54	19.2	3.42
-3.18	25.2	3.55
-3.81	28.5	3.62
-4.45	31.0	3.66
-5.08	32.7	3.69

$V' =$ 28.2 m/min

Profile 0. Sampler model L.

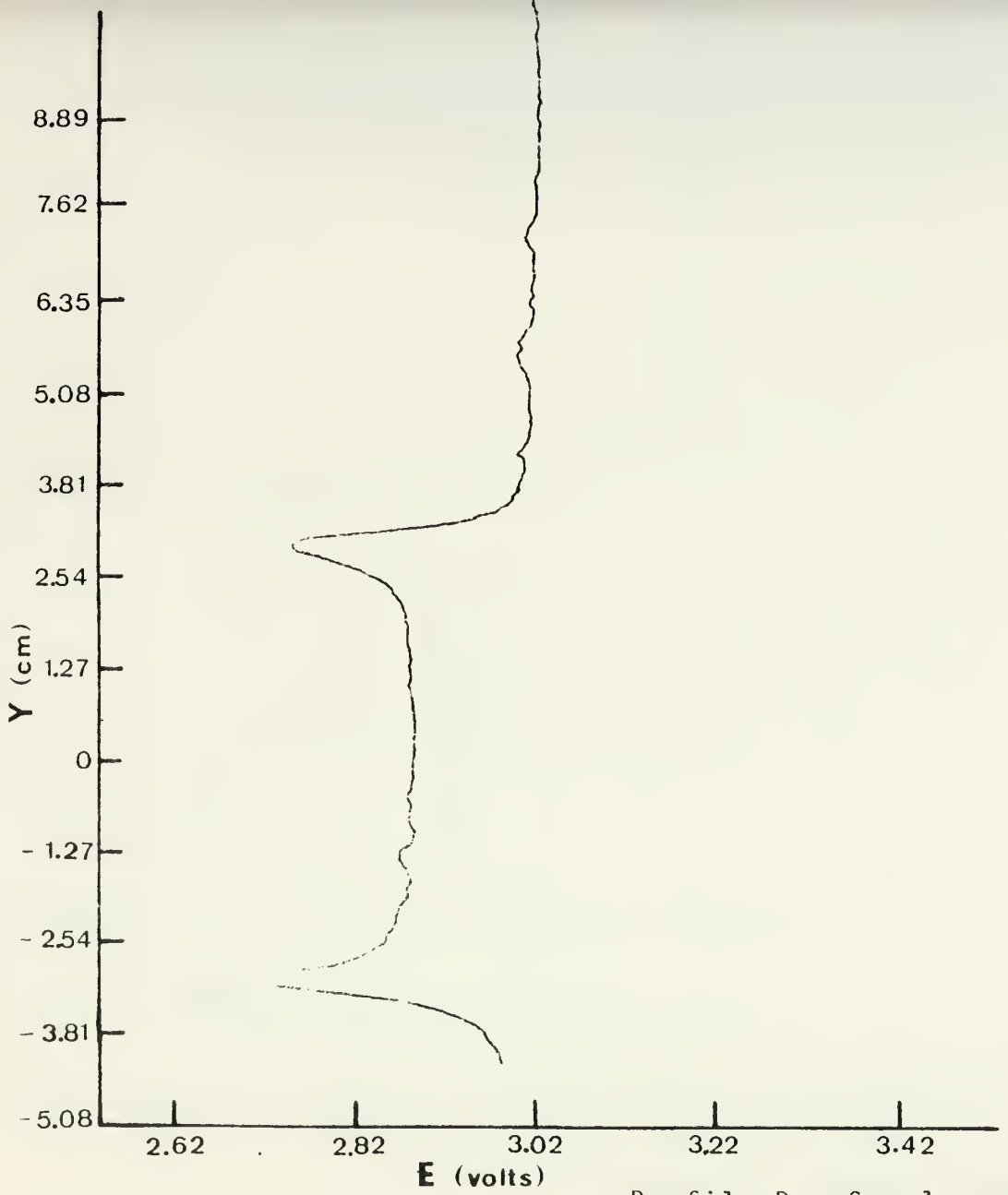

$X = 0^+$ (at mouth of sampler)

Y (cm)	V (m/min)	E (volts)
11.43	40.9	3.02
7.62	40.9	3.02
3.81	39.2	3.00
3.18	31.0	2.89
2.79	27.8	2.84
2.54	28.2	2.85
1.91	30.1	2.88
1.27	31.0	2.89
.635	31.0	2.89
0	31.0	2.89
- .635	31.0	2.89
-1.27	31.0	2.89
-1.91	30.1	2.88
-2.54	28.2	2.85
-2.79	26.1	2.82
-3.18	26.9	2.83
-3.81	37.8	2.98

$V' =$ 29.6 m/min

Profile P. Sampler model M.

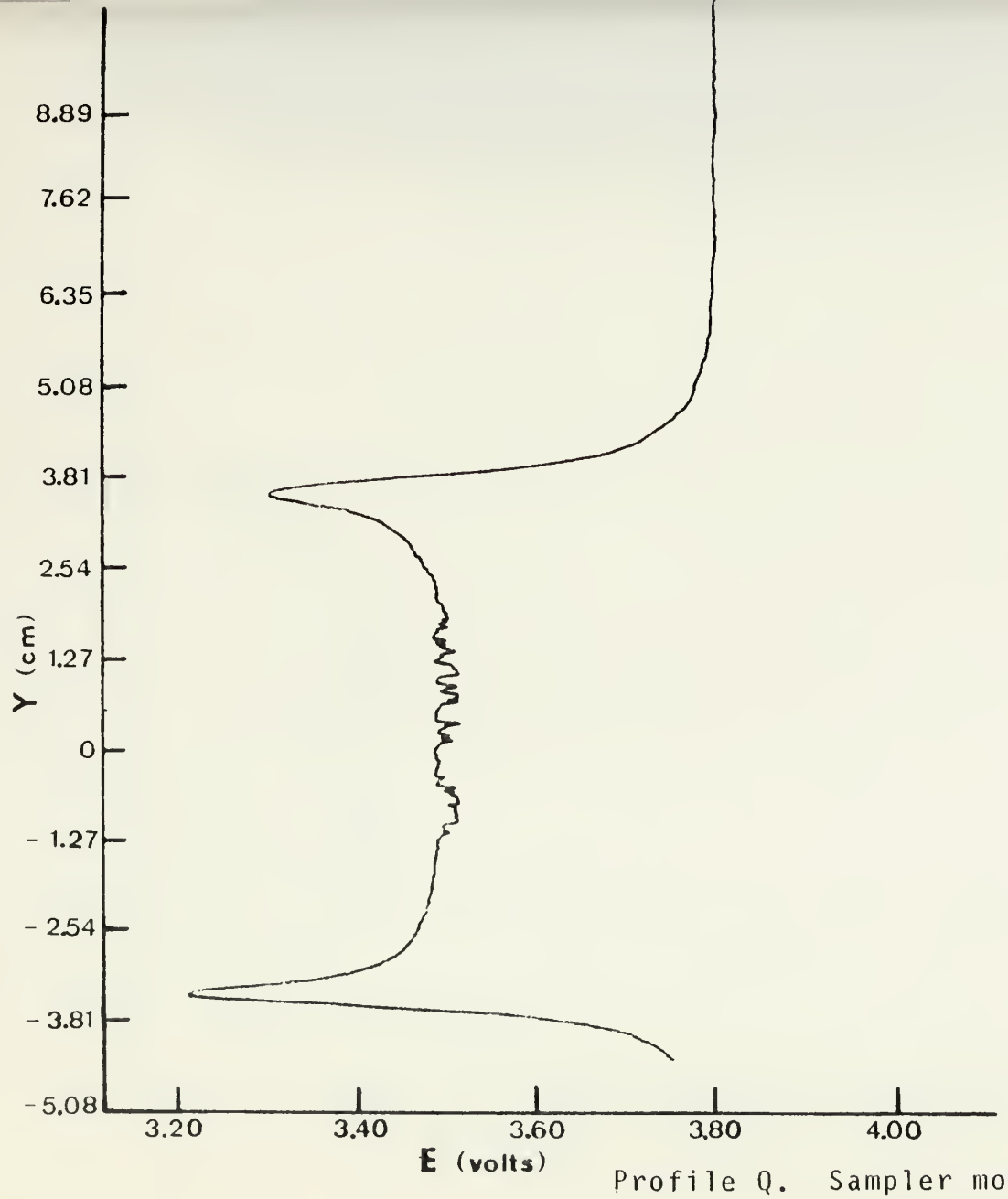

$X = 0^+$ (at mouth of sampler)

Y (cm)	V (m/min)	E (volts)
7.62	39.5	3.8
6.35	39.5	3.8
5.08	39.0	3.79
4.45	36.4	3.75
3.81	25.2	3.55
3.56	15.0	3.31
3.18	19.2	3.42
2.54	21.8	3.48
1.91	22.8	3.5
1.27	22.8	3.5
.635	23.7	3.52
0	22.8	3.5
- .635	23.2	3.51
-1.27	22.8	3.5
-1.91	22.3	3.49
-2.54	21.4	3.47
-3.18	18.0	3.39
-3.56	12.0	3.22
-3.81	27.7	3.6
-4.45	37.0	3.76

$V' =$ 20.6 m/min

Profile Q. Sampler model N.

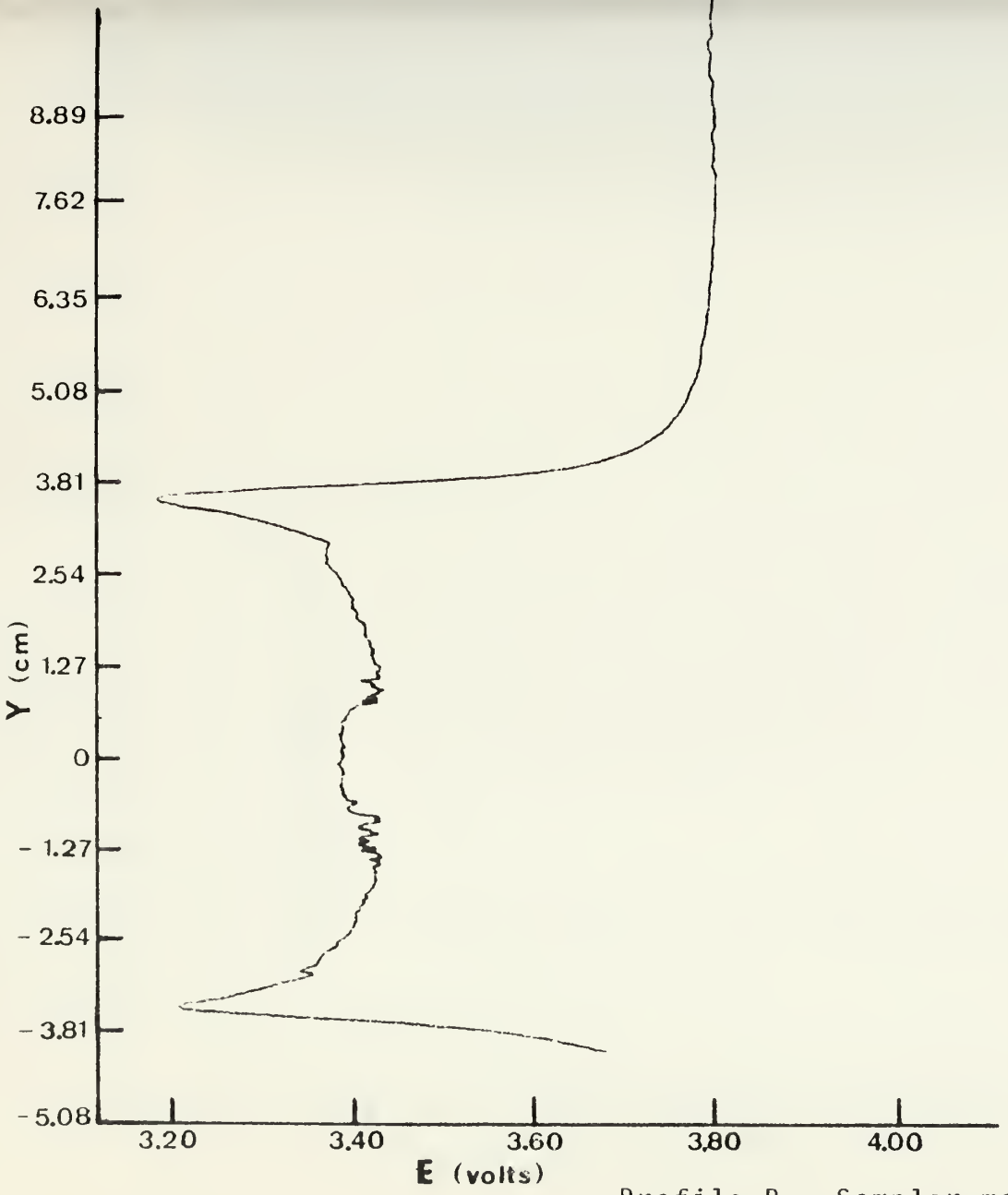

$X = 0^+$ (at mouth of sampler)

Y (cm)	V (m/min)	E (volts)
8.89	39.5	3.8
6.99	39.5	3.8
5.72	39.0	3.79
5.08	38.5	3.78
4.45	36.4	3.75
3.81	23.7	3.52
3.56	11.1	3.19
3.18	15.3	3.32
2.54	18.0	3.39
1.91	18.8	3.41
1.27	19.6	3.43
.635	18.4	3.4
0	18.4	3.4
- .635	18.4	3.4
-1.27	19.2	3.42
-1.91	19.2	3.42
-2.54	18.0	3.39
-3.18	15.0	3.31
-3.56	11.7	3.21
-3.81	26.7	3.58

$V' =$ 17.0 m/min

Profile R. Sampler model 0.

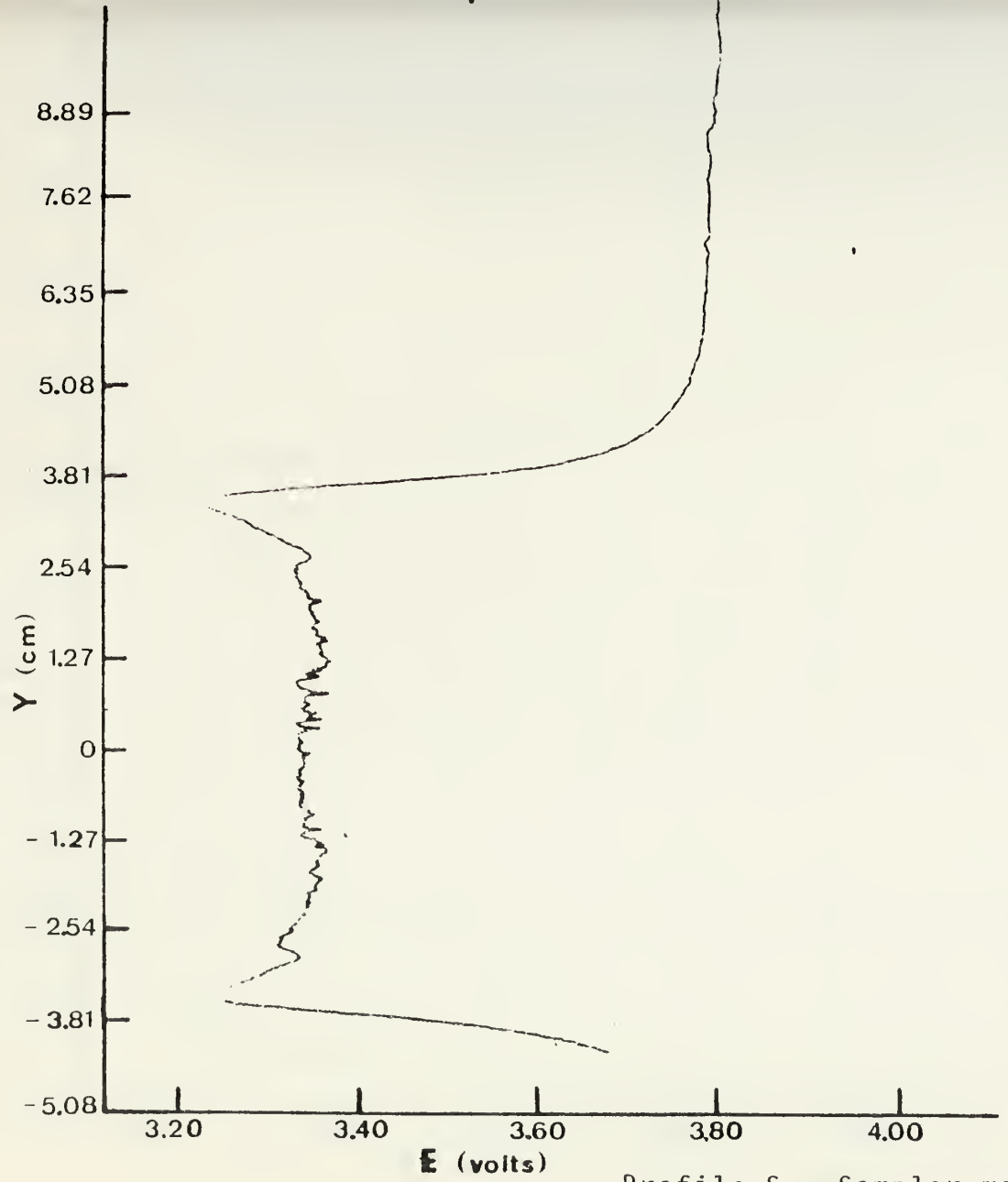

$X = 0^+$ (at mouth of sampler)

Y (cm)	V (m/min)	E (volts)
8.89	39.5	3.8
6.99	39.5	3.8
5.72	39.0	3.79
5.08	37.7	3.77
4.45	34.5	3.72
3.81	21.4	3.47
3.56	12.6	3.24
3.18	14.3	3.29
2.54	16.0	3.34
1.91	16.8	3.36
1.27	17.2	3.37
.635	16.4	3.35
0	16.4	3.35
- .635	16.4	3.35
-1.27	17.2	3.37
-1.91	16.8	3.36
-2.54	15.7	3.33
-3.18	14.0	3.28
-3.56	12.9	3.25
-3.81	25.7	3.56
-4.45	35.8	3.74

$V' =$ 15.6 m/min

Profile S. Sampler model P.

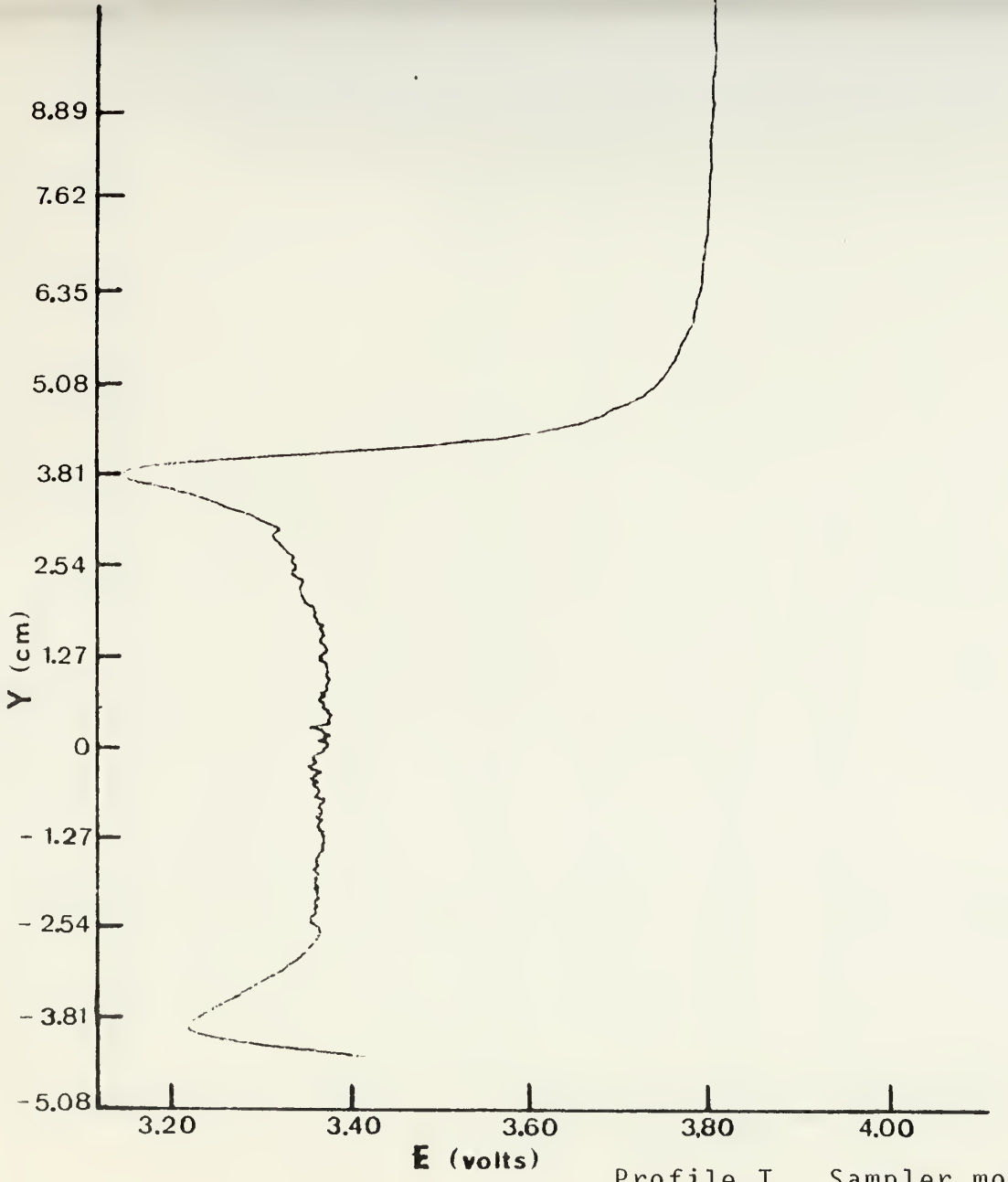

$X = 0^+$ (at mouth of sampler)

Y (cm)	V (m/min)	E (volts)
11.43	39.5	3.8
9.53	39.5	3.8
6.99	39.0	3.79
6.35	38.5	3.78
5.72	37.7	3.77
5.08	35.1	3.73
4.45	28.8	3.62
3.81	9.6	3.14
3.18	14.6	3.3
2.54	15.7	3.33
1.91	16.4	3.35
1.27	16.8	3.36
.635	16.8	3.36
0	16.8	3.36
- .635	16.8	3.36
-1.27	16.8	3.36
-1.91	16.8	3.36
-2.54	16.8	3.36
-3.18	14.6	3.3
-3.81	11.7	3.21
-4.45	22.8	3.5

$V' =$ 15.4 m/min

Profile T. Sampler model Q.

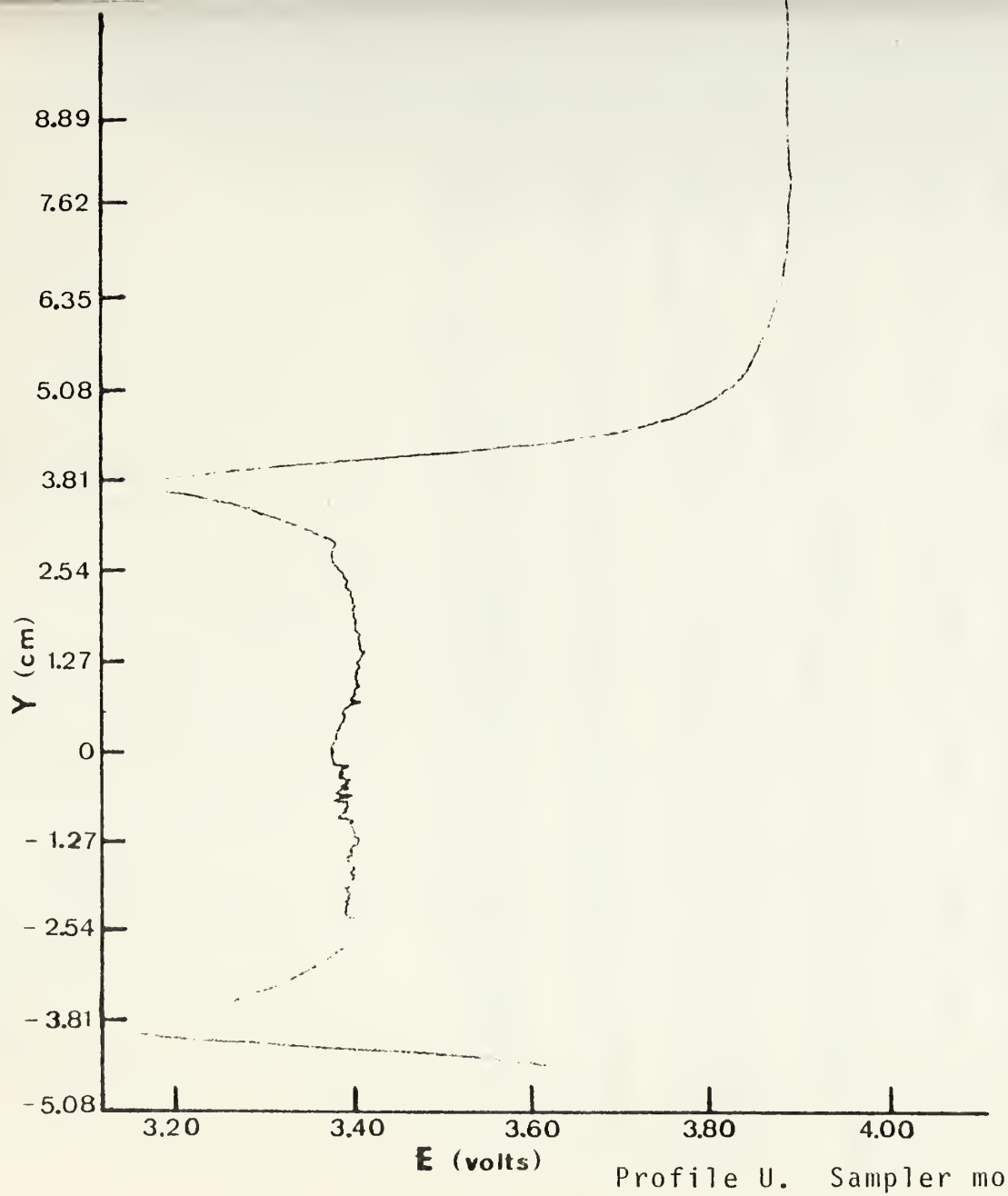

$X = 0^+$ (at mouth of sampler)

Y (cm)	V (m/min)	E (volts)
7.62	39.5	3.8
6.99	39.5	3.8
6.35	39.0	3.79
5.72	37.7	3.77
5.08	35.8	3.74
4.45	29.9	3.64
3.81	8.3	3.09
3.18	12.6	3.24
2.54	14.6	3.3
1.91	15.0	3.31
1.27	15.3	3.32
.635	15.0	3.31
0	14.3	3.29
- .635	14.6	3.3
-1.27	15.3	3.32
-1.91	15.3	3.32
-2.54	15.3	3.32
-3.18	12.6	3.24
-3.81	7.6	3.06
-4.45	23.7	3.52
-5.08	33.3	3.7

$V' = 13.5$ m/min

Profile U. Sampler model R.

REFERENCES

1. Aron, W., E. H. Ahlstrom, B. Bary, A.W.H. Be, and W. D. Clarke, "Towing Characteristics of Plankton Sampling Gear," Limnology and Oceanography, v. 10 (3), 333-340, 1965.

2. Neumann, G. and W. J. Pierson, Principles of Physical Oceanography, Prentice-Hall, 1966.

3. Pankhurst, R. C. and D. W. Holder, Wind Tunnel Technique, London, Pitman, 1952.

4. Pope, A. and J. J. Harper, Low Speed Wind Tunnel Testing, John Wiley and Sons, Inc., 1-4, 1966.

5. Smith, P. E. and R. I. Clutter, "Hydrodynamics of Flow and Collection in Plankton Nets", Ocean Science and Ocean Engineering, n. 1, 515 (abstract), 1965.

6. Streeter, V. L., Fluid Mechanics, McGraw-Hill Book Co., Inc., 8-9, 1960.

7. Tranter, D. J., "A Formula for the Filtration Coefficient of a Plankton Net", Australian Journal of Marine and Freshwater Research, v. 18, 113-121, 1967.

8. Tranter, D. J. and A. C. Heron, "Experiments on Filtration in Plankton Nets", Australian Journal of Marine and Freshwater Research, v. 18, 89-111, 1967.

9. Tranter, D. J. and P. E. Smith, "Filtration Performance", UNESCO Monograph on Oceanographic Methodology, no. 2, 27-56, 1968.

10. Vannucci, M., "Loss of Organisms Through the Meshes," UNESCO Monograph on Oceanographic Methodology, no. 2, 77-86, 1968.

INITIAL DISTRIBUTION LIST

		No. Copies
1.	Defense Documentation Center Cameron Station Alexandria, Virginia 22314	2
2.	Library (Code 0142) Naval Postgraduate School Monterey, California 93940	2
3.	Dr. Eugene D. Traganza Department of Oceanography, Code 68 Naval Postgraduate School Monterey, California 93940	3
4.	LT. Robert P. Mitchke USN 7106 Rook Road Houston, Texas 77017	2
5.	Department of Oceanography, Code 68 Naval Postgraduate School Monterey, California 93940	3
6.	Oceanographer of the Navy Hoffman Building No. 2 200 Stovall Street Alexandria, Virginia 22332	1
7.	Office of Naval Research Code 480 Arlington, Virginia 22217	1
8.	Dr. Robert E. Stevenson Scientific Liaison Office, ONR Scripps Institution of Oceanography La Jolla, California 92037	1
9.	Library, Code 3330 Naval Oceanographic Office Washington, D. C. 20373	1
10.	SIO Library University of California, San Diego P. O. Box 2367 La Jolla, California 92037	1
11.	Department of Oceanography Library University of Washington Seattle, Washington 98105	1

12. Commanding Officer 1
Fleet Numerical Weather Central
Monterey, California 93940

13. Commanding Officer 1
Navy Environmental Prediction Research
Facility
Monterey, California 93940

14. Department of the Navy 1
Commander Oceanographic System Pacific
Box 1390
FPO San Francisco 96610

Thesis 166837
M646 Mitchke
c.1 Design and wind tunnel testing of a size sampling in-situ net system (SSISNET).